2023

# Effects of Phosphorus-binding Agents on Nutrient Dynamics and a Planktothrix Bloom in a Shallow, Semi-enclosed Lake Area

Joseph Lee Davidson
*Wright State University*

# EFFECTS OF PHOSPHORUS-BINDING AGENTS ON NUTRIENT DYNAMICS AND A *PLANKTOTHRIX* BLOOM IN A SHALLOW, SEMI-ENCLOSED LAKE AREA

A thesis submitted in partial fulfillment of the requirements
for the degree of
Master of Science

By

JOSEPH LEE DAVIDSON
B.S., Wright State University, 2020

2023
Wright State University

WRIGHT STATE UNIVERSITY

COLLEGE OF GRADUATE PROGRAMS & HONORS STUDIES

April 21st, 2023

I HEREBY RECOMMEND THAT THE THESIS PREPARED UNDER MY SUPERVISION BY Joseph Lee Davidson ENTITLED Effects of Phosphorus-binding agents on nutrient dynamics and a *Planktothrix* bloom in a shallow, semi-enclosed lake area BE ACCEPTED IN PARTIAL FULFILLMENT OF THE REQUIREMENTS FOR THE DEGREE OF Master of Science.

Silvia E. Newell, Ph.D.
Thesis Director

Abinash Agrawal, Ph.D.
Director of Earth & Environmental Sciences Department

Committee on Final Examination

Mark J. McCarthy, Ph.D.

Stephen J. Jacquemin, Ph.D.

Shu Schiller, Ph.D.
Interim Dean, College of Graduate P
Programs & Honors Studies

# ABSTRACT

Davidson, Joseph Lee. M.S. Department of Earth and Environmental Sciences, Wright State University, 2023. Effects of Phosphorus-binding agents on nutrient dynamics and a Planktothrix bloom in a shallow, semi-enclosed lake area.

Grand Lake St. Marys is the largest (52 $km^2$) inland lake in Ohio, USA, and receives high nutrient loadings (90th percentile for total nitrogen (N) and phosphorus (P) concentrations in the USA) from a watershed dominated by agricultural row-crops and livestock production. Eutrophication has led to cyanobacterial harmful algal blooms, dominated by non-$N_2$ fixing *Planktothrix*, that persist year-round, including in winter months. In summer 2020 and 2021, multiple treatments using P-binding agents within a 3.5 ha swimming enclosure were conducted to remove excess dissolved P from the water column. The objective of this study was to examine pre-and-post treatment biogeochemical and physicochemical conditions in contrast to the surrounding lake, in addition to evaluating anomalous conditions that led to removal of the lake's no-contact advisory for the first time in 12 years. In four out of five treatments across both years, total P and chlorophyll-a (chl-a) values were higher three weeks post-treatment within the treated area, indicating failures of the treatments to reduce biomass long-term. The harsh winter of 2020-2021, along with a dry Spring 2021, led to large, temporary reductions in algal biomass and toxicity and sediment oxygen demand, and allowed for denitrifying bacteria to remove excess N from the water column. However, chl-a levels returned to > 300 μg $L^{-1}$ by July 2021. This study, along with previous studies regarding failures of treatments using P-

binding agents to reduce algal biomass and toxicity long-term, provide further evidence that reducing watershed N and P loads is likely the only long-term solution to mitigating eutrophication and cyanobacteria blooms in GLSM.

# TABLE OF CONTENTS

# LIST OF FIGURES

# LIST OF TABLES

# ACKNOWLEDGEMENTS

I would like to thank my advisors, Drs. Silvia Newell and Mark J. McCarthy, first and foremost, for their guidance and teachings in both my undergraduate and graduate careers. More importantly, I am extremely grateful for their understanding and patience during these tumultuous years that I have been working on my master's degree. They never gave up on me, pushed me to complete my thesis, and went above and beyond their duties as advisors. I certainly could not have finished my master's degree without them, both intellectually and resolutely.

Next, I must thank my other committee member, Dr. Stephen Jacquemin. Dr. Jacquemin has conducted extensive research on GLSM that is vital to reaching a solution to the HAB issue. His weekly data series on the lake was invaluable for my thesis as he provided a sampling resolution that would not have been feasible otherwise, and closed gaps in my records that provided key insights. Additionally, our collection methods would have been far more difficult without the availability of the pontoon boat and dock, along with his laboratory at the Wright State – Lake Campus.

Our laboratory manager, Justin Myers, deserves high praise for continuously being the "go-to-man" and savior for many graduate students in the lab. While completing his own master's degree, Justin was able to partake in nearly all my sampling trips, assisting in the field collection, laboratory setup, and instrument analysis. There is

no doubt that I could not have completed this thesis without his assistance in all areas, especially the organization and analysis of a substantial number of samples.

Additionally, I need to thank a vast number of undergraduate, graduate, and former Newell laboratory colleagues that helped at various times during my sample collection and analysis: Laboratory members - Rufaro Bulathsinghalage, Liam Garry, John Hughes, Marinda Vanhoose, and Dante Villarreal; Graduate colleagues - Marie Bezold, Marissa Despins, Kishan Gomez, and Kayla Gonzalez-Boy; Former Newell laboratory colleagues – Ashlynn Boedecker, Shannon Collins, and Daniel Hoffman. Due to the culture of cooperation created in the Newell laboratory, all of these people (and likely more) had a hand in collecting, organization, and analyzing my data.

Lastly, I need to thank the institutions that made this thesis possible. During my undergraduate and graduate career, Wright State University offered an affordable education with a vast number of opportunities for research that led me to the master's program. The Ohio Sea Grant College Program provided nearly all the funding to complete my thesis. The West Rock Scholar Program awarded me with a $10,000 scholarship to gather substantial supplies for collection and analysis. I had the honor of sharing my research at the 10$^{th}$ annual Shallow Lakes Conference and the 2021 Lahti Lakes Symposium. Finally, Aaron Roerdink and Nancy Miller at the National Center for Water Quality Research at Heidelberg University provided invaluable data for nutrient loading into GLSM that allowed for key insights.

# I. INTRODUCTION

## *i. Global Increases in Eutrophication*

Eutrophication, the overabundance of organic matter (often algal biomass) due to excess nutrient inputs, primarily nitrogen (N) and phosphorus (P), is one of the most prevalent and concerning water quality issues globally. Excess nutrients are a catalyst for algal bloom proliferation, which alters natural ecosystem function, reduces ecosystem services and overall water quality, increases algal toxin production, and has created a combined cost of $2.2-4.6 billion annually for U.S. freshwaters (Treuer et al., 2021). Surpluses of N and P from agricultural soils increased four-fold globally between 1950 and 2000 and are expected to increase in the future (Hamilton et al., 2016). Reactive N is biologically active and chemically reactive, and reactive N fluxes have increased tenfold over the past century (Byrnes et al., 2020; U.S. Environmental Protection Agency, 2011). This increase in reactive N is primarily due to the development and commercialization of the Haber-Bosch process, allowing nitrogen fixation (N-fixation), the conversion of inert atmospheric $N_2$ to $NH_4^+$, on an industrial scale to enrich soils with N fertilizers (Byrnes et al., 2020; Glibert et al., 2014; Hamilton et al., 2016; U.S. Environmental Protection Agency, 2011). Phosphate usage shows a similar trend, as P minerals have been increasingly mined and utilized for P-containing fertilizers, which are then applied at substantial rates – even in soils with adequate P concentrations (Glibert, 2017; Smith et al., 1999). The widespread use of N and P has contributed to their accumulation in surface and

coastal waters, especially when best nutrient management practices for fertilizer application are not followed.

In addition to synthetic fertilizers, manure applications, inadequate wastewater treatment processing, and atmospheric N deposition combine to alter N and P biogeochemical cycling and contribute to eutrophication globally (Glibert, 2017; Smith et al., 1999). Recurring algal blooms have been noted in many of the world's largest inland freshwater lakes, including Lake Victoria (Africa), Lake Erie and Lake Michigan (North American Great Lakes), and Lake Taihu (China; Paerl & Otten, 2013). These freshwater lakes are crucial drinking water resources for millions of people; however, eutrophication has led to harmful algal blooms (HABs), hypoxic conditions in bottom water, reduced recreational opportunities, and declines in near-shore property values in these systems.

*ii. cHABs Produced by Non-diazotrophic Cyanobacteria*

One of the more immediate impacts of eutrophication is often the development and proliferation of cyanobacterial harmful algal blooms (cHABs). Cyanobacteria (formerly blue-green algae) include many species capable of producing toxins, such as the hepatotoxin, microcystin, which can cause acute toxicity in aquatic and terrestrial species (Paerl & Otten, 2013). This algal group has a long and successful evolutionary history (~3.5 billion years), displaying its ability to adapt and outcompete other algal species over time (Paerl & Otten, 2013). Cyanobacteria often have physiological characteristics (e.g., enhanced nutrient uptake strategies, high productivity at elevated temperatures, buoyancy control, etc.) that provide competitive advantages under anthropogenic disturbances (e.g., increased nutrient loading, climate change, etc.; Hamilton et al., 2016; Paerl & Otten, 2013; Paerl & Paul, 2012). These

advantages have contributed to cyanobacterial proliferation in the latter half of the 20th and early 21st century in many large lake ecosystems.

Non-diazotrophic cyanobacteria (non-$N_2$-fixing species) have increased dramatically during this time, although past work suggests that diazotrophs, or $N_2$-fixing species, should hold a competitive advantage in historically N-depleted systems (Conley et al., 2009; Hamilton et al., 2016; Paerl & Otten, 2013; Steffen et al., 2014). Previous dogma suggested that P controls productivity in freshwater ecosystems and that reducing N inputs would not reduce eutrophication and cHABs (Schindler, 2012; Schindler et al., 2008). However, in a single system, there can be a shift from P-control throughout the winter months to N-control at the peak of the bloom season in summer and fall, with dual control of N and P present throughout the year (Paerl et al., 2011). Additionally, in many systems, N and P loads are so high that, even when P is targeted, enough N and P remain to support non-N fixers (Hoffman et al., 2022; Jacquemin et al., 2023).

*iii. Paradigm Shift: Dual-nutrient Management*

Based on whole-lake experiments with P (and carbon) fertilization, and legacy N stores from previous N fertilization, it was assumed that N-fixation by diazotrophs could balance N losses from denitrification, sediment burial, washout, etc. (Schindler, 2012; Schindler et al., 2008). However, more recent studies showed that cyanobacteria relying on energetically costly N-fixation do not offset these N losses on timescales relevant for eutrophication management, and thus still rely on external and internal N sources (Scott & McCarthy, 2010, 2011). Additionally, empirical and modeled evidence showed that eutrophic and hypereutrophic systems become increasingly N-depleted over time due to higher denitrification:N-fixation ratios, with many of these systems dominated by toxic, non-$N_2$-fixing cyanobacterial species (Paerl et al., 2020; Scott

et al., 2019). Therefore, a paradigm shift has occurred, calling for dual nutrient (N & P) management, especially for systems dominated by toxic, non-$N_2$-fixing cyanobacterial species that rely on external and internal N loads to produce biomass and N-rich toxins.

*iv. Reduced N Forms Increasing Toxicity*

Increases in external N loading, especially highly bioavailable, chemically reduced forms of N (urea, $NH_4^+$, and some dissolved organic N (DON)), have created an environment favorable for non-$N_2$-fixing, toxic cyanobacteria, even in N-depleted systems (Hampel et al., 2019; McCarthy, et al., 2013; Newell et al., 2019). This favorable environment is partially a result of the global shift to nitrogenous fertilizers containing $NH_4^+$ and urea, where worldwide use of urea has increased 100-fold and now accounts for ~90% of all N fertilizer in the United States (Glibert et al., 2006). Urea is produced through the Wöhler process, where silver cyanate and ammonia are combined. Urea can be hydrolyzed and become an additional source of $NH_4^+$ for cHABs (Glibert et al., 2016; Solomon et al., 2010). $NH_4^+$ is the preferred N source for primary producers, including non-$N_2$-fixing cyanobacteria, as it requires the least amount of energy to assimilate, and cyanobacteria have superior $NH_4^+$ assimilation capabilities compared to eukaryotes (Gobler et al., 2016; Harke et al., 2016; Monchamp et al., 2014).

Chemically reduced N forms are crucial for microcystin production, since each microcystin-LR molecule, the most ubiquitous microcystin variant, requires at least 10 N atoms ($C_{49}H_{74}N_{10}O_{12}$; Paerl et al., 2020). Reduced N forms enhance toxic cyanobacterial strains more frequently than inorganic P and oxidized N, with reduced N also stimulating overall cyanobacterial populations more frequently than P (Davis et al., 2010, 2015). cHABs in western Lake Erie upregulate *mcyD* gene transcripts during $NH_4^+$ and urea laboratory enrichments, and there was a positive correlation between the microcystin:chl-a ratio and dissolved inorganic N

concentrations during bloom periods (Chaffin et al., 2018, 2021). Overall, total N (TN) concentrations and temperature are the best predictors of cyanobacterial biomass and toxin quotas in lakes, along nearly all trophic gradients (i.e., mesotrophic, eutrophic, hypereutrophic; e.g., Gobler et al., 2016; Harke et al., 2016).

*v. N and P Nutrient Cycling*

Mitigating cHABs requires understanding of internal nutrient cycling (both N and P) in aquatic systems, including internal loads, dominant chemical form, biological and chemical transformations, and potential removal pathways. Both N and P enter aquatic systems via allochthonous sources (e.g., agricultural runoff and treated sewage discharge) or autochthonous sources (e.g., remineralization and resuspension) and contribute to cHAB formation (Heisler et al., 2008; Paerl et al., 2020; Smith et al., 1999). Unlike P, however, which is primarily retained in sediments as legacy stores (unless released during remineralization or anoxic events) or assimilated into biomass, N cycling has many forms and transformation pathways depending on chemical and biological conditions (Paerl et al., 2020). Pathways for N cycling include sources (external loading, atmospheric deposition, and N-fixation), sinks (denitrification or anammox, sediment burial, or export downstream) and links (nitrification $NH_4^+ \rightarrow NO_3^-$; dissimilatory $NO_3^-$ reduction to $NH_4^+$ [DNRA; $NO_3^- \rightarrow NH_4^+$], and organic matter remineralization to $NH_4^+$; An & Gardner, 2002; McCarthy et al., 2007). Denitrification is the stepwise reduction of nitrate ($NO_3^-$) to $N_2$ gas performed by facultative anaerobes during organic matter decomposition (heterotrophic), while anammox (anaerobic ammonium oxidation; [$NH_4^+ + NO_2^- \rightarrow N_2$]) is autotrophic and typically does not represent a large proportion of $N_2$ production in lakes (e.g., Boedecker et al. 2020).

A potentially important N source in lakes is N-fixation, which converts atmospheric $N_2$ gas into $NH_4^+$ and is performed by diazotrophic algal species and bacteria (Canfield et al., 2010). As mentioned previously, N-fixation is energetically costly and requires 16 ATP molecules per molecule of fixed $N_2$ to break the $N_2$ triple bond (Canfield et al., 2010). Cyanobacterial N-fixation usually occurs when inorganic N pools become exhausted, and a low N:P ratio results in N imbalance relative to P (Scott & McCarthy, 2010).

Removal pathways (sinks) for N in lakes include denitrification and anammox. Denitrification occurs anaerobically, when $NO_3^-$ acts as the terminal electron acceptor, and is converted stepwise into nitrite ($NO_2^-$), nitric oxide (NO), nitrous oxide ($N_2O$), and then $N_2$ gas (Burgin & Hamilton, 2007) Anammox is also an anaerobic pathway that utilizes $NO_2^-$, potentially contributed by denitrifying bacteria (Burgin & Hamilton, 2007), to oxidize $NH_4^+$ and form $N_2$ (McCarthy et al., 2016). Since $N_2$ is not bioavailable for most organisms, conversion to $N_2$ is considered permanent removal of N from the system (Burgin & Hamilton, 2007; Scott et al., 2008). Denitrification is more broadly studied and the primary removal pathway for N in freshwater systems; however, anammox may have contributed up to 30% of N removal from a eutrophic lake (McCarthy et al., 2016). The natural removal of N from an aquatic system is key for mitigating eutrophication in systems with high external or internal N loads and represents a valuable ecosystem service (Boedecker et al., 2020).

In eutrophic systems, denitrification is usually enhanced due to the respiration of organic algal material by bacteria and detritivores, leading to hypoxia/anoxia in sediments and overlying water in contact with the sediment surface (Zhu et al., 2020). However, in hypereutrophic systems, including shallow lakes that experience $O_2$ replenishment with wind and wave action, algal accumulation may inhibit denitrification by disrupting nitrification-denitrification coupling

(Zhu et al., 2020). Nitrification converts $NH_4^+$ to $NO_3^-$, supplying $NO_3^-$ to denitrifying bacteria; however, nitrification is an aerobic process, and high respiration rates in hypereutrophic systems can lead to bottom-water hypoxia, decoupling the nitrification-denitrification link (Zhu et al., 2020).

Organic matter remineralization and DNRA are two key N links, providing an internal supply of $NH_4^+$ for primary producers, including cyanobacteria. Both pathways involve the reduction of oxidized N forms ($NO_3^-$ and $NO_2^-$) to $NH_4^+$; however, DNRA occurs in anoxic environments, while respiration (process for organic matter remineralization) is usually an aerobic process (Burgin & Hamilton, 2007). DNRA is an understudied component of the N cycle in freshwater systems, but it is thought to occur in $NO_3^-$ limited systems replete with organic matter (Burgin & Hamilton, 2007). While these pathways provide an additional source of $NH_4^+$, it is difficult to determine $NH_4^+$ availability within the water column due to high biological demand for $NH_4^+$ and rapid turnover rates (Gardner et al., 2017; McCarthy et al., 2013).

*vi. Internal $NH_4^+$ Cycling Sustaining Blooms*

Once N is discharged into aquatic systems, rapid internal $NH_4^+$ cycling allows cHABs to sustain themselves, even during periods of inorganic N depletion and low external N loading (Hampel et al., 2019; McCarthy et al., 2016; McCarthy et al., 2013; Paerl et al., 2011). For example, over three summer months, $NH_4^+$ regeneration rates in Sandusky Bay, Lake Erie, were equivalent to ~77% of the annual, external N load, supporting 36–50% of potential photic $NH_4^+$ uptake (Hampel et al., 2019). In Lake Taihu, China, $NH_4^+$ regeneration rates were about 400% of the annual N loading into the lake (Paerl et al., 2011). Similar results were observed in Missisquoi Bay, Lake Champlain (USA and Canada), where $NH_4^+$ regeneration rates equated to nearly twice the external N load (McCarthy et al., 2013). These $NH_4^+$ regeneration rates can

support cHABs during the bloom season; however, some organic matter will eventually sink to and become buried in the sediments, contributing to legacy N stores and potential internal $NH_4^+$ loading in the future (McCarthy et al., 2016).

*vii. Bloom Formation in Shallow Lake Systems*

In shallow systems, the exchange of nutrients between sediments and overlying water, (benthic-pelagic coupling) is an important factor for understanding eutrophication and developing management strategies (Griffiths et al., 2017). Inorganic N and P are assimilated into biomass, transported to the benthos, and then remineralized within or near the sediment-water interface (SWI; Baustian et al., 2014), although some remineralization can also occur in the water column (McCarthy et al., 2013). In eutrophic or hypereutrophic systems, this remineralization/respiration process can lead to high rates of water column oxygen demand (WCOD) and sediment oxygen demand (SOD), potentially resulting in hypoxic bottom waters (Gardner et al., 2009).

Oxygen controls the redox gradient and is thus the primary control for inorganic nutrient fluxes across the SWI (Baustian et al., 2014). Under oxic conditions, phosphate ($PO_4^{3-}$) adsorbs to sinking sediment particles (i.e., complex with iron or aluminum) and accumulates a P reservoir within the sediments. These complexes prevent P release under oxic conditions (Baustian et al., 2014). However, under anoxic conditions, similar to those noticed in peak bloom conditions during summer months, $PO_4^{3-}$ can be released into the water column, providing bioavailable P substrate for algal growth (Baustian et al., 2014).

$NH_4^+$ displays a similar pattern of release under anoxic conditions, which can fuel toxic strains of cyanobacteria and contribute to the bioavailable inorganic N pool (Gardner et al., 2017). Under anoxic conditions, $NH_4^+$ conversion to $NO_3^-$ via nitrification will not occur, which

subsequently prevents denitrification from removing excess N, especially during periods of $NO_3^-$ depletion due to high HAB biomass. Excess $NH_4^+$ will be released into the water column, where toxic strains of cyanobacteria are able to outcompete nitrifiers. The excess $NH_4^+$ will be rapidly recycled by the cyanobacteria, sustaining HAB biomass and toxin production, while providing more detritus for bacteria to consume oxygen further (Gardner et al., 2017). HAB biomass tends to increase faster than $NH_4^+$ turnover rates, leading to high demand for $NH_4^+$, providing evidence that the internal recycling of this reduced N form is critical for HAB biomass, and mitigating this recycling is vital for eutrophication management (Gardner et al., 2017).

*viii. Importance of GLSM and Previous Treatments*

Chemical alterations to remove these excess nutrients, mainly P, have become prevalent short–term solutions to eutrophication due to practical and economic limitations that hinder long-term methods for reducing nutrient inputs (e.g., restoring natural wetlands, reducing external nutrient loading with best management practices, etc.; Jančula & MarŠálek, 2011; Nogaro et al., 2013). P-binding chemical treatments, such as aluminum sulfate (alum), are popular for removing P from the water column because it complexes with dissolved P and forms floccules that sink to the sediments, rendering them non–bioavailable (Jančula & MarŠálek, 2011; Nogaro et al., 2013). Additionally, these floccules provide a temporary "cap" on the sediments to prevent P release (Jančula & MarŠálek, 2011; Nogaro et al., 2013). While effects of these treatments on P have been well observed, changes in N dynamics during these treatments, and the subsequent impact on cHABs, are not well understood.

Throughout the previous decade (2010-2020), Grand Lake St. Marys (GLSM; Ohio, USA) has experienced recurring cHABs, resulting in overall reductions in lake water quality and recreational value (Jacquemin et al., 2018; Steffen et al., 2014; Wolf & Klaiber, 2017). These

blooms are prevalent due to high external nutrient loads (90th percentile for total N and P concentrations in the USA) from a watershed dominated by agricultural row–crops and livestock production (Figure 1; Hoorman et al., 2008; Jacquemin et al., 2018; OEPA, 2007). GLSM is the largest (52 $km^2$) inland lake in Ohio, USA; however, with a shallow average depth (~1.5-m), nutrient levels can amplify quickly, intensifying eutrophication (Jacquemin et al., 2018). These cHABs persist year–round, including in winter months (e.g., winter 2019-2020; Jacquemin et al., unpublished data), and are dominated by *Planktothrix*, a non-$N_2$-fixing, filamentous algae known to produce microcystin (Steffen et al., 2014). However, at the peak of the annual bloom, another non-$N_2$-fixer, *Microcystis spp.*, has also been observed, often coinciding with highest toxin measurements (Steffen et al., 2014). Total microcystin levels for GLSM are in the $99^{th}$ percentile for the USA, leading to annual "no contact" warnings and watershed-wide "distressed" labels (Jacquemin et al., 2018; Steffen et al., 2012; U.S. Environmental Protection Agency, 2009).

GLSM is a drinking water resource for the city of Celina (population 10,400) and a recreational resource that, in some years, has been valued at US$150 million (Davenport & Drake, 2011; Steffen et al., 2014). Considering its importance to local communities, multiple approaches have been attempted to mitigate the recurring cHABs, such as reducing external nutrient loading, linear aeration, reducing internal loading of accumulated P in the sediment, sediment dredging, and chemical applications, with no long term success (Jacquemin et al., 2018; Nogaro et al., 2013; Steffen et al., 2014). The latest attempts were made within Dog Tale Lake (West Beach), a newly constructed swimming enclosure (32,500 $m^2$) located in the northeastern portion of GLSM (Figure 2). Alum was applied to the enclosure in June 2020, followed by multiple Phoslock (bentonite clay) and SeClear (algaecide) applications in May-July 2021.

Following an alum treatment in the main lake in 2011, undesirable effects on nutrient cycling were observed, while failing to prevent subsequent cHABs (Nogaro et al., 2013). Treated sediments were a source of highly bioavailable $NH_4^+$, potentially enhancing bloom toxicity and providing bioavailable N in a historically N-depleted system (Nogaro et al., 2013; Steffen et al., 2014). Additionally, the study noted an increase in $N_2O$ production ($N_2O$ is a potent greenhouse gas) and a decrease in $N_2$ production (Nogaro et al., 2013). These measurements indicated that denitrification was inhibited within the treated areas, reducing natural N removal from the system (Nogaro et al., 2013). Alum applications may decrease natural denitrification by increasing concentrations of free sulfides, which can block nitrification and the final step of denitrification, thus favoring DNRA and enhancing $NH_4^+$ availability, instead of releasing $N_2O$ or $N_2$ (Burgin & Hamilton, 2007; Nogaro et al., 2013). While these chemical applications have been utilized for decades to reduce P concentrations and cyanobacterial biomass, their unintended consequences on N cycling reduce their effectiveness in GLSM and could enhance bloom toxicity.

*ix. Objective of Current Study*

The objective of this study was to evaluate the effects of these chemical treatments on nutrient dynamics and determine whether the role of SWI nutrient fluxes promoted (via release of bioavailable N and P) or mitigated (N removal via denitrification) cHAB biomass and toxicity within the West Beach enclosure. Additionally, upon further evaluation from collected data, the study also evaluated the onset of the cHAB bloom from year to year to determine potential reasons for the bloom delay in 2021. The following hypotheses were addressed in this study:

(1) Alum and Phoslock/SeClear applications in the enclosure will reduce ambient P concentrations and chlorophyll *a* concentrations compared to the main lake.

(2) Denitrification will be the primary N removal pathway; however, it may be inhibited by alum and Phoslock applications and bottom water hypoxia during peak cHABs.

(3) GLSM sediments will be a source of $NH_4^+$ and P into the water column, with enhanced release of $NH_4^+$ in treated sediments.

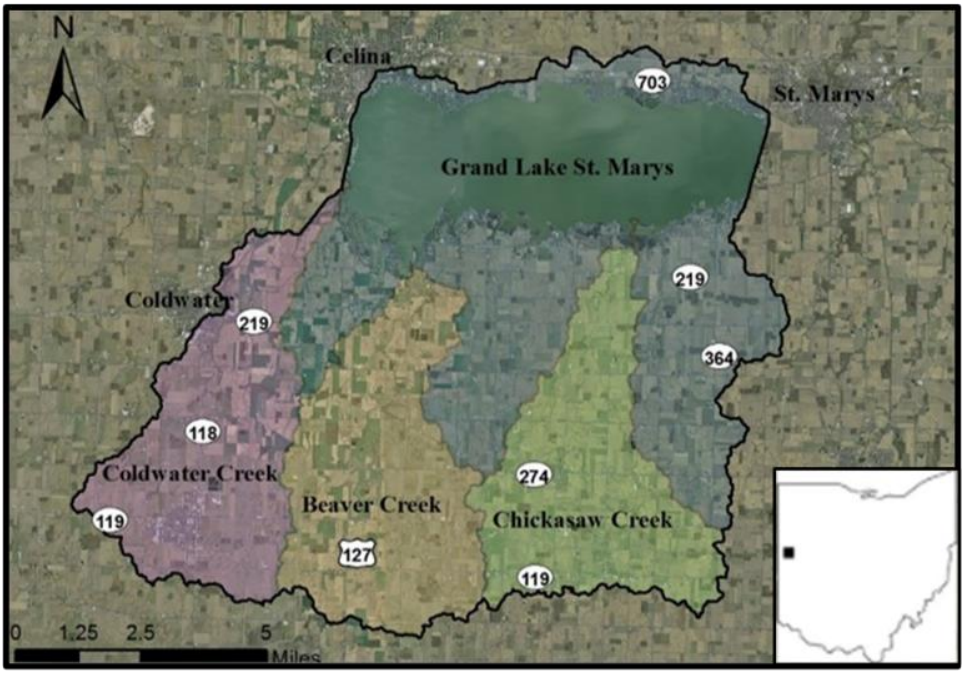


*Figure 1: Grand Lake St. Marys Watershed. (Modified from Stephen Jacquemin/ Grand Lake St. Marys Water Quality Update – September 2020).*

# II. METHODS

## *i. Field Location*

Water and sediment samples were collected from Grand Lake St. Marys from April 2020 through July 2021. The sampling locations were in the northeastern portion of Grand Lake St. Marys near the village of Villa Nova and the town of St. Mary's (USA; Fig. 4). Samples were collected from a site known locally as Dog Tale Lake, which was renamed as the West Beach Enclosure for the purpose of this study. The West Beach Enclosure is roughly 3.25 ha (0.0325 $km^2$) with an average sampled depth of 0.93 m and a maximum sampled depth of 1.51 m. Alterations were made by the Ohio Department of Natural Resources (ODNR) in previous years to slow the exchange of water between the lake and swimming enclosure. Approximately half of the enclosure area was dredged to remove nutrient-rich sediment and replaced with a new sand base. The rock berm was extended by 400 ft (191.9 m), a 50-ft (15.2 m) air curtain was installed, and ~20 aerators were placed throughout the enclosure.

## *ii. P-binding treatments*

The initial alum treatment was conducted on June 9$^{th}$, 2020, where 5,200 lbs. (2358.7 kg) was applied to the West Beach Enclosure (Table 1). Additional treatments did not occur until the summer of 2021. A combination of Phoslock and SeClear were applied every 3-4 weeks from May-July 2021 (Table 1). SeClear was always applied with 250lbs. (113.4kg), and Phoslock was applied at 1,000 lbs. (453.6kg), except for June 11$^{th}$, 2021, where 1,650 lbs. (748.4 kg) were applied.

*Table 1: Application dates and dosages (kg) for alum, SeClear, and Phoslock applications in 2020 and 2021.*

| Date | Alum Application | SeClear Application | Phoslock Application |
|---|---|---|---|
| | kg | | |
| 06/09/2020 | 2358.7 | -- | -- |
| 05/13/2021 | -- | 113.4 | 453.6 |
| 06/11/2021 | -- | 113.4 | 748.4 |
| 07/02/2021 | -- | 113.4 | -- |
| 07/23/2021 | -- | 113.4 | 453.6 |

*iii. Sample Collection*

Water samples and sediment cores were collected from within and directly outside the West Beach Enclosure (Figures 2, 3, & 4). Samples were collected approximately monthly from April to November 2020 and February to July 2021 (15 total sampling events).

Weekly measurements of algal biomass, total microcystin toxins, and total P (TP) concentrations were collected throughout this period, along with water samples for measuring dissolved nutrients, including $NO_3^-$, $NO_2^-$, $NH_4^+$, o-$PO_4^{3-}$, and urea (Tables 3 & 4). Nutrient samples were filtered immediately upon collection through Fisher Scientific Target2 0.22 µm syringe filters (Nylon) into 16 mL Karter Scientific polypropylene test tubes (~12-12.5 mL), transported back to the lab on ice (0-4 °C) and in the dark, and frozen at -20 °C (Tables 5 & 6).

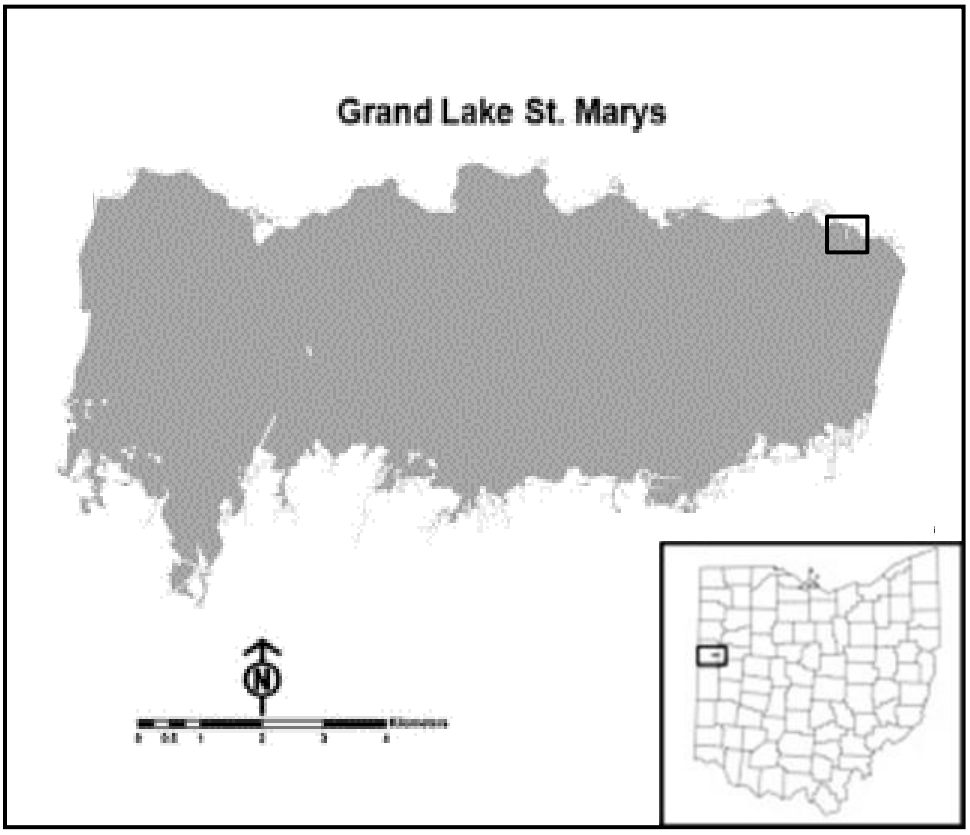


*Figure 2: Silhouette of Grand Lake St. Marys with West Beach Enclosure outlined in black and location in Ohio, USA. (Modified from Steffen et al., 2014).*

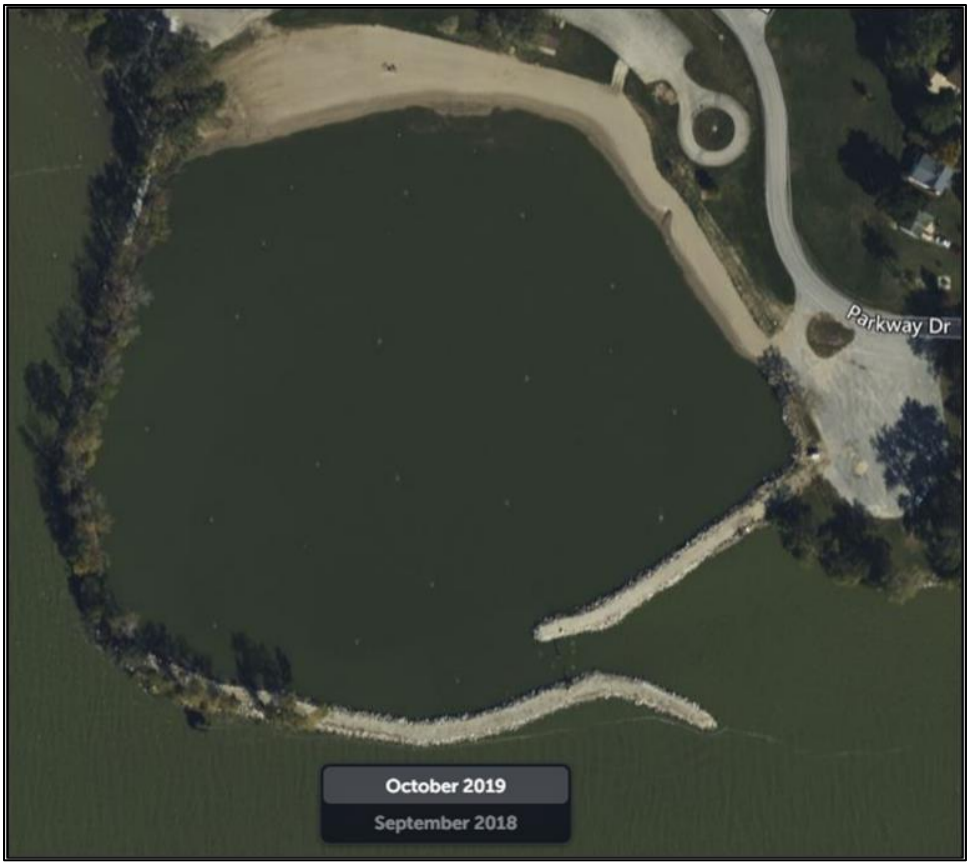


*Figure 3: Updated satellite imagery of West Beach Enclosure following ODNR changes. (Generated within Google Earth Pro v7.3.4).*


*Figure 4: Sampling site locations within the enclosure and the surrounding lake. (Generated within Google Earth Pro v7.3.4).*

*iv. Water Column Respiration Incubations*

Six water samples were collected from each site, with three samples preserved immediately with 200 µL 50% (w/w) $ZnCl_2$. All samples were wrapped twice in aluminum foil to eliminate light exposure and incubated in a nearby pond for ~24 h. After the incubation period, the other three samples were preserved with 200 µL 50% $ZnCl_2$. These samples were then analyzed using Membrane Inlet Mass Spectrometry (MIMS) to determine differences in $O_2$ concentrations and respiration rates.

*v. Physicochemical Parameters*

A Eureka Manta 2 sonde was used to measure temperature, depth, dissolved oxygen (DO) concentration, pH, specific conductance, chlorophyll *a* fluorescence, and cyanobacterial cell density (Tables 3 & 4). A BBE Moldaenke Algae Torch provided additional chlorophyll *a* and phycocyanin pigment (cyanobacteria) concentrations (Tables 3 & 4).

*vi. Sediment Core Incubations*

For each site, six intact sediment cores with overlying water were collected in acrylic core tubes (30 cm length, 7.6 cm diameter) using a PVC pole corer modified from a sediment coring lander (Gardner et al. 2009; Figure 5). Sixty liters of near-bottom water were collected from each sampling site to serve as inflow reservoirs for continuous-flow incubations (e.g., McCarthy et al. 2016). The cores were immediately capped and placed in the dark for transport to the lab at Wright State University (WSU). Overlying water was decanted gently, ensuring not to disturb the SWI, until ~10 cm of overlying water remained. An air- and water-tight plunger (Delrin) containing inflow and outflow tubes (gastight PEEK) was slowly pushed into the sediment core tubes until the inflow tubing was ~1 cm above the sediment surface (Figure 5). Cores were wrapped with aluminum foil to exclude light effects. Peristaltic pumps supplied aerated bottom

water at ~1.25 - 1.5 mL $min^{-1}$ to the overlying water of each intact core (system retention time ~2-3 h). After a pre-incubation period (~12+ h) to re-establish steady-state conditions, sediment cores were incubated over 72 h. Nutrient and dissolved gas samples were collected daily, and near-simultaneously, from inflow reservoirs and core outflows. Nutrient samples were filtered through 0.22 µm syringe filters and immediately frozen. Dissolved gas samples were immediately analyzed when feasible; however, from April to August 2020 and November 2020, dissolved gas samples were preserved with 200 µL 50% $ZnCl_2$ and analyzed within two weeks.

Duplicate intact sediment cores for each site received ~20 µM $^{15}NH_4^+$, ~100 µM $^{15}NO_3^-$, or unamended bottom water. Immediately after isotope addition, nutrient samples were collected from the bottom water reservoirs to verify spike amounts. Unamended cores were used to determine net $^{28}N_2$, $O_2$, and nutrient fluxes. The $^{15}NH_4^+$ (A) cores were used to determine possible anaerobic $NH_4^+$ oxidation (anammox). Note that the incubation system used here maintains near in situ redox conditions, which allows nitrification to proceed and prevents conclusive determination of anammox, as opposed to coupled nitrification-denitrification (e.g., Hoffman et al. 2019). $^{15}NO_3^-$ (N) cores were used to estimate potential denitrification and dissimilatory nitrate reduction to ammonium (DNRA) rates, as well as N-fixation occurring simultaneously with denitrification (An et al. 2001; McCarthy et al. 2016).

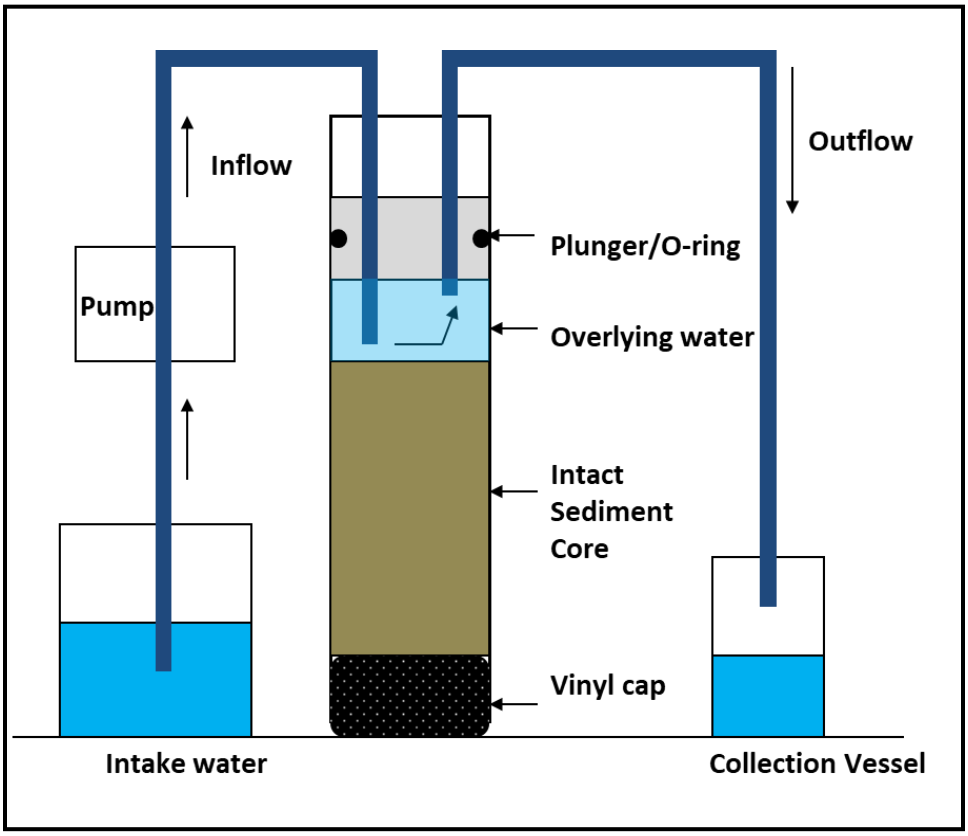


*Figure 5: Schematic diagram of continuous-flow sediment core incubation system. (Adapted from Lavrentyev et al., 2000).*

*vii. Dissolved Gases*

Dissolved gases ($O_2$, $^{28}N_2$, $^{29}N_2$, $^{30}N_2$) were measured using MIMS (Kana et al., 1994). Inflow and outflow samples were collected and analyzed daily over a three-day incubation period. Outflow samples were collected in tall, glass tubes (low surface area-to-volume ratio) after allowing the sample to overflow the tube multiple times (>15 min). These samples were analyzed immediately, when possible, to avoid atmospheric contamination. When samples were unable to be analyzed immediately, they were preserved with 200 µl 50% ZnCl2 (w/w), capped with ground glass stoppers, and submerged in water until analysis. Inflow samples were collected in identical tubes after transferring the sample from the inflow reservoir using a 60-mL syringe. These samples were also analyzed immediately when feasible. Preserved respiration samples were typically analyzed the day after completing the 24-h incubation.

*viii. Dissolved Nutrients*

Nutrient samples were analyzed using colorimetric flow injection analysis (FIA) on a Lachat Quikchem 8500 using methods for low-ammonia ($NH_3$-N), high-ammonia ($NH_3$-N), ortho-phosphate (ortho-P), nitrate + nitrite ($NO_x$), and urea (N as urea; Table 2). Two methods (QuikChem® methods 31-107-06-1-F & 31-107-06-1-G) for $NH_3$-N were utilized to cover a wider applicable concentration range. Both methods are based on the Berthelot reaction, where ammonia reacts with alkaline phenol and sodium hypochlorite to form indophenol blue, with sodium nitroprusside added for enhanced sensitivity. The absorbance was measured at 630 nm, and the standards were made using $NH_4Cl$ (0, 0.1, 0.25, 0.,75, 1.5, 2.5, 5, 10, and 25 µM). The ortho-P method (QuikChem® method 31-115-01-1-I) relies on the reaction between $NH_4^+$ molybdate and antimony potassium tartrate in an acid medium with phosphate, which forms a complex that produces a blue color. The absorbance was measured at 880 nm, and the standards

were made using potassium phosphate (0, 0.03, 0.1, 0.5, 1, 2, 5, and 10 µM). $NO_x$ analysis (QuikChem® method 31-107-04-1-E) occurred on two separate Lachat columns, one measuring $NO_2^-$ only, and the other measuring both $NO_3^-$ and $NO_2^-$ by reducing the $NO_3^-$ to $NO_2^-$ using a granulated copper-cadmium column. Thus, total $NO_x$ and $NO_2^-$ were measured, and $[NO_3^-]$ was determined as $[NO_x] – [NO_2]$. The absorbance was measured at 540 nm, and the standards were prepared using $NaNO_2$ (0, 0.1, 0.25, 0.5, 1, 5, 10, 20, and 40 µM). The urea method (QuikChem® method 31-206-1-A) hydrolyzes diacetyl monoxime in an acidic solution to diacetyl, which reacts with urea present in the sample when acidic ferric ions are present. Thiosemicarbazide is added to increase the color intensity. The absorbance is measured at 530 nm, and the standards were prepared using 1 mM Urea-N (0, 0.25, 0.37, 0.75, 1.0, 2.5, 5.0, 10.0, and 20.0 µM).

*Table 2: Lachat Quikchem 8500 Analysis Methods and Detection Limits. Applicable ranges and detection limits were obtained from manufacturer operating manuals.*

| Analyte | Lachat Method | Applicable Range | Detection Limit | Standard Range |
|---|---|---|---|---|
| | | | (µM N or P) | |
| Low-Ammonia | 31-107-06-1-G | 0.09 – 7.14 | 0.03 | 0 – 25 |
| High-Ammonia | 31-107-06-1-F | 0.36 – 143 | 0.19 | 0 – 25 |
| Ortho-Phosphate | 31-115-01-1-I | 0.03 – 3.23 | 0.01 | 0 – 10 |
| $NO_x$ | 31-107-04-1-E* | 0.36 – 28.57 | 0.04 | 0 – 40 |
| Urea | 31-206-1-A | 0.71 – 28.57 | 0.21 | 0 – 20 |

*Nitrite-only run simultaneously with NOx on a separate channel with no Cd column for total nitrite. $[NO_3^-] = [NO_x] – [NO_2]$

*ix. Statistics*

Monthly precipitation records were provided by the United States Geological Survey (USGS) for the rain gauge near the Great Miami River in Sidney, OH (03261500), which is roughly 48.3 km southeast of GLSM (Figure 8). Nutrient loading data from Chickasaw Creek were provided by the National Center for Water Quality Research at Heidelberg University (Figure 9). All figures for these data were generated using the ggplot2 (Wickham 2009) package in R (version 4.0.4, R Core Team). Comparisons between years were performed using a paired two-way analysis of variance (ANOVA).

# III. RESULTS

## *i. Treatment effects on chl-a and total P values*

Pre-and-post treatment results for each of the five P-binding treatments are shown in Figure 7. For all five P-binding treatments within the enclosure, average TP concentrations were higher three weeks post-treatment (Figure 7). In most applications, TP concentrations dropped immediately after treatment; however, concentrations rebounded within the subsequent weeks. In four out of five P-binding treatments, average chl-a values increased three weeks post-treatment (Figure 6). Similarly, and potentially related to TP concentrations, average chl-a values had an immediate reduction, followed by an increase in subsequent weeks.

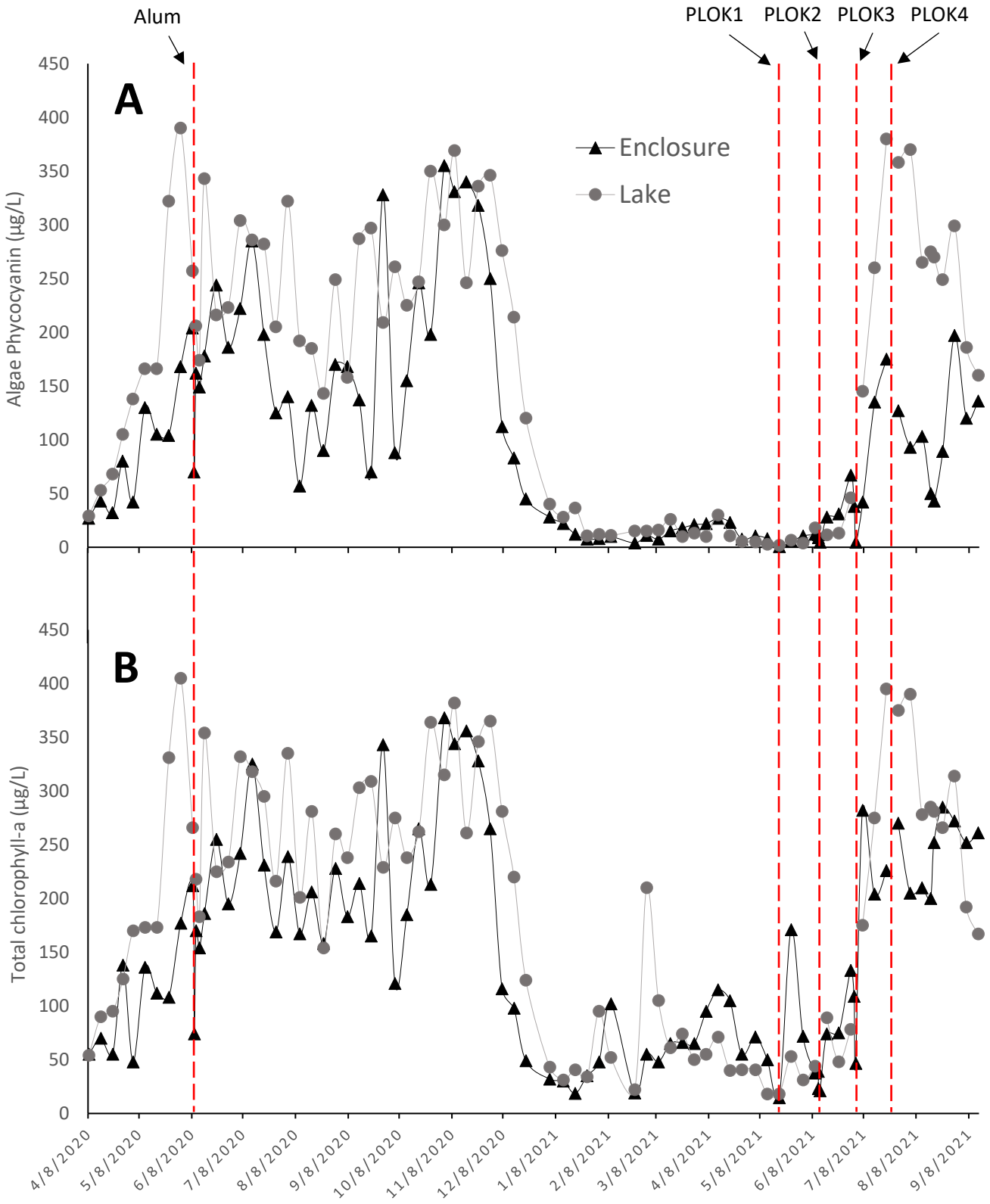


*Figure 6: Algal biomass throughout the entire sampling period. (A) phycocyanin levels, and (B) total chlorophyll-a levels.*

For the initial alum treatment in June 2020, there were no differences in any key indicator (i.e., TP, chl-a, phycocyanin, microcystin) that would suggest treatment success. As expected, chl-a values in the enclosure decreased immediately (within a day of treatment) from 212 µg $L^{-1}$ to 74 µg $L^{-1}$. However, average chl-a values changed from 166 ± 30.6 µg $L^{-1}$ pre-treatment to 191 ± 22.2 µg $L^{-1}$ post-treatment. Average TP concentrations also increased in the enclosure from 8.91 ± 1.66 µM pre-treatment to 9.50 ± 0.81 µM post-treatment.

For the first Phoslock treatment (PLOK1; Figure 7) in May 2021, average TP concentrations increased in the enclosure from 2.43 ± 0.15 µM pre-treatment to 3.46 ± 0.17 µM post-treatment (ANOVA; $p = 0.021$). Chl-a values decreased from 50 µg $L^{-1}$ to 14.5 µg $L^{-1}$ immediately following treatment; however, a week later, values increased to 171 µg $L^{-1}$, which is well above the average pre-treatment value of 58.7 ± 6.33 µg $L^{-1}$ (Figure 6) and higher than the chlorophyll concentration in the lake on the same day (53 µg L-1).

Average TP concentrations increased in the enclosure from 3.49 ± 0.16 µM pre-treatment to 6.68 ± 1.67 µM post-treatment (ANOVA; $p = 0.022$) after the second Phoslock treatment (PLOK2; Figure 7) in June 2021. Despite the increase in average TP concentrations, chl-a values were essentially unchanged from 79.8 ± 31.4 µg $L^{-1}$ pre-treatment to 65.2 ± 20.6 µg $L^{-1}$ post-treatment (Figure 6). No differences in physicochemical parameters occurred within the enclosure between pre-and-post treatment.

After the third Phoslock treatment (PLOK3; Figure 7) in early July 2021, average TP concentrations in the enclosure were 6.68 ± 1.67 µM pre-treatment and 7.13 ± 0.65 µM post-treatment. As expected, chl-a values in the enclosure decreased immediately (within a day of treatment) from 109 µg $L^{-1}$ to 46.5 µg $L^{-1}$ (Figure 6). However, chl-a values increased in the enclosure from 82.4 ± 18.9 µg $L^{-1}$ pre-treatment to 190 ± 50.5 µg $L^{-1}$ post-treatment.

For the fourth Phoslock treatment (PLOK4; Figure 7) in late July 2021, average TP concentrations increased in the enclosure from 7.45 ± 0.56 µM pre-treatment to 10.0 ± 0.44 µM post-treatment. Chl-a values did not change in the enclosure, with 234 ± 16.7 µg $L^{-1}$ pre-treatment to 227 ± 14.1 µg $L^{-1}$ post-treatment (Figure 6).

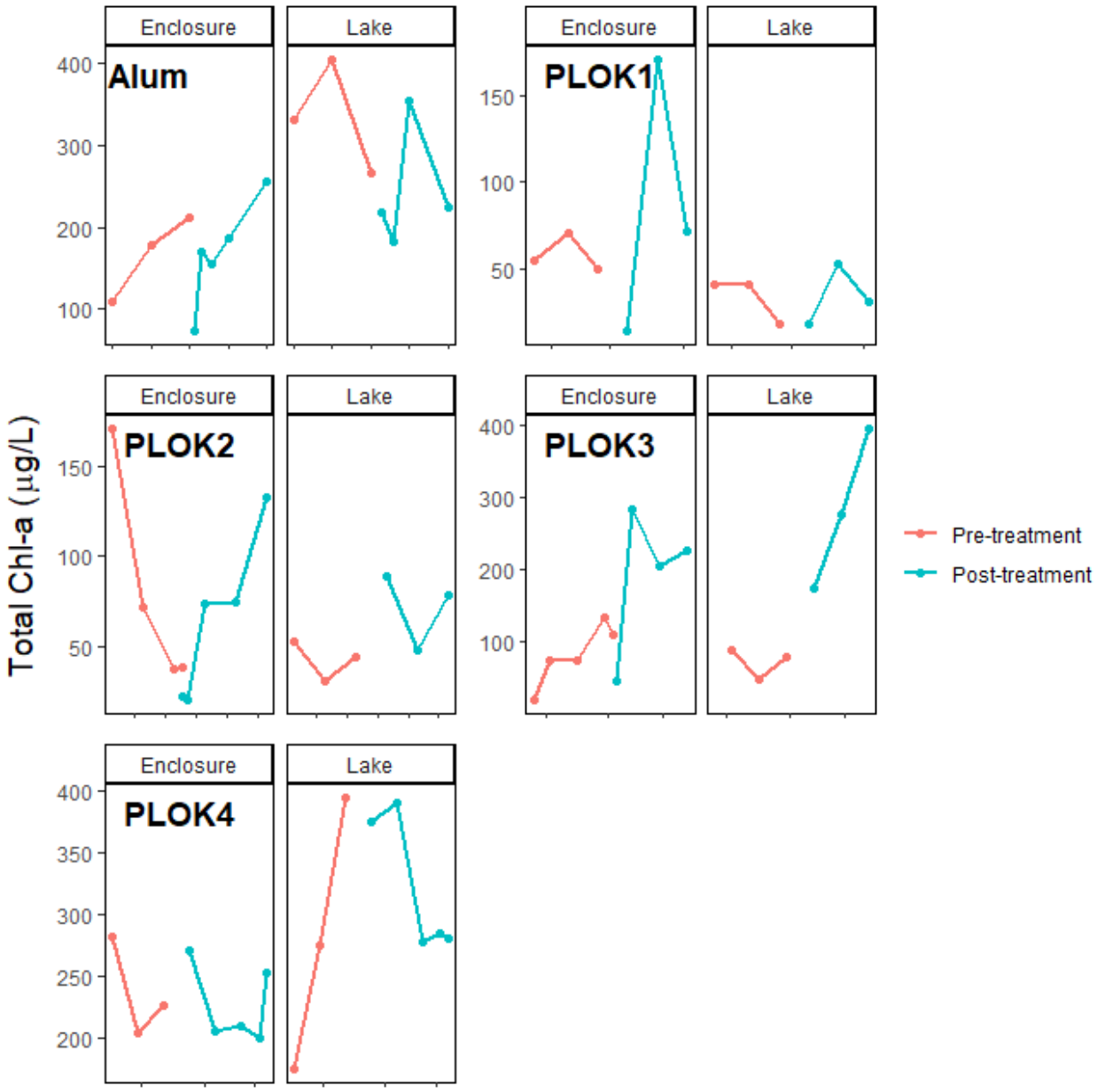


*Figure 7: Total chl-a concentrations for three weeks pre-and-post chemical treatments within the enclosure and lake.*

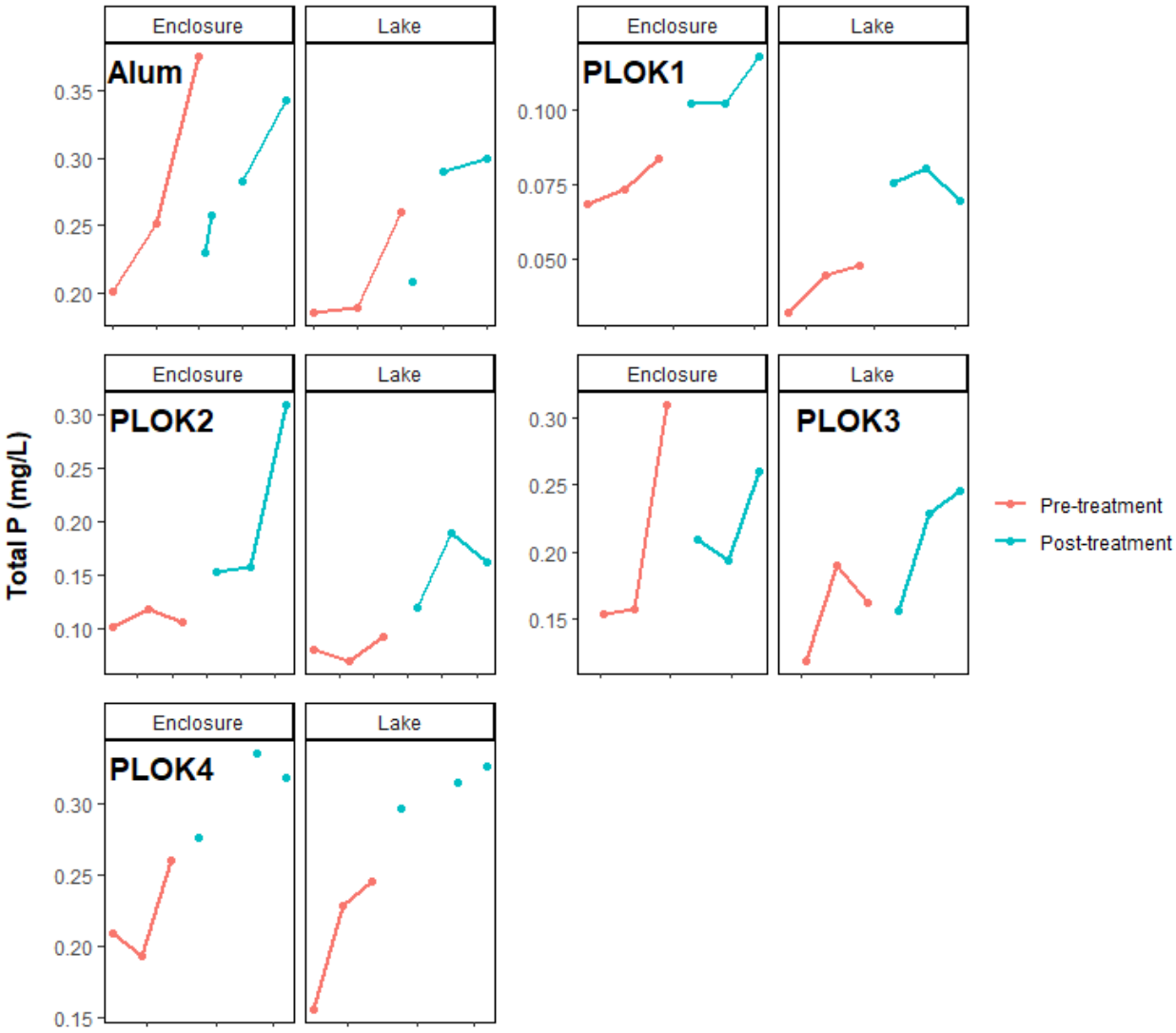


*Figure 8: Total phosphorus (TP) concentrations for three weeks pre-and-post chemical treatments within the enclosure and lake.*

*ii. Precipitation and Nutrient Loading Between Years*

Average monthly precipitation values, gathered from the Great Miami River station (03261500) in Sidney, OH, are shown in Figure 8. Precipitation at the beginning of each year, from January through July, differed from 61.6 cm in 2020 to 45.8 cm in 2021. More importantly, from January through March, precipitation differed from 31.6 cm in 2020 to 14.4 cm in 2021. March 2020 generated the largest monthly precipitation throughout the sampling period at 15.4 cm, which was larger than the first three months of 2021 combined. As a result, discharge from Chickasaw Creek (a GLSM tributary) from January through July 2021 was ~43% of overall discharge from January through July 2020. Chickasaw Creek is one of the main tributaries to GLSM, accounting for ~25% of total drainage from the overall watershed, with characteristics indicative of the entire watershed (i.e., similar soils, tile drainage, channelized streams, and land usage of ~80-90% row crops and livestock production; Jacquemin et al., 2018). Additionally, data from Chickasaw Creek spanned the entirety of the sampling period.

Consequently, as shown in Figure 9, external nutrient loads for $NO_3^-$, TP, SRP, and TN from Chickasaw Creek all decreased from January through July between years. $NO_3^-$ loading from January through July 2021 ($6.00 \times 10^9$ mg $NO_3^-$) was ~41% of loading for the same months in 2020 ($1.45 \times 10^{10}$ mg $NO_3^-$). TP loading from January through July 2021 ($9.09 \times 10^7$ mg TP) was ~28% of loading for the same months in 2020 ($3.22 \times 10^8$ mg TP). SRP loading from January through July 2021 ($5.25 \times 10^7$ mg SRP) was ~23% of loading for the same months in 2020 ($2.28 \times 10^8$ mg SRP). TN loading from January through July 2021 ($6.62 \times 10^9$ mg TN) was ~56% of loading for the same months in 2020 ($1.19 \times 10^{10}$ mg TN). TKN from January through July 2021 ($6.24 \times 10^8$ mg TKN) was ~58% of loading for the same months in 2020 ($1.08 \times 10^9$ mg TKN).

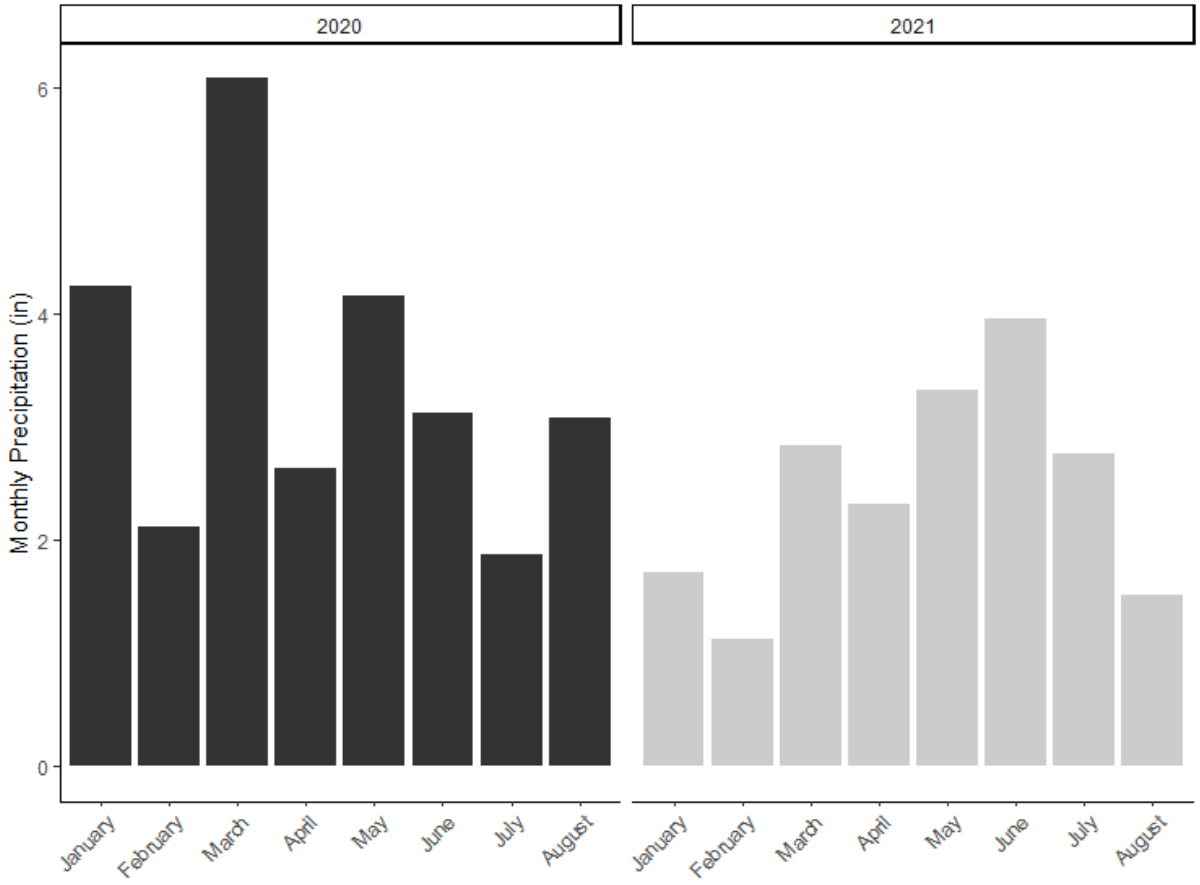


*Figure 9: Monthly precipitation from Great Miami River station (03261500) in Sidney, OH (~48 km) southeast of Grand Lake St. Marys).*

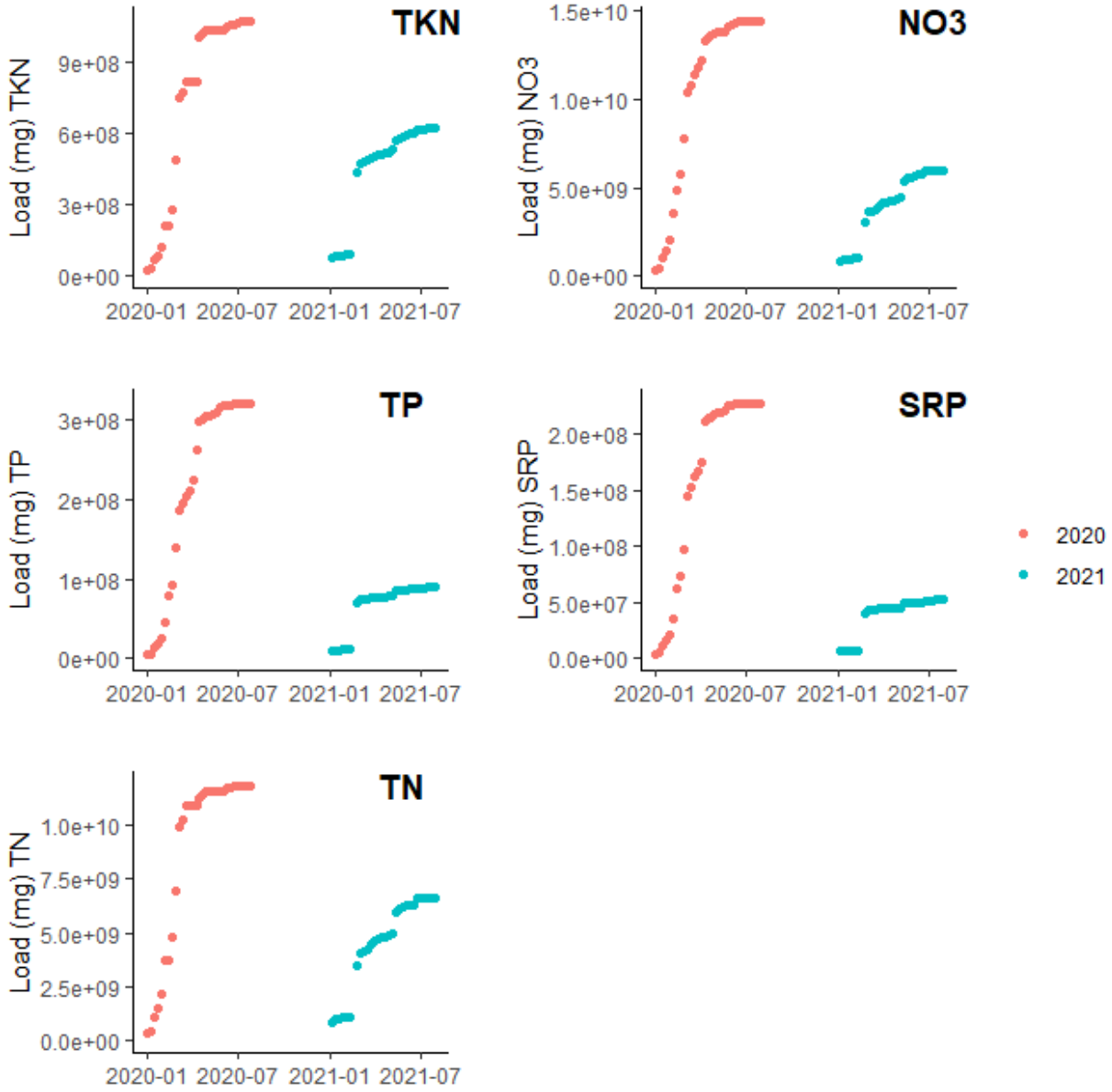


*Figure 10: Cumulative loading for total Kjeldahl nitrogen (TKN), nitrate ($NO_3^-$), total phosphorus (TP), soluble reactive phosphorus (SRP), and total nitrogen (TN) for the Chickasaw Creek tributary from January through July for each year. Data from the National Center for Water Quality Research at Heidelberg University.*

*iii. Environmental Parameters*

Sonde measurements, including temperature, DO, pH, and specific conductivity, are shown in Tables 3 & 4 for the enclosure and lake, respectively. Measurements for algal indicators of chl-a, phycocyanin, and microcystin toxins are also included in Tables 3 & 4.

Water temperature followed expected seasonal trends for the lake and enclosure in each year (Tables 3 & 4). The enclosure was colder in the spring (April and May; 2020 average = 12.9 ± 2.0 °C; 2021 average = 15.9 ± 1.5 °C), hottest in mid-summer (June, July, and August; 2020 average = 25.2 ± 0.6 °C; 2021 average = 25.9 ± 0.6 °C), and cooler again in the fall (September; 2020 average = 20.0 ± 1.4 °C; 2021 average = 23.1 ± 0.2 °C). The lake was also colder in the spring (2020 average = 12.9 ± 1.8 °C; 2021 average = 15.7 ± 1.5 °C), hottest in mid-summer (2020 average = 24.9 ± 0.7 °C; 2021 average = 25.3 ± 0.7 °C), and cooler again in the fall (2020 average = 20.1 ± 1.1 °C; 2021 average = 22.5 ± 0.1 °C). GLSM was (unusually) ice-covered in winter 2020-2021, with under-ice water temperatures at 1.1 °C in the enclosure and 0.5 °C in the surrounding lake in February 2021.

DO concentrations in both the enclosure (Table 3) and lake (Table 4) followed similar patterns. DO concentrations in 2020 averaged 11.9 ± 0.4 mg $L^{-1}$ and 11.8 ± 0.5 mg $L^{-1}$ for the enclosure and lake, respectively. At the bloom peak in mid-summer 2020, DO concentrations averaged 6.8 ± 0.6 mg $L^{-1}$ and 5.89 ± 0.7 mg $L^{-1}$ for the enclosure and lake, respectively, as respiration rates and temperatures increased. DO concentrations rose throughout the winter in both the lake and enclosure, as expected since cooler water has higher saturation concentrations for dissolved gases. DO levels reached near hypoxic levels (below 3 mg $L^{-1}$) within the surrounding lake in July 2020, corresponding with a large fish kill. The lowest recorded DO

concentration in the enclosure was 3.7 mg $L^{-1}$. There were no differences in DO concentrations between the lake and enclosure in either year.

In the enclosure from April through July, specific conductance averaged 403 ± 6.59 µg $L^{-1}$ in 2020 and 507 ± 9.45 µg $L^{-1}$ in 2021 (Tables 3 & 4). In the lake, specific conductance averaged 391 ± 7.45 µg $L^{-1}$ in 2020 and 503 ± 10.7 µg $L^{-1}$ in 2021. For both sites, the maximum specific conductance occurred under ice cover in February 2021, with maxima of 563 µS $cm^{-1}$ and 522 µS $cm^{-1}$ for the enclosure and lake, respectively.

*Table 3: Weekly monitoring data from bottom water (within 1 m above sediment surface) using a multiparameter sonde from every sampling event within the enclosure. Missing data is indicated with ND. Temp = Temperature, Sp. Cond. = Specific Conductance, and DO = Dissolved Oxygen. Temp, DO, pH, and Sp. Cond. were measured during each sampling event using a Eureka Manta 2 Water Quality Sonde. Chl-a and phycocyanin were measured with a BBE Moldaenke Algae Torch.*

| Date | Temp | DO | Sp. Cond. | pH | TP | Chl-a | Phycocyanin | Microcystin |
|---|---|---|---|---|---|---|---|---|
| | °C | mg $L^{-1}$ | µS $cm^{-1}$ | | µM | | µg $L^{-1}$ | |
| 04/08/2020 | 7.20 | 10.6 | 407 | 7.80 | 5.07 | 55.0 | 27.0 | ND |
| 04/15/2020 | 8.50 | 13.5 | 430 | 7.80 | 4.71 | 70.0 | 43.0 | ND |
| 04/22/2020 | 9.30 | 11.9 | 450 | 8.00 | 5.24 | 55.0 | 32.0 | ND |
| 04/28/2020 | 10.8 | 10.7 | 452 | 9.00 | 5.72 | 138 | 80.0 | 20.1 |
| 05/04/2020 | 18.0 | 13.1 | 406 | 9.20 | 7.07 | 48.0 | 42.0 | 30.8 |
| 05/11/2020 | 9.60 | 11.1 | 440 | 9.30 | 6.53 | 136 | 130 | 45.6 |
| 05/18/2020 | 18.0 | 11.1 | 440 | 9.30 | 7.78 | 112 | 105 | 46.9 |
| 05/25/2020 | 22.1 | 13.5 | 370 | 9.50 | 6.51 | 108 | 104 | 42.6 |
| 06/01/2020 | 20.0 | 10.9 | 380 | 9.50 | 8.13 | 177 | 168 | 68.2 |
| 06/08/2020 | 25.1 | 8.10 | 375 | 9.00 | 12.1 | 212 | 204 | 45.6 |
| 06/09/2020 | 27.0 | 11.5 | 360 | 7.14 | 7.43 | 74.0 | 70.0 | ND |
| 06/10/2020 | 25.0 | 6.90 | 375 | 7.80 | 8.32 | 170 | 162 | 41.5 |
| 06/12/2020 | 24.5 | 11.0 | 376 | 9.06 | ND | 154 | 149 | ND |
| 06/15/2020 | 20.1 | 8.20 | 400 | 9.50 | 9.14 | 186 | 178 | 65.0 |
| 06/22/2020 | 25.9 | 7.00 | 380 | 9.15 | 11.1 | 255 | 244 | 66.4 |
| 06/29/2020 | 27.6 | 7.10 | 368 | 9.15 | 9.59 | 195 | 186 | 40.9 |
| 07/06/2020 | 28.1 | 4.20 | 430 | 8.57 | 11.8 | 242 | 222 | 7.90 |
| 07/13/2020 | 25.1 | 4.78 | 415 | 8.60 | 11.5 | 325 | 285 | 37.1 |
| 07/20/2020 | 26.4 | 3.70 | 400 | 8.78 | 11.1 | 231 | 198 | 40.7 |
| 07/27/2020 | 29.1 | 5.95 | 403 | 8.84 | 9.64 | 169 | 125 | 15.8 |
| 08/03/2020 | 23.7 | 6.10 | 406 | 9.05 | 11.1 | 239 | 140 | 5.70 |
| 08/10/2020 | 26.4 | 5.52 | 388 | 8.77 | 10.7 | 167 | 57.0 | 5.90 |
| 08/17/2020 | 24.7 | 5.84 | 396 | 8.78 | 12.4 | 206 | 132 | 25.7 |
| 08/24/2020 | 26.7 | 4.79 | 394 | 8.64 | 11.9 | 158 | 90.0 | 17.3 |
| 08/31/2020 | 23.3 | 4.62 | 422 | 8.64 | 11.8 | 228 | 170 | 15.9 |
| 09/07/2020 | 22.3 | 6.12 | 415 | 8.67 | 14.0 | 183 | 168 | 24.7 |
| 09/14/2020 | 21.4 | 7.50 | 376 | 8.76 | 13.2 | 214 | 137 | 25.9 |
| 09/21/2020 | 16.2 | 6.19 | 385 | 9.29 | 11.3 | 165 | 70.0 | ND |
| 09/28/2020 | 20.2 | 6.22 | 386 | 8.76 | 10.6 | 343 | 328 | 17.6 |

| | | | | | | | | |
|---|---|---|---|---|---|---|---|---|
| 10/05/2020 | 12.0 | 4.90 | 427 | 8.69 | 11.8 | 121 | 88.0 | 21.4 |
| 10/12/2020 | 18.6 | 8.37 | 404 | 9.29 | 11.8 | 185 | 155 | 56.2 |
| 10/19/2020 | 10.7 | 10.1 | 407 | 8.62 | 11.3 | 265 | 246 | 65.2 |
| 10/26/2020 | 11.6 | 9.62 | 419 | 9.16 | 10.7 | 213 | 198 | 39.4 |
| 11/03/2020 | 6.30 | 13.2 | 379 | 9.30 | 9.92 | 368 | 355 | 61.5 |
| 11/09/2020 | 12.0 | 9.20 | 417 | 9.58 | 9.04 | 344 | 331 | 55.6 |
| 11/16/2020 | 6.20 | 13.3 | 385 | 8.73 | 10.7 | 356 | 340 | 49.0 |
| 11/23/2020 | 5.30 | 10.7 | 445 | 8.86 | 8.69 | 328 | 318 | 10.4 |
| 11/30/2020 | 6.00 | 11.8 | 425 | 9.02 | 7.04 | 265 | 250 | 2.10 |
| 12/07/2020 | 1.60 | 13.9 | 423 | 8.84 | 3.68 | 116 | 112 | 5.60 |
| 12/14/2020 | 4.30 | 15.2 | 394 | 8.78 | 3.58 | 98.0 | 83.0 | 5.80 |
| 12/21/2020 | 1.10 | 16.0 | 452 | 9.15 | 3.31 | 49.0 | 45.0 | 2.20 |
| 01/04/2021 | 1.60 | 10.9 | 473 | 8.73 | 2.53 | 32.0 | 28.0 | ND |
| 01/12/2021 | 1.10 | 12.7 | 509 | 8.76 | 1.97 | 30.0 | 22.0 | 0.89 |
| 01/19/2021 | 0.20 | 14.8 | 523 | 8.98 | 1.39 | 19.0 | 12.0 | 1.00 |
| 01/26/2021 | 1.80 | 11.8 | 553 | 8.58 | 1.58 | 35.0 | 7.50 | 0.90 |
| 02/02/2021 | 2.00 | 12.9 | 424 | 9.11 | 2.86 | 48.0 | 8.00 | ND |
| 02/09/2021 | 1.00 | 6.68 | 505 | 8.44 | 2.74 | 102 | 10.0 | ND |
| 02/23/2021 | 2.80 | 15.8 | 212 | 9.03 | 1.74 | 19.0 | 4.00 | ND |
| 03/02/2021 | 2.90 | 9.90 | 519 | 8.85 | 2.84 | 55.0 | 11.0 | ND |
| 03/09/2021 | 6.60 | 11.3 | 492 | 8.79 | 2.90 | 48.0 | 7.50 | 1.90 |
| 03/16/2021 | 6.60 | 10.4 | 506 | 8.96 | 3.01 | 65.0 | 15.2 | 1.30 |
| 03/23/2021 | 10.7 | 10.7 | 494 | 8.62 | 3.59 | 66.0 | 18.0 | 1.80 |
| 03/30/2021 | 10.0 | 10.4 | 470 | 9.04 | 2.92 | 65.0 | 21.0 | ND |
| 04/06/2021 | 13.0 | 10.0 | 517 | 9.10 | 2.65 | 95.0 | 22.0 | 0.50 |
| 04/13/2021 | 13.1 | 11.7 | 519 | 8.96 | 3.59 | 115 | 27.0 | 0.30 |
| 04/20/2021 | 12.5 | 9.53 | 544 | 9.00 | 4.04 | 105 | 23.0 | 4.20 |
| 04/27/2021 | 14.3 | 9.10 | 507 | 8.73 | 2.21 | 55.0 | 7.50 | 0.40 |
| 05/05/2021 | 16.0 | 8.60 | 540 | 8.80 | 2.37 | 71.0 | 10.5 | 0.72 |
| 05/12/2021 | 13.2 | 11.0 | 509 | 9.10 | 2.71 | 50.0 | 8.00 | 0.41 |
| 05/19/2021 | 20.0 | 6.25 | 508 | 8.48 | 3.28 | 15.0 | 0.50 | 0.32 |
| 05/26/2021 | 24.7 | 7.80 | 502 | 8.84 | 3.28 | 171 | 5.50 | 0.30 |
| 06/02/2021 | 19.9 | 7.38 | 537 | 8.85 | 3.80 | 72.0 | 10.5 | 0.30 |
| 06/09/2021 | 24.8 | 4.70 | 547 | 8.53 | 3.39 | 38.0 | 12.0 | 0.63 |
| 06/11/2021 | 26.5 | 4.50 | 540 | 8.36 | ND | 39.0 | 11.5 | ND |
| 06/11/2021 | ND | 4.20 | ND | 7.67 | ND | 23.0 | 9.00 | ND |

| | | | | | | | | |
|---|---|---|---|---|---|---|---|---|
| 06/12/2021 | 28.1 | 5.70 | 525 | 7.88 | ND | 21.0 | 4.50 | ND |
| 06/16/2021 | 24.3 | 6.95 | 560 | 8.76 | 4.96 | 74.0 | 28.0 | 0.38 |
| 06/23/2021 | 22.1 | 6.21 | 528 | 8.50 | 5.07 | 75.0 | 31.0 | 1.30 |
| 06/30/2021 | 27.9 | 5.70 | 512 | 8.26 | 10.0 | 133 | 67.0 | 50.0 |
| 07/02/2021 | ND | ND | ND | ND | ND | 109 | 38.0 | ND |
| 07/03/2021 | ND | ND | ND | NF | ND | 47.0 | 4.60 | ND |
| 07/07/2021 | 28.7 | 10.3 | 446 | 8.62 | 6.77 | 282 | 42.0 | 1.60 |
| 07/14/2021 | 25.2 | ND | 441 | 8.70 | 6.23 | 204 | 135 | 4.98 |
| 07/21/2021 | 26.7 | 5.00 | 446 | 8.32 | 8.40 | 226 | 175 | 0.30 |
| 07/28/2021 | 28.7 | 11.4 | 413 | 8.90 | 8.93 | 270 | 127 | 0.30 |
| 08/04/2021 | 24.5 | 5.40 | ND | 8.80 | ND | 205 | 93.0 | 1.01 |
| 08/11/2021 | 26.5 | 4.67 | 432 | 8.00 | 10.8 | 210 | 103 | 2.16 |
| 08/16/2021 | 25.0 | 7.25 | 438 | 8.10 | ND | 200 | 50.0 | ND |
| 08/18/2021 | 25.1 | 7.30 | 447 | 8.56 | 10.3 | 252 | 43.0 | 0.83 |
| 08/23/2021 | 29.1 | 5.76 | 422 | 8.30 | 12.2 | 285 | 89.0 | 3.31 |
| 08/30/2021 | 27.0 | 5.21 | 408 | 8.46 | 11.8 | 272 | 197 | 2.13 |
| 09/06/2021 | 23.3 | 7.10 | 408 | 9.10 | 10.4 | 252 | 120 | 3.15 |
| 09/13/2021 | 22.9 | 7.75 | 434 | 8.86 | 10.8 | 261 | 136 | 2.97 |

*Table 4: Weekly monitoring data from bottom water (within 1 m above sediment surface) using a multiparameter sonde from every sampling event within the lake. Missing data is indicated with ND. Temp = Temperature, Sp. Cond. = Specific Conductance, and DO = Dissolved Oxygen. Temp, DO, pH, and Sp. Cond. were measured during each sampling event using a Eureka Manta 2 Water Quality Sonde. Chl-a and phycocyanin were measured with a BBE Moldaenke Algae Torch.*

| Date | Temp | DO | Sp. Cond. | pH | TP | Chl-a | Phycocyanin | Microcystin |
|---|---|---|---|---|---|---|---|---|
| | °C | mg $L^{-1}$ | µS $cm^{-1}$ | | µM | µg $L^{-1}$ | | |
| 04/08/2020 | 7.50 | 11.7 | 368 | 8.20 | 3.68 | 54.0 | 29.0 | ND |
| 04/15/2020 | 8.40 | 13.0 | 420 | 7.50 | 5.37 | 90.0 | 53.0 | ND |
| 04/22/2020 | 9.70 | 11.6 | 448 | 8.10 | 4.40 | 95.0 | 68.0 | ND |
| 04/28/2020 | 10.5 | 10.5 | 449 | 9.20 | 4.83 | 125 | 105 | 22.2 |
| 05/04/2020 | 18.6 | 13.8 | 420 | 9.30 | 4.41 | 170 | 138 | 41.4 |
| 05/11/2020 | 10.0 | 11.2 | 418 | 8.90 | 5.94 | 173 | 166 | 49.1 |
| 05/18/2020 | 18.4 | 9.70 | 410 | 9.60 | 7.05 | 173 | 166 | 62.1 |
| 05/25/2020 | 20.1 | 13.1 | 375 | 9.30 | 6.02 | 331 | 322 | 77.9 |
| 06/01/2020 | 19.7 | 8.60 | 400 | 9.10 | 6.13 | 405 | 390 | 74.4 |
| 06/08/2020 | 24.5 | 6.50 | 350 | 8.10 | 8.39 | 266 | 257 | 40.9 |
| 06/10/2020 | 24.9 | 4.30 | 335 | 8.60 | 6.73 | 218 | 206 | 57.8 |
| 06/12/2020 | 23.5 | 9.70 | 343 | 9.02 | ND | 183 | 174 | ND |
| 06/15/2020 | 19.7 | 6.40 | 370 | 8.82 | 9.35 | 354 | 343 | 55.4 |
| 06/22/2020 | 26.1 | 4.40 | 376 | 8.85 | 9.66 | 225 | 216 | 58.2 |
| 06/29/2020 | 27.5 | 12.0 | 365 | 10.0 | 9.39 | 234 | 223 | 48.1 |
| 07/06/2020 | 27.1 | 2.50 | 397 | 8.10 | 25.2 | 332 | 304 | 20.0 |
| 07/13/2020 | 25.1 | 4.10 | 400 | 8.30 | 10.8 | 318 | 286 | 44.5 |
| 07/20/2020 | 26.1 | 3.00 | 400 | 8.83 | 11.8 | 295 | 282 | 45.5 |
| 07/27/2020 | 29.4 | 5.60 | 382 | 9.62 | 11.7 | 216 | 205 | 30.5 |
| 08/03/2020 | 23.3 | 6.40 | 380 | 8.84 | 13.7 | 335 | 322 | 7.00 |
| 08/10/2020 | 27.4 | 7.80 | 398 | 9.70 | 11.0 | 201 | 192 | 39.7 |
| 08/17/2020 | 24.5 | 5.90 | 400 | 9.34 | 15.1 | 281 | 185 | 75.0 |
| 08/24/2020 | 26.8 | 2.70 | 427 | 8.76 | 13.8 | 154 | 143 | 31.2 |
| 08/31/2020 | 22.8 | 4.40 | 420 | 8.81 | 14.7 | 260 | 249 | 34.5 |
| 09/07/2020 | 22.1 | 6.20 | 396 | 8.64 | 15.0 | 238 | 158 | 39.8 |
| 09/14/2020 | 21.2 | 6.70 | 406 | 9.29 | 13.7 | 303 | 287 | 63.7 |
| 09/21/2020 | 16.9 | 8.70 | 400 | 9.45 | 11.2 | 309 | 297 | ND |
| 09/28/2020 | 20.2 | 6.60 | 388 | 9.15 | 12.4 | 229 | 209 | 36.2 |
| 10/05/2020 | 12.6 | 9.00 | 410 | 9.33 | 11.8 | 275 | 261 | 40.3 |

| | | | | | | | | |
|---|---|---|---|---|---|---|---|---|
| 10/12/2020 | 17.6 | 8.60 | 386 | 9.37 | 11.1 | 238 | 225 | 70.4 |
| 10/19/2020 | 10.8 | 10.7 | 350 | 9.02 | 11.3 | 262 | 247 | 60.8 |
| 10/26/2020 | 11.8 | 9.40 | 417 | 8.88 | 10.3 | 364 | 350 | 42.0 |
| 11/03/2020 | 6.70 | 14.2 | 405 | 8.80 | 12.2 | 315 | 300 | 47.3 |
| 11/09/2020 | 11.9 | 11.6 | 414 | 9.05 | 9.84 | 382 | 369 | 48.4 |
| 11/16/2020 | 6.30 | 13.2 | 421 | 8.86 | 16.6 | 261 | 246 | 51.6 |
| 11/23/2020 | 5.40 | 10.2 | 399 | 8.71 | 10.2 | 346 | 336 | 13.2 |
| 11/30/2020 | 7.00 | 10.7 | 410 | 9.02 | 7.39 | 365 | 346 | 8.30 |
| 12/07/2020 | 2.30 | 15.7 | 420 | 8.75 | 5.87 | 281 | 276 | 11.6 |
| 12/14/2020 | 4.40 | 14.9 | 436 | 9.18 | 5.13 | 220 | 214 | 14.5 |
| 12/21/2020 | 1.10 | 17.7 | 435 | 9.12 | 4.37 | 124 | 120 | 7.40 |
| 01/04/2021 | 0.70 | 15.0 | 382 | 9.30 | 1.02 | 43.0 | 40.0 | ND |
| 01/12/2021 | 0.80 | 13.5 | 454 | 9.23 | 2.14 | 31.2 | 28.0 | 0.94 |
| 01/19/2021 | 0.20 | 13.1 | 460 | 9.15 | 2.16 | 40.5 | 36.5 | 4.70 |
| 01/26/2021 | 0.80 | 8.50 | 434 | 9.32 | 1.98 | 34.0 | 10.5 | 2.70 |
| 02/02/2021 | 2.50 | 11.4 | 553 | 9.38 | 3.32 | 95.0 | 12.0 | 1.90 |
| 02/09/2021 | 1.90 | 11.3 | 528 | 8.80 | 1.71 | 52.0 | 11.0 | 1.40 |
| 02/23/2021 | 3.00 | 11.7 | 513 | 8.99 | 2.93 | 22.0 | 15.0 | 1.20 |
| 03/02/2021 | 5.20 | 9.70 | 372 | 9.12 | 5.99 | 210 | 15.0 | 0.90 |
| 03/09/2021 | 5.00 | 9.70 | 450 | 8.93 | 3.75 | 105 | 15.9 | 3.80 |
| 03/16/2021 | 6.30 | 10.4 | 460 | 9.02 | 4.26 | 61.0 | 26.0 | 2.40 |
| 03/23/2021 | 10.4 | 10.5 | 502 | 8.86 | 2.42 | 74.0 | 10.0 | 0.40 |
| 03/30/2021 | 9.30 | 11.6 | 500 | 9.11 | 3.41 | 50.0 | 13.0 | 0.90 |
| 04/06/2021 | 12.2 | 12.4 | 495 | 9.30 | 3.54 | 55.0 | 10.0 | 5.0 |
| 04/13/2021 | 13.6 | 9.30 | 488 | 8.75 | 2.65 | 71.0 | 30.0 | 4.9 |
| 04/20/2021 | 13.5 | 10.3 | 535 | 8.35 | 2.76 | 40.0 | 11.0 | 4.9 |
| 04/27/2021 | 14.4 | 8.50 | 487 | 8.81 | 1.05 | 40.5 | 6.00 | 0.59 |
| 05/05/2021 | 14.8 | 8.50 | 520 | 9.10 | 1.45 | 40.5 | 5.00 | 0.54 |
| 05/12/2021 | 13.3 | 9.70 | 508 | 9.10 | 1.56 | 18.0 | 3.00 | 0.34 |
| 05/19/2021 | 19.8 | 6.20 | 530 | 8.20 | 2.44 | 18.0 | 2.00 | 1.10 |
| 05/26/2021 | 24.2 | 5.80 | 558 | 8.85 | 2.59 | 53.0 | 7.00 | 0.39 |
| 06/02/2021 | 19.1 | 7.80 | 554 | 9.10 | 2.25 | 31.0 | 4.0 | 0.40 |
| 06/09/2021 | 24.4 | 3.60 | 548 | 8.51 | 2.95 | 44.0 | 18.0 | 0.96 |
| 06/16/2021 | 24.5 | 5.50 | 553 | 8.66 | 3.84 | 89.0 | 12 | 0.42 |
| 06/23/2021 | 21.1 | ND | 528 | 8.90 | 6.12 | 48.0 | 13 | 1.44 |

| | | | | | | | | |
|---|---|---|---|---|---|---|---|---|
| 06/30/2021 | 28.2 | 2.70 | 492 | 7.60 | 5.25 | 78.2 | 46 | 2.41 |
| 07/07/2021 | 27.8 | 2.90 | 474 | 8.40 | 5.04 | 175 | 145 | 3.10 |
| 07/14/2021 | 25.0 | ND | 445 | 8.40 | 7.39 | 275 | 260 | 2.82 |
| 07/21/2021 | 26.5 | 5.20 | 426 | 9.24 | 7.94 | 395 | 380 | 4.03 |
| 07/28/2021 | 27.9 | 8.70 | 418 | 9.50 | 9.59 | 375 | 358 | 2.30 |
| 08/04/2021 | 22.6 | 3.60 | 422 | 8.40 | ND | 390 | 370 | 4.26 |
| 08/11/2021 | 26.2 | 3.40 | 430 | 9.10 | 10.2 | 278 | 265 | 4.71 |
| 08/16/2021 | 25.0 | 6.80 | 441 | 8.70 | ND | 285 | 275 | ND |
| 08/18/2021 | 25.2 | 4.30 | 454 | 8.90 | 10.5 | 281 | 270 | 3.30 |
| 08/23/2021 | 28.3 | 7.00 | 437 | 9.21 | 10.8 | 266 | 249 | 6.50 |
| 08/30/2021 | 27.0 | 3.10 | 412 | 8.80 | 11.6 | 314 | 299 | 3.52 |
| 09/06/2021 | 22.4 | 8.90 | 430 | 9.20 | 12.4 | 192 | 186 | 4.02 |
| 09/13/2021 | 22.5 | 4.30 | 440 | 8.80 | 11.1 | 167 | 160 | 9.27 |

*iv. Cyanobacterial Biomass and Toxins Between Years*

Microcystin concentrations were different between years for both sites (ANOVA; $p < 0.0001$), with much lower concentrations in 2021. Toxin levels peaked at 66.4 µg $L^{-1}$ (Table 3) in the enclosure in June 2020 and 70.4 µg $L^{-1}$ (Table 4) in the lake in October 2020, which are well above the recreational exposure limit set by the World Health Organization (24 µg $L^{-1}$; WHO, 2021). From April through July 2020, average microcystin concentrations were 41.0 ± 19.6 µg $L^{-1}$ and 48.5 ± 4.32 µg $L^{-1}$ for the enclosure and lake, respectively. From March through July 2021, average microcystin concentrations were 3.94 ± 1.90 µg $L^{-1}$ and 2.10 ± 0.42 µg $L^{-1}$ for the enclosure and lake, respectively (Figure 10). No differences in microcystin concentrations were noted between the sites for either year.

Phycocyanin concentrations were different between years for both sites (ANOVA; $p < 0.0001$), with much lower phycocyanin concentrations in 2021. Phycocyanin peaked at 331 µg $L^{-1}$ (Table 3) in the enclosure in November 2020 and 380 µg $L^{-1}$ (Table 4) in the lake in July 2021. From April through July 2020, average phycocyanin concentrations were 138 ± 16.7 µg $L^{-1}$ and 207 ± 23.2 µg $L^{-1}$ for the enclosure and lake, respectively. From March through July 2021, average phycocyanin concentrations were 36.3 ± 10.2 µg $L^{-1}$ and 76.9 ± 31.2 µg $L^{-1}$ in the enclosure and lake, respectively.

Chl-a concentrations were different between years for both sites (ANOVA; $p = 0.03$). Maximum chl-a concentrations were 344 µg $L^{-1}$ (Table 3) in November 2020 in the enclosure and 395 µg $L^{-1}$ (Table 4) in the lake in July 2021. From April through July 2020, average chl-a concentrations were 156 ± 16.9 µg $L^{-1}$ and 224 ± 22.4 µg $L^{-1}$ in the enclosure and lake, respectively. From March through July 2021, mean chl-a concentrations were 104 ± 16.9 µg $L^{-1}$ and 109 ± 29.6 µg $L^{-1}$ in the enclosure and lake, respectively.

Although the cyanobacterial bloom remained at high levels (>300 µg $L^{-1}$) in the enclosure and lake until November 2020, the harsh winter of 2020-2021 limited the bloom size. From December 2020 through February 2021, microcystins decreased to 0.89 and 0.94 µg $L^{-1}$ for the enclosure and lake, respectively. Similarly, during the same period, phycocyanin and total chl-a levels decreased to 4.00 and 19.0 and 10.5 and 31.2 µg $L^{-1}$, for the enclosure and lake, respectively.

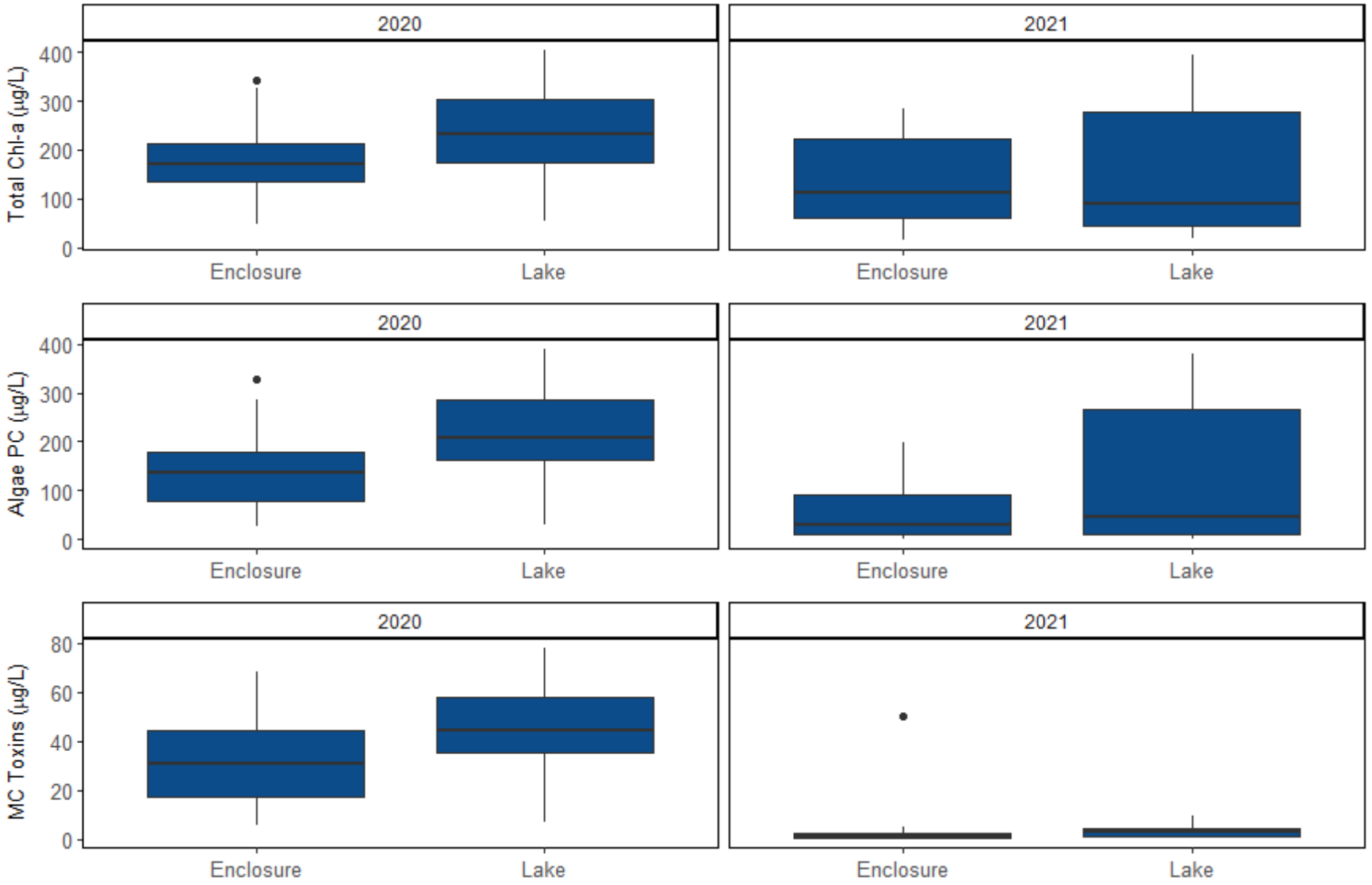


*Figure 11: Total chlorophyll-a, algae phycocyanin, and microcystin toxins measured from April through September in 2020 and 2021 for both the enclosure and lake.*

*v. Ambient Nutrient Concentrations (March through July)*

While nutrient loading decreased in 2021 compared to 2020, ambient nutrient concentrations for N-species increased, as the cyanobacterial bloom did not initiate until July. Average $NH_4^+$ concentrations in the enclosure from March through July of each year increased from 1.02 ± 0.63 µM in 2020 to 16.8 ± 6.45 µM in 2021 (Table 5). In the lake, average $NH_4^+$ concentrations increased from 0.76 ± 0.42 µM in 2020 to 21.0 ± 4.14 µM in 2021 (Table 6).

Nitrite concentrations remained below the detection limit for nearly the entirety of spring and summer 2020 (Table 5 & 6); however, from March through July 2021, $NO_2^-$ concentrations averaged 1.30 ± 0.32 µM and 1.44 ± 0.51 µM for the enclosure and lake, respectively. Average $NO_3^-$ concentrations from March through July of each year increased from 8.98 ± 8.92 µM in 2020 to 28.8 ± 14.1 µM in 2021 in the enclosure (Table 5). In the lake during those months, $NO_3^-$ concentrations were 20.6 ± 20.5 µM in 2020 and 26.8 ± 11.5 µM in 2021 (Table 6).

Urea had the largest increase among the bioavailable N forms in both the enclosure and lake. From April through July in the enclosure, urea increased from 1.15 ± 0.17 µM in 2020 to 6.84 ± 3.06 µM in 2021 (Table 5). In the lake during the same period, average urea concentrations increased from 1.39 ± 0.28 µM in 2020 to 11.8 ± 4.11 µM in 2021 (Table 6).

In contrast to the dissolved inorganic nitrogen fluxes ambient ortho-P concentrations decreased on average from March through July of each year. Ortho-P concentrations in the enclosure were 0.11 ± 0.07 µM in 2020 and 0.06 ± 0.02 µM in 2021 (Table 5). In the lake during the same period, ortho-P concentrations were 1.14 ± 0.97 µM in 2020 and 0.08 ± 0.02 µM in 2021 (Table 6).

*Table 5: Ambient nutrient data collected at each sampling event within the enclosure. Units are µM N or µM P. Measurements below the detection limit are reported as BDL (0.04 µM for NOx, 0.03 for µM $NH_4^+$, 0.01 µM for ortho-P, and 0.21 µM for urea-N).*

| Date | $NH_4^+$ | $NO_2^-$ | $NO_3^-$ | Urea-N | Ortho-P |
|---|---|---|---|---|---|
| | | | µM | | |
| ***Spring*** | | | | | |
| 04/08/2020 | 1.88 | 2.42 | 44.7 | 1.06 | 0.015 |
| 05/22/2020 | 0.032 | BDL | 0.103 | 0.774 | 0.016 |
| ***Summer*** | | | | | |
| 06/12/2020 | 0.022 | BDL | 0.045 | 0.977 | 0.015 |
| 06/24/2020 | 0.060 | BDL | BDL | 1.19 | 0.092 |
| 07/08/2020 | 3.11 | BDL | 0.077 | 1.77 | 0.394 |
| 08/11/2020 | BDL | BDL | 0.137 | 0.897 | 0.030 |
| ***Fall*** | | | | | |
| 09/15/2020 | 1.07 | BDL | 0.061 | 0.913 | 0.019 |
| 10/13/2020 | 0.530 | BDL | BDL | 0.916 | 0.018 |
| ***Winter*** | | | | | |
| 11/10/2020 | 55.1 | 1.18 | 16.5 | 0.705 | 0.010 |
| 02/10/2021 | 55.1 | 0.203 | 21.4 | 4.30 | 0.071 |
| ***Spring*** | | | | | |
| 03/21/2021 | 25.6 | 1.58 | 52.7 | 2.11 | 0.028 |
| 05/11/2021 | 0.198 | 1.89 | 53.6 | 9.39 | 0.047 |
| ***Summer*** | | | | | |
| 06/06/2021 | 13.1 | 1.32 | 7.32 | 14.3 | 0.049 |
| 07/19/2021 | 28.3 | 0.402 | 1.57 | 1.57 | 0.122 |

*Table 6: Ambient nutrient data collected at each sampling event within the lake. Units are µM N or µM P. Measurements below the detection limit are reported as BDL (0.04 µM for NOx, 0.03 µM for $NH_4^+$, 0.01 µM for ortho-P, and 0.21 µM for urea-N).*

| Date | $NH_4^+$ | $NO_2^-$ | $NO_3^-$ | Urea-N | Ortho-P |
|---|---|---|---|---|---|
| | | | µM | | |
| ***Spring*** | | | | | |
| 04/08/2020 | 2.31 | 3.13 | 103 | 1.12 | BDL |
| 05/22/2020 | 0.176 | BDL | 0.089 | 0.907 | 0.015 |
| ***Summer*** | | | | | |
| 06/12/2020 | 0.114 | BDL | 0.044 | 0.992 | 0.045 |
| 06/24/2020 | 0.152 | BDL | 0.062 | 1.50 | 0.666 |
| 07/08/2020 | 1.07 | BDL | 0.342 | 2.43 | 4.97 |
| 08/11/2020 | BDL | BDL | BDL | 0.737 | 0.526 |
| ***Fall*** | | | | | |
| 09/15/2020 | 0.183 | BDL | 0.064 | 0.753 | 0.262 |
| 10/13/2020 | 0.738 | BDL | BDL | 0.904 | 0.035 |
| ***Winter*** | | | | | |
| 11/10/2020 | 58.0 | 1.23 | 19.5 | 1.10 | 0.012 |
| 02/10/2021 | 51.6 | 0.629 | 43.3 | 3.27 | 0.063 |
| ***Spring*** | | | | | |
| 03/21/2021 | 24.7 | 1.50 | 65.7 | 10.8 | 0.140 |
| 05/11/2021 | 8.61 | 1.76 | 28.5 | 15.0 | 0.052 |
| ***Summer*** | | | | | |
| 06/06/2021 | 25.4 | 2.48 | 12.4 | 20.3 | 0.042 |
| 07/19/2021 | 25.4 | 0.032 | 0.545 | 0.872 | 0.083 |

*vi. Oxygen Demand*

SOD within the enclosure differed between years (ANOVA; $p = 0.018$). From April through July 2020 in the enclosure, SOD ranged from 1119 in April 2020 to 2093 µmol $O_2$ $m^{-2}$ $hr^{-1}$ in June 2020, averaging 1751 ± 173.0 µmol $O_2$ $m^{-2}$ $hr^{-1}$ (Figure 11). From March through July 2021, SOD ranged from 871 in May to 1398 µmol $O_2$ $m^{-2}$ $hr^{-1}$ in the enclosure, averaging 1062 ± 174 µmol $O_2$ $m^{-2}$ $hr^{-1}$.

SOD within the lake differed between years (ANOVA; $p = 0.032$) and showed similar differences between years, ranging from 962 in April 2020 to 2266 µmol $O_2$ $m^{-2}$ $hr^{-1}$ on June 24, 2020, averaging 1602 ± 228 µmol $O_2$ $m^{-2}$ $hr^{-1}$ (Figure 11). From March through July 2021, SOD ranged from 614 in July to 1168 µmol $O_2$ $m^{-2}$ $hr^{-1}$ in June, averaging 862 ± 115 µmol $O_2$ $m^{-2}$ $hr^{-1}$.

From April through July 2020 in the enclosure, WCOD ranged from 1672 in April 2020 to 7939 µmol $O_2$ $m^{-2}$ $hr^{-1}$ on June 12, 2020, averaging 5168 ± 1224 µmol $O_2$ $m^{-2}$ $hr^{-1}$ (Figure 11). From March through July 2021, WCOD ranged from 640 in March to 9244 µmol $O_2$ $m^{-2}$ $hr^{-1}$ in June, averaging 4124 ± 1820 µmol $O_2$ $m^{-2}$ $hr^{-1}$.

WCOD in the lake showed similar differences between years, ranging from 2303 in April 2020 to 11151 µmol $O_2$ $m^{-2}$ $hr^{-1}$ in July 2020, averaging 5809 ± 1571 µmol $O_2$ $m^{-2}$ $hr^{-1}$ (Figure 11). From March through July 2021 in the lake, WCOD ranged from 1382 in May to 9657 µmol $O_2$ $m^{-2}$ $hr^{-1}$ in July, averaging 4203 ± 1944 µmol $O_2$ $m^{-2}$ $hr^{-1}$. Peak combined SOD and WCOD in July 2020 (12800 µmol $O_2$ $m^{-2}$ $hr^{-1}$) coincided with a fish kill within the lake.

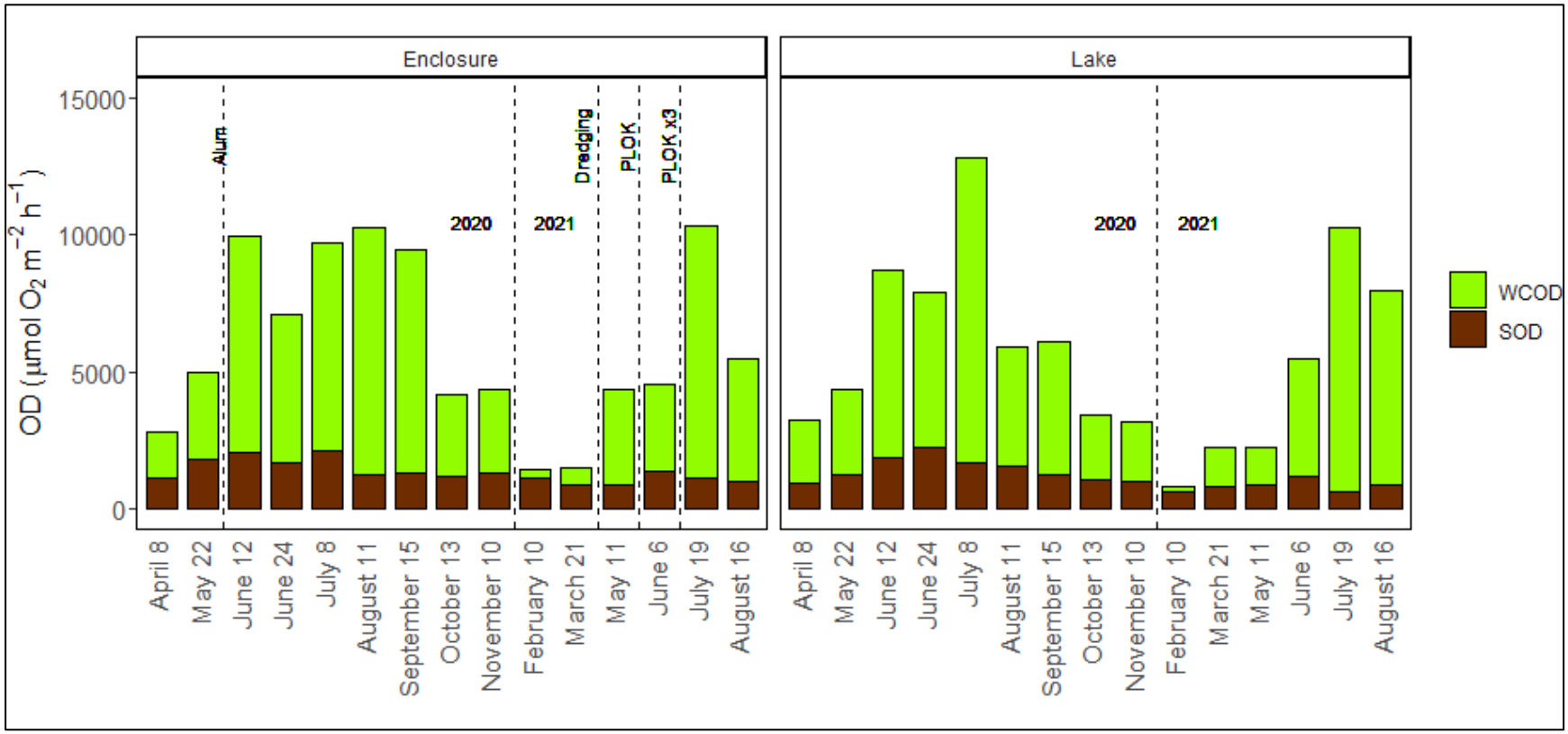


*Figure 12: Water column oxygen demand (WCOD) and sediment oxygen demand (SOD) for each site during each sampling event.*

*vii. Unamended Sediment Core Incubations*

Net nutrient fluxes were calculated from unamended sediment cores. Bars with positive values indicate an efflux of the specified nutrient from the sediments to the overlying water column. Negative values indicate an influx of the specified nutrient from the overlying water column into sediments. Errors bars show the standard error of rates calculated from duplicate sediment cores over three days of incubation (i.e., n = 6). Errors bars overlapping with zero indicate variations between influx and efflux during the three-day incubation.

Ambient concentrations of $NO_2^-$ were mostly BDL in both years, likely contributing to low net sediment fluxes (Figure 12). From April through July 2020 in the enclosure, $NO_2^-$ fluxes ranged from a net sink of -0.49 µmol N $m^{-2}$ $h^{-1}$ in April to 91.8 µmol N $m^{-2}$ $h^{-1}$ in July, averaging 18.2 ± 18.4 µmol N $m^{-2}$ $h^{-1}$. From March through July 2021, sediments were nearly always a net $NO_2^-$ source, except for June (-2.22 µmol N $m^{-2}$ $h^{-1}$), averaging 0.68 ± 1.15 µmol N $m^{-2}$ $h^{-1}$ in the enclosure. From April through July 2020 in the lake, $NO_2^-$ fluxes ranged from a net sink of -0.02 µmol N $m^{-2}$ $h^{-1}$ in May to 18.1 µmol N $m^{-2}$ $h^{-1}$ in July, averaging 7.92 ± 3.60 µmol N $m^{-2}$ $h^{-1}$. From March through July 2021 in the lake, sediments were nearly always a net $NO_2^-$ source, except for June (-4.75 µmol N $m^{-2}$ $h^{-1}$), averaging 3.94 ± 3.00 µmol N $m^{-2}$ $h^{-1}$.

From April through July 2020 in the enclosure, $NO_3^-$ fluxes ranged from a net sink of -95.0 µmol N $m^{-2}$ $h^{-1}$ in April to 56.3 µmol N $m^{-2}$ $h^{-1}$ in July, averaging -7.54 ± 24.4 µmol N $m^{-2}$ $h^{-1}$ (Figure 13). From March through July 2021 in the enclosure, sediments were always a net $NO_3^-$ sink, ranging from -162 µmol N $m^{-2}$ $h^{-1}$ in May to -1.77 µmol N $m^{-2}$ $h^{-1}$ in July, averaging -73.2 ± 37.7 µmol N $m^{-2}$ $h^{-1}$. From April through July 2020 in the lake, $NO_3^-$ fluxes ranged from a net sink of -254 µmol N $m^{-2}$ $h^{-1}$ in April to 5.55 µmol N $m^{-2}$ $h^{-1}$ in July, averaging -49.2 ± 51.3

μmol N $m^{-2}$ $h^{-1}$. From March through July 2021 in the lake, sediments were nearly always a net $NO_3^-$ source, except for March (-83.8 μmol N $m^{-2}$ $h^{-1}$), averaging 8.99 ± 36.4 μmol N $m^{-2}$ $h^{-1}$.

Sediments were mainly a net $NH_4^+$ source in 2020 and 2021 for both the lake and enclosure (Figure 14). From April through July 2020, $NH_4^+$ fluxes in the enclosure ranged from a net source of 279 μmol N $m^{-2}$ $h^{-1}$ in April 2020 to a net sink of -0.83 μmol N $m^{-2}$ $h^{-1}$ on June 24, 2020. Average net $NH_4^+$ fluxes during this period were 74.3 ± 54.3 μmol N $m^{-2}$ $h^{-1}$. From March through July 2021, sediments were always a net $NH_4^+$ source in the enclosure, averaging 128 ± 14.0 μmol N $m^{-2}$ $h^{-1}$. During winter 2020-2021, $NH_4^+$ fluxes in the enclosure ranged from a net sink of -0.3 μmol N $m^{-2}$ $h^{-1}$ in October to a net source of 48.1 μmol N $m^{-2}$ $h^{-1}$ in February. From April through July 2020, $NH_4^+$ fluxes in the lake ranged from a net source of 404 μmol N $m^{-2}$ $h^{-1}$ in July 2020 to a net sink of -0.07 μmol N $m^{-2}$ $h^{-1}$ on June 24, 2020. Average net $NH_4^+$ fluxes during this period were 96.3 ± 78.3 μmol N $m^{-2}$ $h^{-1}$. Similar to the enclosure, from March through July 2021, sediments were always a net $NH_4^+$ source to the lake, averaging 40.5 ± 16.9 μmol N $m^{-2}$ $h^{-1}$. During winter 2020-2021, $NH_4^+$ fluxes in the lake ranged from a net sink of -16.2 μmol N $m^{-2}$ $h^{-1}$ in February to a net source of 107 μmol N $m^{-2}$ $h^{-1}$ in November.

Ambient concentrations and net sediment fluxes for ortho-P were low throughout the sampling period (Figure 15). From April through July 2020 in the enclosure, net ortho-P fluxes ranged from -1.20 μmol P $m^{-2}$ $h^{-1}$ in May to 3.02 μmol P $m^{-2}$ $h^{-1}$ on June 24, averaging 0.52 ± 0.62 μmol P $m^{-2}$ $h^{-1}$. From March through July 2021 in the enclosure, net ortho-P fluxes ranged from -0.45 μmol P $m^{-2}$ $h^{-1}$ in July to 0.27 μmol P $m^{-2}$ $h^{-1}$ in March averaging -0.13 ± 0.15 μmol P $m^{-2}$ $h^{-1}$. From April through July 2020 in the lake, net ortho-P fluxes ranged from -0.28 μmol P $m^{-2}$ $h^{-1}$ in April to 19.8 μmol P $m^{-2}$ $h^{-1}$ in July, averaging 5.45 ± 3.65 μmol P $m^{-2}$ $h^{-1}$. From

March through July 2021 in the lake, net ortho-P fluxes ranged from -0.21 µmol P $m^{-2}$ $h^{-1}$ in March to 0.25 µmol P $m^{-2}$ $h^{-1}$ in May, averaging -0.12 ± 0.20 µmol P $m^{-2}$ $h^{-1}$.

For both the lake and enclosure, sediments were nearly always a net source of urea, except in July (-9.95 µmol N $m^{-2}$ $h^{-1}$) and August (-0.14 µmol N $m^{-2}$ $h^{-1}$) 2021 in the lake (Figure 16). From April through July 2020 in the enclosure, net urea fluxes ranged from 1.95 µmol N $m^{-2}$ $h^{-1}$ on June 12 to 13.8 µmol N $m^{-2}$ $h^{-1}$ in April, averaging 7.22 ± 2.33 µmol N $m^{-2}$ $h^{-1}$. From March through July 2021 in the enclosure, net urea fluxes ranged from 7.26 µmol N $m^{-2}$ $h^{-1}$ on June 6 to 23.2 µmol N $m^{-2}$ $h^{-1}$ in July, averaging 15.4 ± 4.45 µmol N $m^{-2}$ $h^{-1}$. From April through July 2020 in the lake, net urea fluxes ranged from -9.95 µmol N $m^{-2}$ $h^{-1}$ in July to 7.40 µmol N $m^{-2}$ $h^{-1}$ on June 12, averaging 2.09 ± 3.08 µmol N $m^{-2}$ $h^{-1}$. From March through July 2021 in the lake, sediments were always a net urea source, with fluxes ranging from 17.7 µmol N $m^{-2}$ $h^{-1}$ on June 6 to 40.1 µmol N $m^{-2}$ $h^{-1}$ in May, averaging 31.1 ± 4.79 µmol N $m^{-2}$ $h^{-1}$.

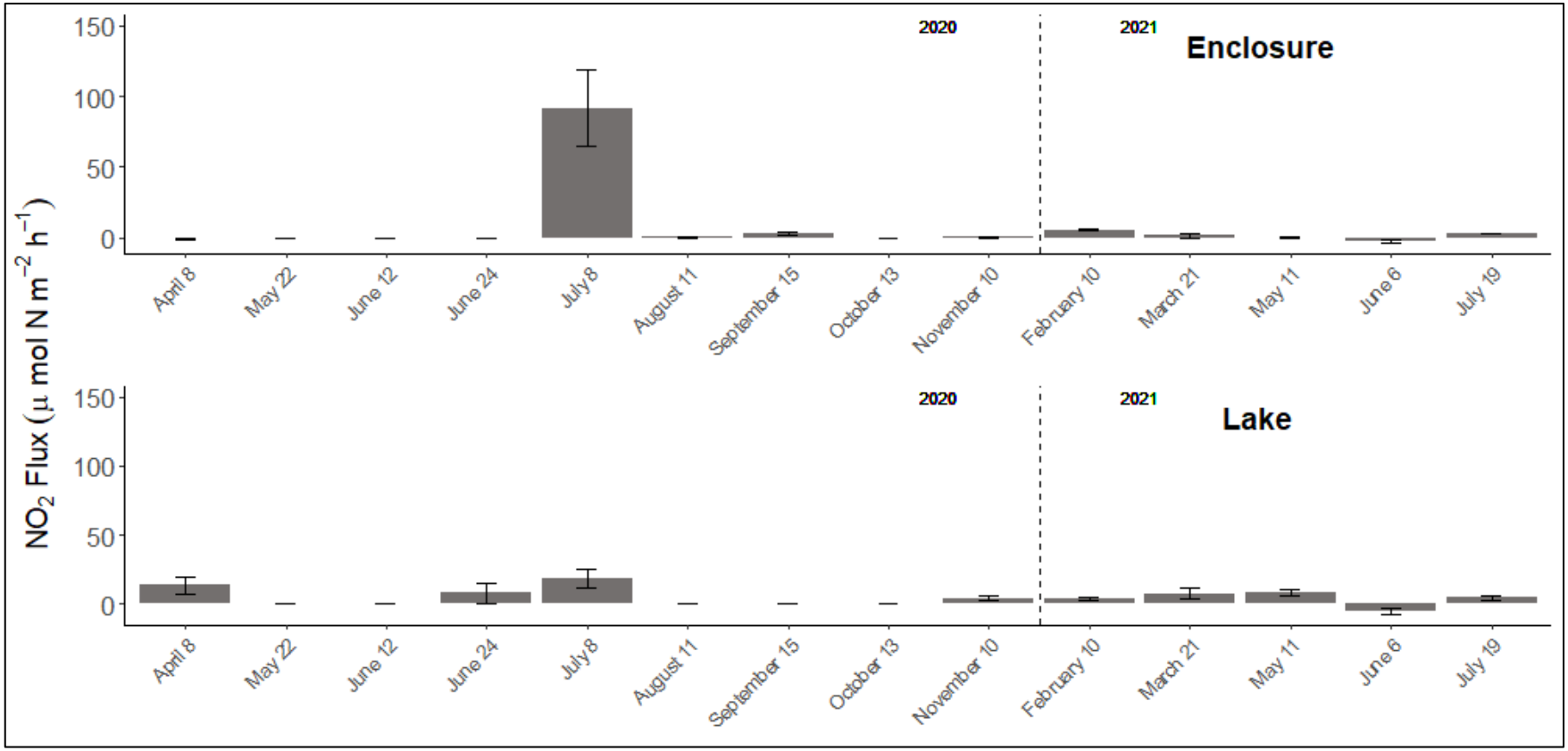


*Figure 13: Net nitrite ($NO_2^-$) fluxes from sediments at both sites from April 2020 through July 2021. Positive values indicate a net efflux from sediments (source), while a negative value indicates a net influx into sediments (sink).*

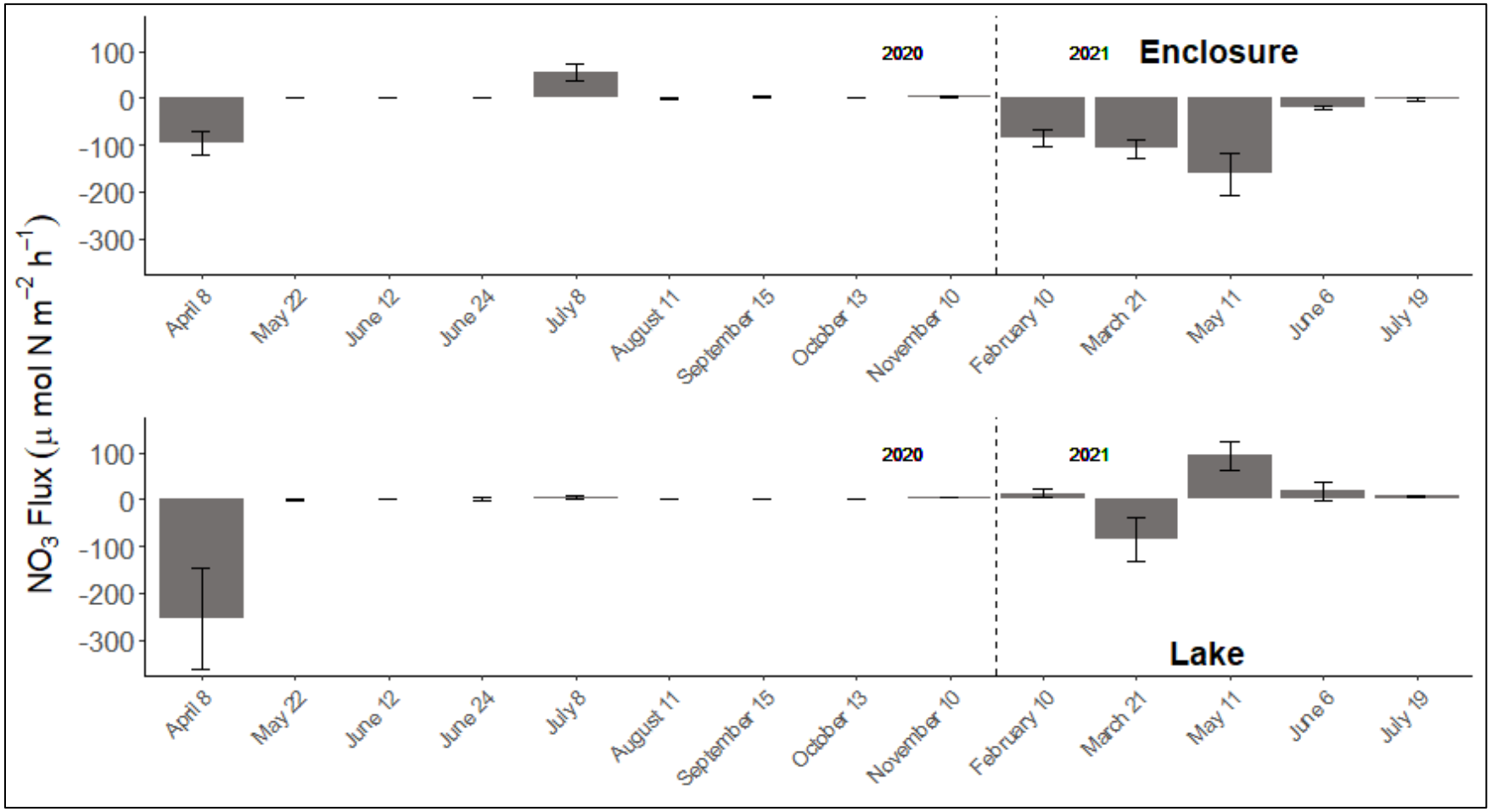


*Figure 14: Net nitrate ($NO_3^-$) fluxes from sediments at both sites from April 2020 through July 2021. Positive values indicate a net efflux from sediments (source), while a negative value indicates a net influx into sediments (sink).*

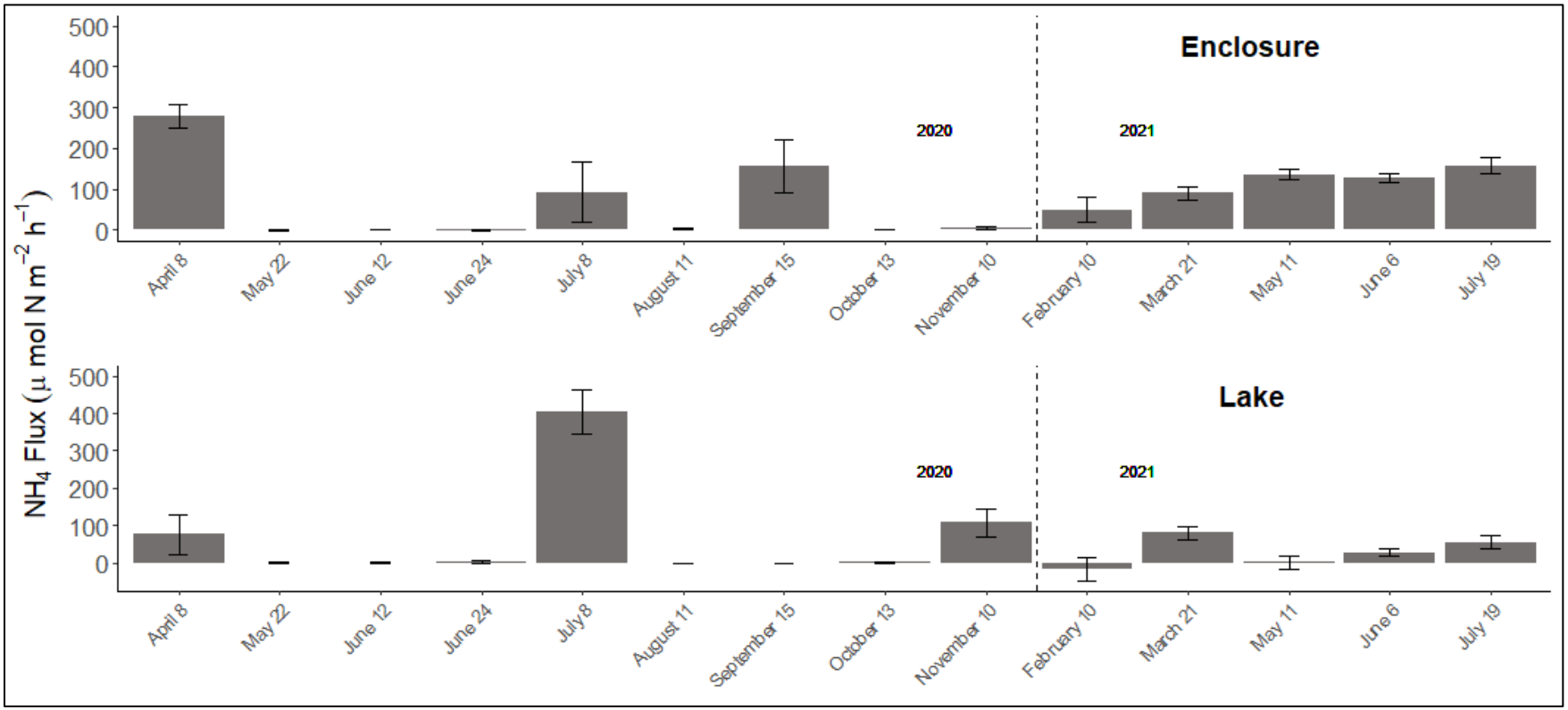


*Figure 15: Net ammonium ($NH_4^+$) fluxes from sediments at both sites from April 2020 through July 2021. Positive values indicate a net efflux from sediments (source), while a negative value indicates a net influx into sediments (sink).*

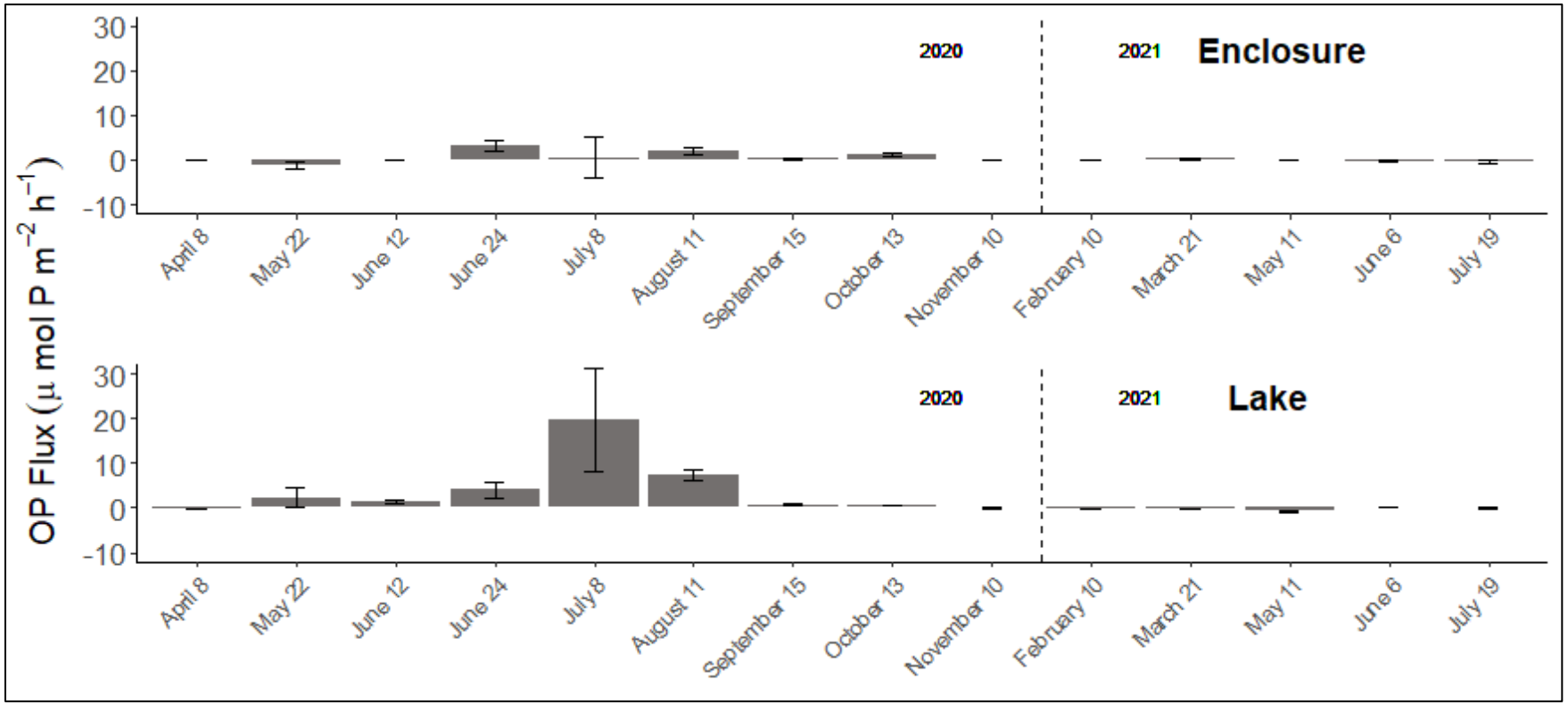


*Figure 16: Net ortho-phosphate (ortho-P) fluxes from sediments at both sites from April 2020 through July 2021. Positive values indicate a net efflux from sediments (source), while a negative value indicates a net influx into sediments (sink).*

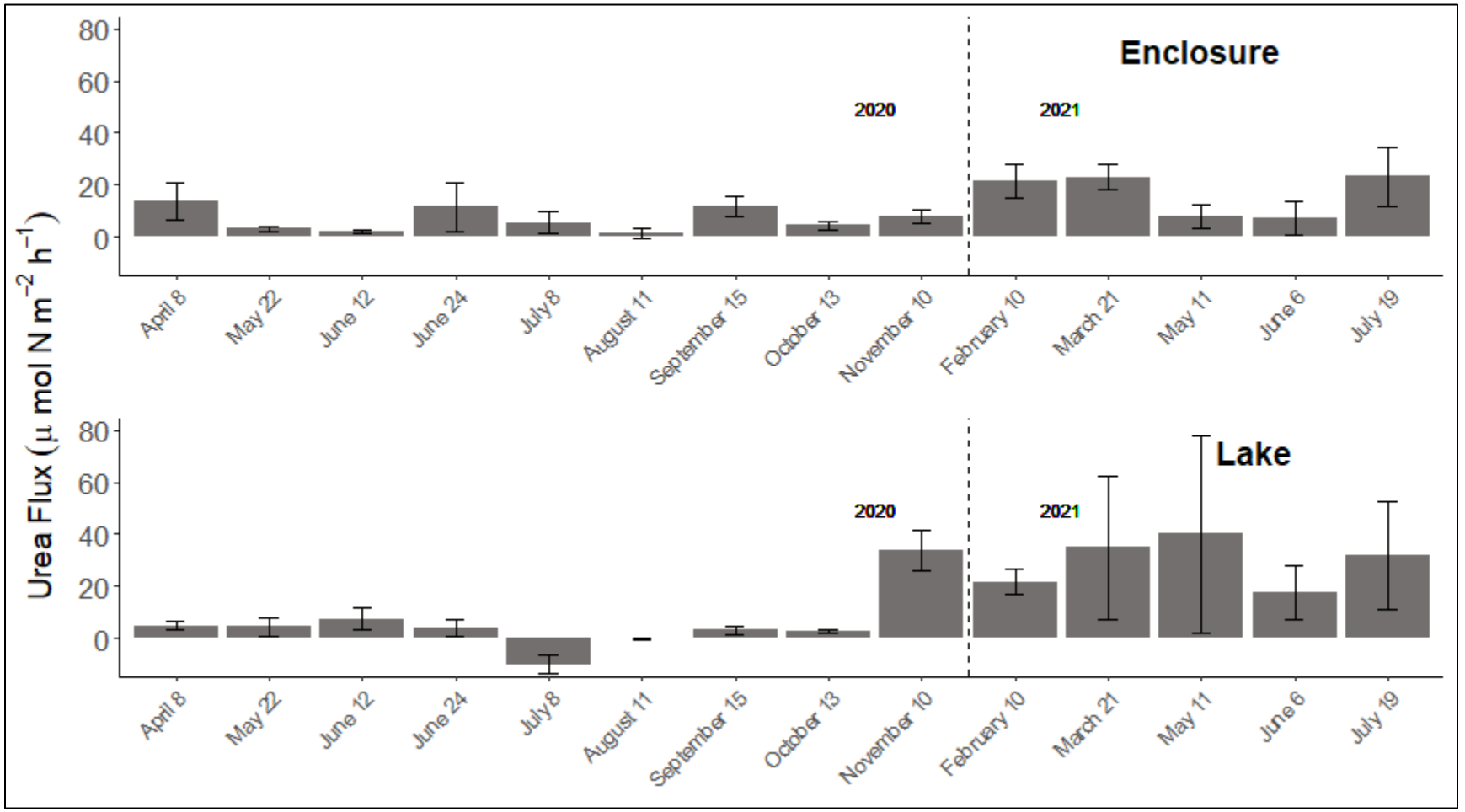


*Figure 17: Net urea fluxes from sediments at both sites from April 2020 through July 2021. Positive values indicate a net efflux from sediments (source), while a negative value indicates a net influx into sediments (sink).*

*viii. Overall sediment-water interface nutrient fluxes*

In the enclosure, sediments were nearly always a net DIN ($NO_3^-$, $NO_2^-$, $NH_4^+$) + urea source (Figure 17), except for February 2021 (-8.83 µmol N $m^{-2}$ $h^{-1}$) and May 2021 (-18.3 µmol N $m^{-2}$ $h^{-1}$). These two negative net DIN + urea fluxes were mainly comprised of $NO_3^-$. In 2020, the enclosure had three large positive pulses of DIN + urea (April, July, and September 2020), mainly comprised of $NH_4^+$. For most of 2020, net DIN + urea fluxes in the enclosure were low (< 20 µmol N $m^{-2}$ $h^{-1}$). During each sampling month in 2021 within the enclosure, a positive net $NH_4^+$ flux was measured, ranging from 48.1 in February to 158 µmol N $m^{-2}$ $h^{-1}$ in July. During these same months, a negative net $NO_3^-$ flux was measured, ranging from -162 in May to -1.78 µmol N $m^{-2}$ $h^{-1}$ in July.

In the lake, sediments were nearly always a net DIN + urea source (Figure 18), except for April 2020 (-160 µmol N $m^{-2}$ $h^{-1}$) and August 2020 (-0.57 µmol N $m^{-2}$ $h^{-1}$). The two negative fluxes of DIN + urea were mainly comprised of $NO_3^-$ (-254 µmol N $m^{-2}$ $h^{-1}$) and $NH_4^+$ (-0.44 µmol N $m^{-2}$ $h^{-1}$), respectively. In 2020, the lake had three large positive pulses of DIN + urea (April, July, and November), mainly comprised of $NH_4^+$. For most of 2020, net DIN + urea fluxes were low (< 20 µmol N $m^{-2}$ $h^{-1}$). During each sampling month in 2021 within the lake, a positive urea flux was measured, ranging from 17.7 in June to 40.1 µmol N $m^{-2}$ $h^{-1}$ in May.

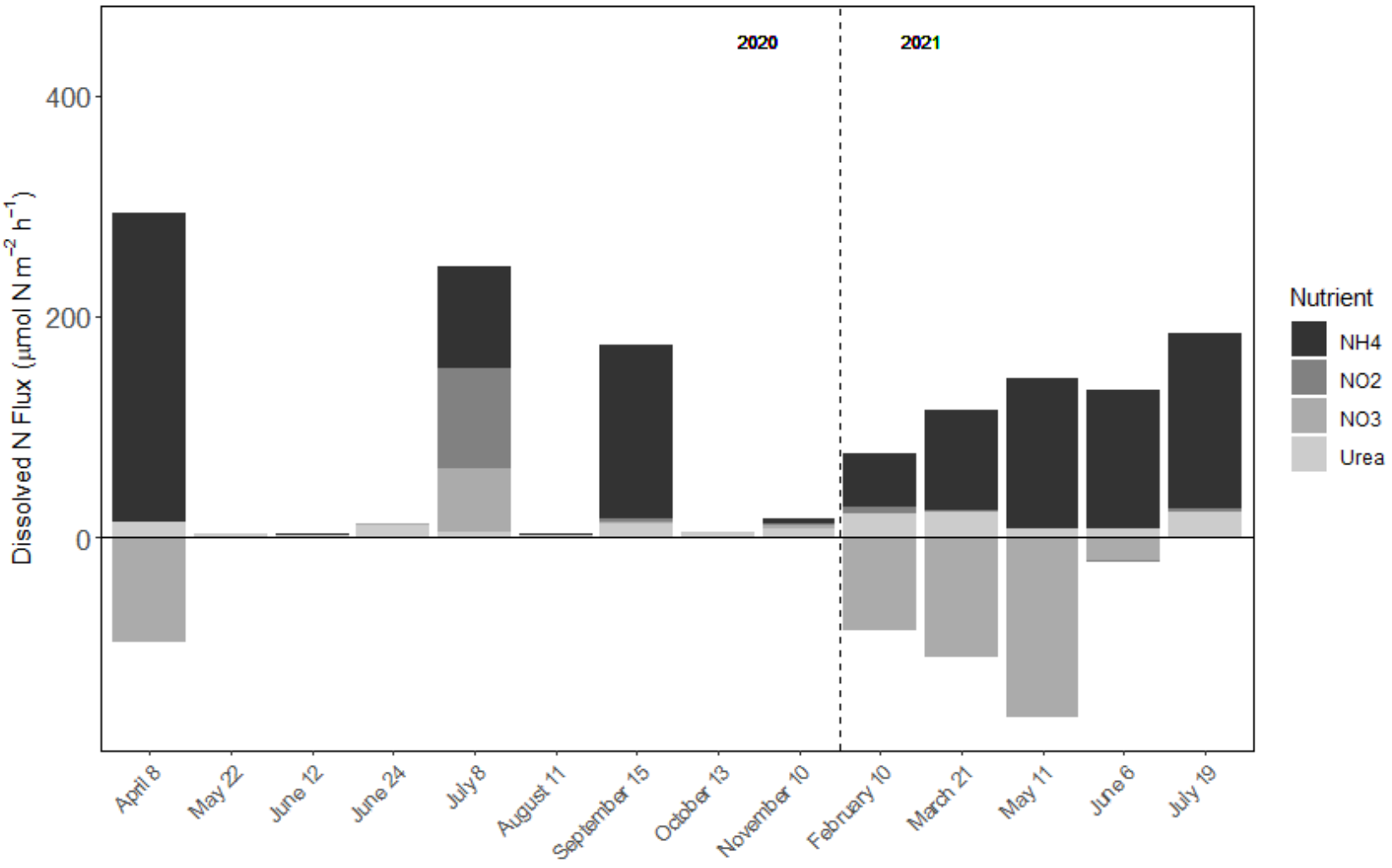


*Figure 18: Overall net DIN fluxes, plus urea, from sediments in the enclosure from April 2020 through July 2021. Positive values indicate a net efflux from sediments (source), while a negative value indicates a net influx into sediments (sink).*

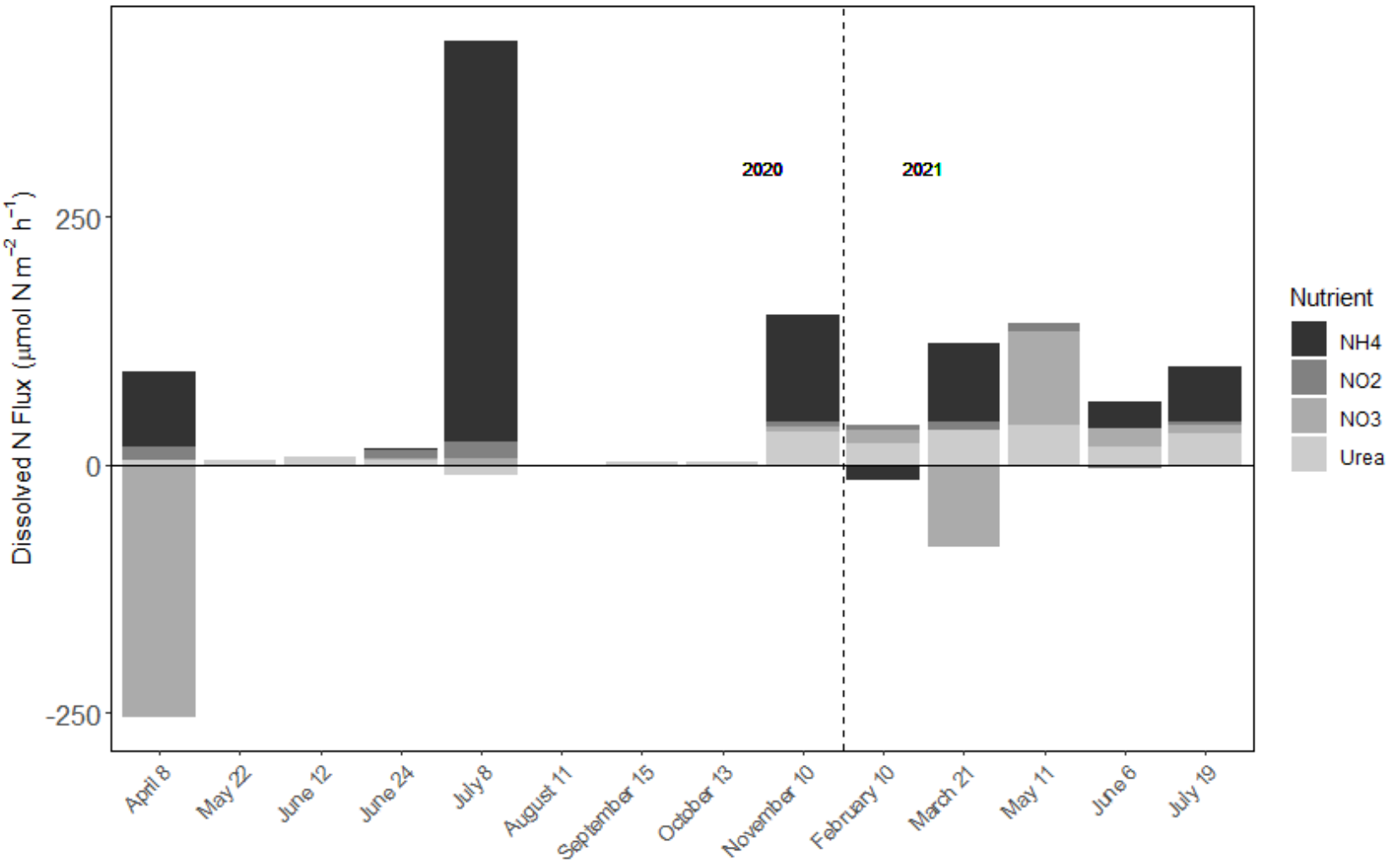


*Figure 19: Overall net DIN fluxes, plus urea, from sediments in the lake from April 2020 through July 2021. Positive values indicate a net efflux from sediments (source), while a negative value indicates a net influx into sediments (sink).*

*ix. Nitrogen cycling rates from sediment core incubations*

The net balance between $N_2$ fixation and denitrification throughout the sampling period (as net $^{28}N_2$ flux in unamended cores) is shown in Figure 19. Positive values indicate net denitrification, while negative values indicate net $N_2$ fixation. For all sampling events in 2020, except April in the enclosure, in-situ net $N_2$ fluxes were negative, indicating net $N_2$ fixation. In 2021, in-situ net $N_2$ fluxes showed net denitrification for all sampling events. In 2020 at both sites, net sediment $N_2$-fixation was observed in unamended cores at all sampling events except April. In 2021 at both sites, net denitrification was observed at all sampling events. Net sediment $N_2$ fixation differed between years in the enclosure (ANOVA; $p = 0.030$). From April through July 2020 within the enclosure, net $^{28}N_2$ fluxes from sediments ranged from -40.2 in May to 64.7 μmol N $m^{-2}$ $hr^{-1}$ in April, with an overall average of -2.76 ± 18.7 μmol N $m^{-2}$ $hr^{-1}$. From March through July 2021 within the enclosure, net $^{28}N_2$ fluxes ranged from 37.0 in May to 91.4 μmol N $m^{-2}$ $hr^{-1}$ in June, with an overall average of 62.1 ± 12.4 μmol N $m^{-2}$ $hr^{-1}$. From April through July 2020 within the lake, net sediment $^{28}N_2$ fluxes in unamended cores ranged from -74.2 in May to 105.1 μmol N $m^{-2}$ $hr^{-1}$ in April, with an overall average of -3.95 ± 30.6 μmol N $m^{-2}$ $hr^{-1}$. From March through July 2021 within the lake, net $^{28}N_2$ fluxes ranged from 21.8 in March to 120 μmol N $m^{-2}$ $hr^{-1}$ in June, with an overall average of 63.9 ± 23.5 μmol N $m^{-2}$ $hr^{-1}$.

Potential denitrification rates, measured from $^{15}NO_3^-$-amended sediment cores (as $^{28+29+30}N_2$ production plus calculated N fixation, if any) did not differ for either site between years. Potential denitrification rates in the enclosure from April through July 2020 ranged from 110 in May to 329 μmol N $m^{-2}$ $hr^{-1}$ in June, with an overall average of 203 ± 43.0 μmol N $m^{-2}$ $hr^{-1}$. From March through July 2021 within the enclosure, potential denitrification rates ranged from 133 in May to 278 μmol N $m^{-2}$ $hr^{-1}$, with an overall average of 200 ± 34.1 μmol N $m^{-2}$ $hr^{-1}$.

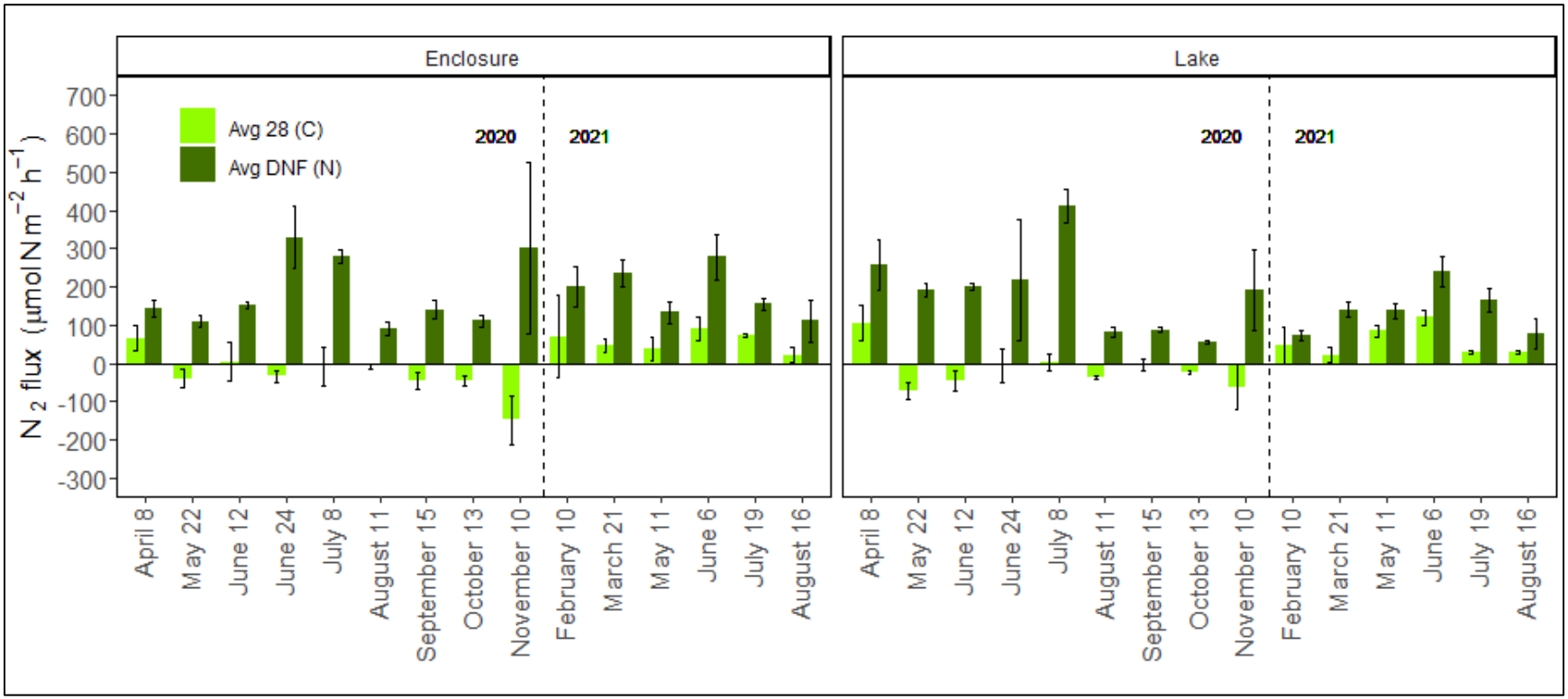


*Figure 20: Net $^{28}N_2$ fluxes from unamended cores and potential denitrification (DNF; $^{28+29+30}N_2$ production plus calculated N fixation, if any) from $^{15}$N-nitrate amended cores.*

# IV. DISCUSSION

## *i. P-binding treatments*

This study evaluated the effectiveness of P-binding agents (i.e., alum, Phoslock, and SeClear) to reduce P concentrations and, subsequently, inhibit cHAB blooms in a shallow, semi-enclosed area of GLSM. The study also evaluated the onset of the cHAB bloom in consecutive years to examine potential reasons for the delay in bloom initiation in 2021. The overall outcome of the study, based on these evaluations, was to provide further evidence for the need for long-term reductions of both N and P loading from watersheds, instead of short-term, expensive applications that may not be effective in large, hyper-eutrophic lakes, such as GLSM.

For decades, water quality standards calling for P reductions have been in place, as it is generally accepted that P can limit productivity in lakes (Schindler, 2012). However, lakes with substantial P legacy stores in sediments can delay water quality improvements after external nutrient loading reductions, which explains why P-binding agents have been used for decades to remove excess P from the water column and inhibit its release from sediments (Huser et al., 2016). While these treatments have been effective in many lakes globally, results are variable based on dosage, morphology of the treatment area, and water residence time (Huser et al., 2016). Correct dosages and applications are highly dependent on accurate estimates of P inputs from the sediments; thus, many treatment failures are a result of a lack of full understanding of the system (Huser et al., 2016; Nogaro et al., 2013).

GLSM is a large, shallow, hyper-eutrophic, polymictic lake with a large, agricultural watershed, making it a difficult system to treat, as shown through failures of previous P-binding treatments (Nogaro et al., 2013). The residence time for GLSM is in excess of 500 d (Filbrun et al., 2013). Higher residence times favor the proliferation of *Planktothrix* blooms, as cyanobacteria have slower growth rates than eukaryotes (Hamilton et al., 2016; Steffen et al., 2014). No studies have established baseline conditions for the West Beach enclosure, specifically before treatments occurred, indicating a possible lack of understanding of nutrient inputs into the semi-enclosed system.

During the initial alum treatment in 2020, which was delayed until June 2020 due to the COVID-19 pandemic, the cyanobacterial bloom was well underway, with chl-a, phycocyanin, and microcystin concentrations of 212, 205, and 45.6 µg $L^{-1}$, respectively, on the day before alum application (06/08/2020). Chl-a and phycocyanin levels dropped to 74.0 and 70.0, respectively, on the day of alum treatment, perhaps indicating an immediate effect from the treatment. Decreases in overall biomass likely led to a decrease in DO concentration, from 11.5 mg $L^{-1}$ on the day of the treatment to 6.9 mg $L^{-1}$ the day after the treatment, as algal biomass was decomposed, leading to remineralization of N and P. Roughly two weeks later, on 06/22/2020, chlorophyll-a, phycocyanin, and microcystin levels increased to 255, 244, and 66.4 µg $L^{-1}$, respectively.

Weeks before the treatment (05/22/2020), ortho-P concentrations were near detection limits in the enclosure (0.016 µM), indicating that most of the bioavailable P in the water column had already been sequestered into biomass. While TP concentration in the enclosure decreased from 12.1 to 8.32 µM from 06/08/2020 to 06/10/2020, TP concentrations quickly rebounded (Figure 6) to 9.14 µM on 06/12/2020 and 11.1 µM on 06/15/2020. Additionally, TP

concentrations in the lake decreased from 8.39 to 6.73 µM from 06/08/2020 to 06/10/2020, indicating that other factors, beyond the alum treatment, influenced overall TP concentrations.

Likely due to the harsh winter of 2020-2021 and lower spring nutrient loading, the bloom in spring to early summer 2021 was smaller than the bloom in 2020, with chl-a, phycocyanin, and microcystin levels at 50, 8, and 0.41 µg $L^{-1}$, respectively, on 05/12/2021, a day before the first Phoslock treatment. Similar to the alum treatment, chlorophyll-a and phycocyanin concentrations decreased to 14.5 and 0.5 mg $L^{-1}$, respectively, on 05/19/2021, while DO levels decreased from 11 to 6.25 mg $L^{-1}$. Reductions in chlorophyll-a and phycocyanin, lasting about one week, indicated some initial success from the treatment. TP concentrations increased from 2.71 µM the day before treatment to 3.28 µM on multiple weeks after treatment. A week later, on 05/26/2021, chlorophyll-a reached 171 µg $L^{-1}$; however, phycocyanin and microcystin concentrations remained low (5.5 and 0.3 µg $L^{-1}$, respectively), indicating that non-cyanobacterial species may have benefitted from higher TP concentrations and temperatures.

After the first Phoslock treatment in May 2021, chl-a concentrations decreased to 37.5 and 31 µg $L^{-1}$ in the enclosure and lake, respectively. Since the lake and enclosure both experienced decreased algal biomass, it is unlikely that the Phoslock treatment can explain the decrease in algal biomass in the enclosure. Chl-a and phycocyanin concentrations remained lower for roughly a week after Phoslock application. However, after the second Phoslock treatment on 06/11/2021, in both the enclosure and lake, TP, chlorophyll-a, and phycocyanin levels increased beyond pre-treatment levels in subsequent weeks. Unlike the first two treatments, no decrease in DO was detected; however, increases in turbidity after Phoslock treatment suggested resuspension of nutrient-rich sediments, leading to the highest biomass and TP concentrations of the growing season to that point.

The third Phoslock treatment (07/02/2021) followed the heaviest precipitation month for the 2021 sampling period, which was observed in the lake as decreased conductivity, increased turbidity, and increased TP following the treatment, indicating that external nutrient loading may have impacted treatment effectiveness. While chl-a and phycocyanin decreased from 109 and 38 to 46.5 and 4.6 µg $L^{-1}$, respectively, from the day before to the day after treatment, these values increased to 282 and 42 µg $L^{-1}$, respectively, only five days after the treatment.

The fourth Phoslock treatment displayed similar effects as the first three treatments; however, perhaps due to increases in external nutrient loading, TP concentrations were high, reflecting a larger amount of biomass. Algal biomass did not decrease immediately as in the previous treatments; however, the lake saw decreases in total chl-a that was not experienced within the enclosure. The stability of chl-a within the enclosure, in comparison to the decreases in the surrounding lake, indicates that external influences were stabilizing biomass levels.

*ii. Ice cover, and reductions in precipitation and nutrient loading between years*

Combined with the complete ice-over of GLSM in Feb. 2021 (at least 10 cm of ice cover), reduced precipitation and associated nutrient loading likely inhibited cyanobacterial growth that typically occurs in spring and early summer and impacted cyanobacterial bloom dynamics for summer 2021. Bloom initiation was delayed by ~3 months in 2021, and an unusually small bloom developed in comparison to individual years in the previous decade (Jacquemin et al., 2023). As a result, the state's "no-contact" advisory was lifted in late May 2021 for the first time in twelve years.

Ice cover in lakes, while largely understudied, negatively affects algal communities due to low water temperatures, isolation from the atmosphere and surrounding landscape, and reduced light penetration (Bertilsson et al., 2013; Cavaliere & Baulch, 2019). Increasing ice-free

years is changing the phytoplankton communities in some lakes (Hampton et al., 2017). Under-ice denitrification affects $NO_3^-$ availability in the spring, which may be an important control on spring diatom blooms (Cavaliere & Baulch, 2019). In ice-free winters, rather than $NO_3^-$ concentrations building up under the ice due to nitrification and fewer phytoplankton, $NO_3^-$ concentrations can remain low while cyanobacterial biomass remains high, which will limit the spring diatom bloom (Cavaliere & Baulch, 2019). Considering that it is not uncommon for GLSM to experience a year-round cyanobacterial bloom, microcystin, phycocyanin, and chl-a concentrations decreasing below 1, 20, and 35 µg L-1, respectively, in 2021 was historically unusual (Jacquemin et al., 2023).

In a changing world, harsh winters with ice cover may become less frequent on GLSM, reducing the strength of factors that can inhibit cyanobacterial blooms, and allowing for 'seeding' blooms to persist over the winter and into early spring. Globally, lakes have warmed by 0.34°C decade$^{-1}$ between 1985 and 2009, and the most rapidly warming lakes are warming at 0.53 to 0.72°C decade$^{-1}$ (O'Reilly et al., 2015). Lakes in the Great Lakes region, such as GLSM, are within one region that is warming faster than the global average (O'Reilly et al., 2015). Thus, the anomalous winter of 2020-2021 is likely to occur less frequently in the future.

Historical data for GLSM over the past decade indicates that there have been multiple years (i.e., 2009, 2010, 2014, 2017) where temperatures dropped low enough to produce ice coverage, similar to 2020-2021, but precipitation and nutrient loading remained consistent (Jacquemin et al., 2023). These other years did not exhibit a similar delay in cyanobacterial bloom onset as in 2021, with the difference possibly explained by reduced external nutrient loading due to a dryer than usual late winter/early spring period. Nutrient (N and P) loading for winter 2020-2021 from Chickasaw Creek was the lowest of the last decade (Jacquemin et al.,

2023). Overall, reductions in spring N and P loading may have delayed cyanobacteria proliferation and dominance in GLSM, which is uncharacteristic of the past decade in the lake (Jacquemin et al., 2023). However, average nutrient loading levels returned in summer, and bloom biomass returned to > 300 µg $L^{-1}$ by July 2021.

Additionally, since both the lake and enclosure had biomass differences between years but not sites, we can conclude that the treatments had little to no effect on cyanobacteria bloom dynamics in the enclosure. Biomass differences between years for each site are likely best explained by reduced nutrient loading, but other factors cannot be excluded. Since microcystin and phycocyanin are indicative of cyanobacterial blooms, the lower values in 2021 indicate that it is likely other algal taxa dominated the phytoplankton community in late spring 2021. Diatoms are competitive at $NO_3^-$ uptake and storage, while cyanobacteria outcompete other species for $NH_4^+$ and urea (Lomas & Glibert, 2000 and Herrero et al., 2001, respectively).

Multiple studies show the importance of reducing external nutrient loading into GLSM during winter and spring (Filbrun et al., 2013; Jacquemin et al., 2018, 2023). The timing of nutrient reduction is important because cyanobacteria can sustain bloom biomass by accessing remineralized and recycled N and P in the water column and released from sediments (Filbrun et al., 2013; Hampel et al, 2019), often referred to as internal nutrient loading. Filbrun et al. (2013) conducted mesocosm experiments mimicking GLSM and found that decoupling GLSM from external nutrient loading during summer did not affect short-term improvements in water quality due to internal P loading (internal N loading was not examined; Filbrun et al., 2013).

In this study, it was found that internal loading of ortho-P from April through July 2020 was 24 to 124 times larger ($5.50 \times 10^9$ to $2.84 \times 10^{10}$ mg ortho-P) than external loading ($2.28 \times 10^8$ mg SRP) from Chickasaw Creek, from January through July 2020, depending on if the

abnormally high ortho-P flux month of July 2020 is included. In 2021, internal loading of ortho-P from March through July 2021 was a net sink (-5.14 x $10^8$ mg ortho-P), which more than accounted for the external SRP loading from Chickasaw Creek from January through July 2021 (5.25 x $10^7$ mg SRP). It must be noted that internal load is ultimately driven by external load, and the focus of this study was within the most productive months of the year; thus, analysis over the full year will bring the external and internal loads closer. However, these results ultimately mean that if we reduce the external load during the winter and spring months, we will reduce the internal load during the summer months, which is shown to be inadequate to drive the bloom alone.

Filbrun et al. (2013) concluded that tributary P loading during late winter to early spring supplies sufficient P to meet cyanobacterial growth and maintenance requirements, including from internal P loading during summer (Filbrun et al., 2013). These conclusions were supported by model outputs showing that week-to-week variability in summer toxin concentrations were unlikely to be influenced by that week's nutrient loading, but rather that summer biomass is linked to total external nutrient load (Jacquemin et al., 2023). Positive effects on GLSM water quality after application of manure during winter was prohibited provides additional credence to this interpretation (Jacquemin et al., 2018). These findings suggest that external nutrient loading (P and N) is critical for bloom formation, and that internal nutrient loading from organic matter remineralization, supplemented with episodic external loads during summer, allows the bloom to sustain itself during warm, rapid growth periods that often coincide with lower precipitation.

*iii. Water Quality Improvements – Net Denitrification in Unamended Cores*

GLSM is often N-stressed during peak bloom months, likely due to early and rapid N uptake by cyanobacteria, which supports production of nitrogenous microcystins (Paerl et al., 2020;

Steffen et al., 2014). In 2020 for both the lake and enclosure, possible N-stress is evident as early as May, as $NH_4^+$, $NO_3^-$, urea, and $NO_2^-$ concentrations were either at or near detection limits from May through July 2020 (Tables 5 & 6). Phycocyanin concentrations were already in excess of 125 µg $L^{-1}$, and microcystin concentrations were well above the 24 µg $L^{-1}$ recreational exposure limit set by the World Health Organization (WHO, 2021). Even during N-stress, algal biomass and toxins remained high during the summer, indicating that internal N loads were supporting the bloom.

In 2020, net denitrification was observed in unamended cores only in April, when water column $NO_3^-$ was abundant (Figure 19). Net N fixation was observed in unamended cores for all other 2020 sampling events (Figure 21). However, $N_2$ production, likely via denitrification, (annamox accounted for less than 10% in all months; Figure 24) was stimulated when $NO_3^-$ was introduced to the system in $^{15}NO_3^-$ amended cores, indicating that denitrifying bacteria were limited by $NO_3^-$ availability, not organic matter. HAB biomass provides organic matter to support denitrification, but $NO_3^-$ availability limiting denitrification has been shown in hypereutrophic lakes in China (Wu et al. 2019) and western Lake Erie (Boedecker et al., 2020). Other studies on lakes in agricultural systems with low $NO_3^-$ concentrations have also shown relatively low denitrification rates, suggesting that denitrification is limited by both $NO_3^-$ and temperature when DIN is low but biomass is high (Cavaliere & Baulch, 2019).

In both the lake and enclosure, a transition occurred from net N fixation during nearly all sampling events in 2020 to net denitrification in 2021 (as net $^{28}N_2$ flux; Figure 20 & 23), and lower cyanobacterial biomass may have contributed to this shift. Denitrification is the reduction of $NO_3^-$ to $N_2$, which is not bioavailable for most organisms, thus removing N from the system (Burgin & Hamilton, 2007; Scott et al., 2008). Removal of N is an important ecosystem service

because TN concentration is correlated to microcystin concentrations in GLSM (Jacquemin et al., 2023), and non-N-fixing cyanobacteria require combined N to produce biomass and toxins.

In 2020, net denitrification in April accounted for the removal of 2.81 x $10^{10}$ mg N when extrapolated for the entire lake; however, it did not nearly account for the external and internal load from January through July 2020 (2.94 x $10^{11}$ mg N). Denitrification did account for the external loading from Chickasaw Creek from January through July 2020, as it was ~2.5 times larger than the external load (1.19 x $10^{10}$ mg N). In 2021, net denitrification occurred in June and July, removing 7.82 x $10^{10}$ mg N; however, it did not account for the external and internal load from January through July 2021 (2.18 x $10^{11}$ mg N). Denitrification did account for the external loading from Chickasaw Creek from January through July 2021, as it was ~12 times larger than the external load (6.62 x $10^{9}$ mg N). Since Chickasaw Creek accounts for a quarter to a fifth of all external loading, it could be stated that denitrification in 2021 may account for the entirety of external N loading (Jacquemin et al., 2018). By delaying the onset of the cyanobacterial bloom with reduced external nutrient loading, denitrifying bacteria may be able to remove a substantial portion of the N in the system that would otherwise be cycled internally to provide substrate for producing bloom biomass and toxicity.

Net $^{28}N_2$ fluxes in unamended cores were similar to those observed in sediments in other eutrophic systems, such as Lake Taihu (McCarthy et al., 2007), Lake Okeechobee (James et al., 2011), Waquoit Bay, MA (Newell et al., 2016), western Lake Erie (Boedecker et al., 2020) and Texas reservoirs (Grantz et al., 2012). There were no indications that denitrification was limited by the P-binding treatments, as noted in a previous study, considering there was no significant difference in denitrification rates between the lake and enclosure in either year.

*iv. Water Quality Improvements - Oxygen Demand*

Analyzing oxygen demand in the water column and sediments provides a better understanding of biomass remineralization, which can release nutrients into the water column and decrease DO levels at the SWI, potentially leading to further nutrient releases from sediments (Gardner et al., 2009). The lower SOD in 2021 for both sites may be related to reduced nutrient loading, and subsequently lower biomass, over the winter and spring months. Higher biomass in 2020 may have both caused higher volumetric rates of respiration in the water column, and, ultimately, allowed more organic matter to sink to the sediments, where it could be remineralized, generating higher SOD. High SOD (>1500 μmol $O_2$ $m^{-2}$ $hr^{-1}$) in GLSM in summer is comparable to other productive systems, such as western Lake Erie (Boedecker et al., 2020) and hypoxic zones in the Gulf of Mexico (McCarthy et al., 2013), which are similarly affected by cHABs. Sediment $NH_4^+$ and P release were correlated ($R^2 = 0.265$) in this study, as expected.

WCOD did not differ between years for either site, indicating that microbial respiration, including remineralization of algal biomass, remained consistent despite the differences in algal biomass between years. Internal recycling of both N and P can sustain algal productivity in other shallow, hypereutrophic lakes, such as Lake Taihu in China (Xu et al., 2021) . DO concentrations decreased immediately following multiple treatments, suggesting that organic matter remineralization may have been stimulated. This remineralization likely released N and P, which may have enhanced the bloom in the weeks after treatments.

*v. Lack of N management*

While removing excess P from the water column is useful for controlling algal biomass, P-binding treatments do not provide a solution for excess N in the water column or release of bioavailable N from sediments. In this study, the main N forms released from sediments were

$NH_4^+$ and urea, which are highly bioavailable, chemically reduced forms of N that are favorable for non-$N_2$-fixing, toxic cyanobacteria, even in N-depleted systems (Hampel et al., 2019; McCarthy, et al., 2013; Newell et al., 2019). Internal regeneration and recycling of $NH_4^+$ supports cHAB blooms in N-stressed systems, with regeneration rates far in excess of external N loading (McCarthy, et al., 2013; Paerl et al., 2011; Xu et al., 2021). Although external nutrient loading was reduced in late winter to early spring, legacy loads of $NH_4^+$ and urea were still released into the water column, providing additional substrate for the bloom to sustain itself.

From April through July 2020, internal loading of DIN and urea was ~5 to 24 times larger ($5.80 \times 10^{10}$ to $2.82 \times 10^{11}$ mg of N) than external TN loading ($1.19 \times 10^{10}$ mg of N) from January through July 2020, depending on if the abnormally high N flux month of July 2020 is included. From April through July 2021, internal loading of DIN and urea was ~32 times larger ($2.12 \times 10^{11}$ mg of N) than external TN loading ($6.62 \times 10^{9}$ mg of N) from January through July 2021. In both years, $NH_4^+$ and urea were the dominant forms of DIN in the water column. However, as mentioned previously, the internal load is ultimately fed by the external load, and cyanoHAB bloom biomass is directly related to the external nutrients (Jacquemin et al., 2023; Kane et al., 2014). Biomass respiration drives the internal load in any given year, thus reducing the external load will reduce internal load, as demonstrated in 2021.

In this study, enhanced rates of $NH_4^+$ flux were shown in the treated sediments within the enclosure in June and July 2021. The enclosure had an $NH_4^+$ flux of 126 and 158 µmol N $m^{-2}$ $hr^{-1}$ in June and July 2021, compared to 27.8 and 54.4 µmol N $m^{-2}$ $hr^{-1}$ for June and July 2021 in the lake. A previous study monitoring alum treatments on GLSM showed similar effects in each of their treatment sites (Nogaro et al., 2013). The release of highly bioavailable ammonium from

the treated sediments can enhance biomass and toxicity of non-N-fixing cyanobacteria (Davis et al., 2015; Hampel et al., 2018).

TN, especially reduced N forms, is a key driver of cHAB blooms in multiple shallow, eutrophic lakes, including GLSM (Hoffman et al., 2022; Jacquemin et al., 2023; McCarthy et al., 2016; Newell et al., 2019; Steffen et al., 2014). Additionally, recent research has suggested that sole reduction of P loads have caused imbalances in eutrophic systems that favor non-diazotrophic cHABs (Gobler et al., 2016; Hellweger et al., 2022). The western basin of Lake Erie is a prime example of this concept, as prior to P load reductions in the 1970s, diazotrophic cHABs were common; however, a shift occurred in the mid-1990s to a dominance of non-diazotrophic cyanobacteria, such as *Microcystis* (Newell et al., 2019). By continuing to focus only on P load reductions in GLSM, nutrient imbalances will continue to expand and favor the already dominant non-diazotrophic cyanobacteria.

# V. CONCLUSION

This study was conducted on one of the most nutrient polluted lakes in the USA and illustrates that chemical treatments aimed at reducing P concentrations, although effective in some cases, may not be effective in large, shallow, hyper-eutrophic systems like GLSM. The chemical treatments, linear aeration, sediment dredging, and attempts at reductions in water transfer between the lake and enclosure did not result in long-term reductions in cyanobacteria biomass and toxicity. Short-term interventions for lake nutrient and cyanobacteria bloom management were not effective for more than a week in GLSM, if at all, and long-term solutions require that external loads of both N and P are reduced. Additionally, although not specified in this study, based on previous chemical interventions with alum on GLSM, treatments may have adverse effects on N cycling and denitrification that can enhance, instead of inhibit, bloom biomass (Nogaro et al., 2013) and toxicity.

The potential for long-term reductions in external nutrient loads, such as implementing best management practices (BMPs) and the restoration or creation of wetlands surrounding the lake, should continue to be the focus of lake managers for GLSM. The distressed watershed rules package, established in 2011, is one such initiative that has shown success in GLSM by reducing external nutrient loads; however, additional efforts are necessary to reduce both the overall volume and concentration of external loads (Hoorman et al., 2008).

Dual nutrient management, focused on reducing external loading, especially from late winter to early spring, is likely the only long-term solution to eutrophication and cyanobacteria blooms in GLSM and similar lakes afflicted with non-N-fixing, toxin-producing cyanobacterial taxa. The harsh winter of 2020-2021 and reduction of overall nutrient loading within the early months of 2021 were anomalies that likely inhibited the ability of cyanobacteria to outcompete other algal species, leading to reduced toxicity and enhanced denitrification rates. Denitrification is a valuable ecosystem service that removes excess N that non-N-fixing cyanobacteria, such as *Planktothrix* and *Microcystis*, thrive on. The overall reduction in biomass coincided with lower SOD in 2021. The fish kill in 2020, which affected the lake and surrounding community, could probably be avoided by reducing external nutrient loads, and, subsequently, algal biomass. Additionally, lower biomass can lead to improved oxygen conditions in bottom water (via lower SOD), thus inhibiting internal loading from sediments, which provide additional nutrients for sustaining these recurring algal blooms.

While removing excess P is vital for eutrophication and algal bloom management, external and internal loads of both N and P in GLSM are substantial and contribute to bloom formation in both the short and long-term. Furthermore, with no attention on managing external and internal N loading, which drives biomass and toxin production for these blooms, leading to non-contact advisories, lake management efforts are likely to be unsuccessful. In shallow lakes, such as GLSM, precipitation events, storms, and natural disturbances, may provide sufficient nutrients to initiate a bloom, which may then rely on internal nutrient loading to sustain biomass. As observed over the past decade, toxin-producing cyanobacteria can proliferate throughout summer months, and even through winter, unless anomalous conditions are present, such as during the winter and early spring 2021.

The most effective approach to returning GLSM to a lake providing recreational and commercial opportunities for local and regional economies is to continue nutrient and ecosystem monitoring and establish policies that govern maximum daily and seasonal loads of both N and P. Chemical treatments targeting P-inactivation have proven ineffective in multiple attempts. Implementing agricultural BMPs, which has already shown a promising start in reduced nutrient loads (Jacquemin et al., 2018; Jacquemin et al. 2023), along with constructing wetlands (Jacquemin et al., 2020), will aid in achieving the overall nutrient loading reductions needed to improve water quality and delivery of ecosystem services in GLSM and similarly affected lakes.

# VI. REFERENCES

An, S., & Gardner, W. S. (2002). Dissimilatory nitrate reduction to ammonium (DNRA) as a nitrogen link, versus denitrification as a sink in a shallow estuary (Laguna Madre/Baffin Bay, Texas). *Marine Ecology Progress Series, 237*, 41–50. https://doi.org/10.3354/meps237041

Baustian, M. M., Hansen, G. J. a., de Kluijver, A., Robinson, K., Henry, E. N., Knoll, L. B., Rose, K. C., & Carey, C. C. (2014). Linking the bottom to the top in aquatic ecosystems: mechanisms and stressors of benthic-pelagic coupling. *Eco-DAS X Symposium Proceedings*, 25–47. https://doi.org10.4319/ecodas.2014.978-0-9845591-4-5.25

Bertilsson, S., Burgin, A., Carey, C. C., Fey, S. B., Grossart, H. P., Grubisic, L. M., Jones, I. D., Kirillin, G., Lennon, J. T., Shade, A., & Smyth, R. L. (2013). The under-ice microbiome of seasonally frozen lakes. *Limnology and Oceanography*, *58*(6), 1998–2012. https://doi.org/10.4319/lo.2013.58.6.1998

Boedecker, A. R., Niewinski, D. N., Newell, S. E., Chaffin, J. D., & McCarthy, M. J. (2020). Evaluating sediments as an ecosystem service in western Lake Erie via quantification of nutrient cycling pathways and selected gene abundances. *Journal of Great Lakes Research*, 48, 920–932, https://doi.org/10.1016/j.jglr.2020.04.010

Burgin, A. J., & Hamilton, S. K. (2007). Have we overemphasized the role of denitrification in aquatic ecosystems? A review of nitrate removal pathways. *Frontiers in Ecology and the*

*Environment*, *5*(2), 89–96. https://doi.org/10.1890/1540-9295(2007)5[89:HWOTRO]2.0.CO;2

Byrnes, D. K., Van Meter, K. J., & Basu, N. B. (2020). Long-term shifts in U.S. nitrogen sources and sinks revealed by the new TREND-nitrogen data set (1930–2017). *Global Biogeochemical Cycles*, *34*(9), 1–16. https://doi.org/10.1029/2020GB006626

Canfield, D. E., Glazer, A. N., & Falkowski, P. G. (2010). The evolution and future of earth's nitrogen cycle. *Science*, *330*(6001), 192–196. https://doi.org/10.1126/science.1186120

Cavaliere, E., & Baulch, H. M. (2019). Winter nitrification in ice-covered lakes. *PLoS ONE*, *14*(11), 1–21. https://doi.org/10.1371/journal.pone.0224864

Chaffin, J. D., Bratton, J. F., Verhamme, E. M., Bair, H. B., Beecher, A. A., Binding, C. E., Birbeck, J. A., Bridgeman, T. B., Chang, X., Crossman, J., Currie, W. J. S., Davis, T. W., Dick, G. J., Drouillard, K. G., Errera, R. M., Frenken, T., MacIsaac, H. J., McClure, A., McKay, R. M., … Zhou, X. (2021). The Lake Erie HABs Grab: A binational collaboration to characterize the western basin cyanobacterial harmful algal blooms at an unprecedented high-resolution spatial scale. *Harmful Algae*, *108*(July), 102080. https://doi.org/10.1016/j.hal.2021.102080

Chaffin, J. D., Davis, T. W., Smith, D. J., Baer, M. M., & Dick, G. J. (2018). Interactions between nitrogen form, loading rate, and light intensity on *Microcystis* and *Planktothrix* growth and microcystin production. *Harmful Algae*, *73*, 84–97. https://doi.org/10.1016/j.hal.2018.02.001

Conley, D. J., Paerl, H. W., Howarth, R. W., Boesch, D. F., Seitzinger, S. P., Havens, K. E., Lancelot, C., & Likens, G. E. (2009). Controlling eutrophication: nitrogen and phosphorus. *Science*, *323*(5917), 1014–1015 http://www.jstor.org/stable/20403108.

Davenport, T., & Drake, W. (2011). Grand Lake St. Marys, Ohio - The case for source water protection: nutrients and algae blooms. In *LakeLine Magazine* (Vol. 31, Issue 3, pp. 41–46). https://www.nalms.org/wp-content/uploads/2018/09/31-3-11.pdf

Davis, T. W., Bullerjahn, G. S., Tuttle, T., McKay, R. M., & Watson, S. B. (2015). Effects of increasing nitrogen and phosphorus concentrations on phytoplankton community growth and toxicity during planktothrix blooms in Sandusky Bay, Lake Erie. *Environmental Science and Technology*, *49*(12), 7197–7207. https://doi.org/10.1021/acs.est.5b00799

Davis, T. W., Harke, M. J., Marcoval, M. A., Goleski, J., Orano-Dawson, C., Berry, D. L., & Gobler, C. J. (2010). Effects of nitrogenous compounds and phosphorus on the growth of toxic and non-toxic strains of *Microcystis* during cyanobacterial blooms. *Aquatic Microbial Ecology*, *61*(2), 149–162. https://doi.org/10.3354/ame01445

Filbrun, J. E., Conroy, J. D., & Culver, D. A. (2013). Understanding seasonal phosphorus dynamics to guide effective management of shallow, hypereutrophic Grand Lake St. Marys, Ohio. *Lake and Reservoir Management*, *29*(3), 165–178. https://doi.org/10.1080/10402381.2013.823469

Gardner, W. S., McCarthy, M. J., Carini, S. A., Souza, A. C., Lijun, H., McNeal, K. S., Puckett, M. K., & Pennington, J. (2009). Collection of intact sediment cores with overlying water to study nitrogen- and oxygen-dynamics in regions with seasonal hypoxia. *Continental Shelf Research*, *29*(18), 2207–2213. https://doi.org/10.1016/j.csr.2009.08.012

Gardner, W. S., Newell, S. E., McCarthy, M. J., Hoffman, D. K., Lu, K., Lavrentyev, P. J., Hellweger, F. L., Wilhelm, S. W., Liu, Z., Bruesewitz, D. A., & Paerl, H. W. (2017). Community biological ammonium demand: A conceptual model for cyanobacteria blooms

in eutrophic lakes. *Environmental Science and Technology*, *51*(14), 7785–7793. https://doi.org/10.1021/acs.est.6b06296

Glibert, P. M. (2017). Eutrophication, harmful algae and biodiversity — Challenging paradigms in a world of complex nutrient changes. *Marine Pollution Bulletin*, *124*(2), 591–606. https://doi.org/10.1016/j.marpolbul.2017.04.027

Glibert, P. M., Harrison, J., Heil, C., & Seitzinger, S. (2006). Escalating worldwide use of urea - A global change contributing to coastal eutrophication. *Biogeochemistry*, *77*(3), 441–463. https://doi.org/10.1007/s10533-005-3070-5

Glibert, P. M., Maranger, R., Sobota, D. J., & Bouwman, L. (2014). The Haber Bosch – harmful algal bloom (HB–HAB) link. *Environ. Res. Lett.*, *9*, https://doi.org/10.1088/1748-9326/9/10/105001

Glibert, P. M., Wilkerson, F. P., Dugdale, R. C., Raven, J. A., Dupont, C. L., Leavitt, P. R., Parker, A. E., Burkholder, J. M., & Kana, T. M. (2016). Pluses and minuses of ammonium and nitrate uptake and assimilation by phytoplankton and implications for productivity and community composition, with emphasis on nitrogen-enriched conditions. *Limnology and Oceanography*, *61*(1), 165–197. https://doi.org/10.1002/lno.10203

Gobler, C. J., Burkholder, J. M., Davis, T. W., Harke, M. J., Johengen, T., Stow, C. A., & Van de Waal, D. B. (2016). The dual role of nitrogen supply in controlling the growth and toxicity of cyanobacterial blooms. *Harmful Algae*, *54*, 87–97. https://doi.org/10.1016/j.hal.2016.01.010

Grantz, E. M., Kogo, A., & Thad Scott, J. (2012). Partitioning whole-lake denitrification using in situ dinitrogen gas accumulation and intact sediment core experiments. *Limnology and*

*Oceanography*, *57*(4), 925–935. https://doi.org/10.4319/lo.2012.57.4.0925

Griffiths, J. R., Kadin, M., Nascimento, F. J. A., Tamelander, T., Törnroos, A., Bonaglia, S., Bonsdorff, E., Brüchert, V., Gårdmark, A., Järnström, M., Kotta, J., Lindegren, M., Nordström, M. C., Norkko, A., Olsson, J., Weigel, B., Žydelis, R., Blenckner, T., Niiranen, S., & Winder, M. (2017). The importance of benthic–pelagic coupling for marine ecosystem functioning in a changing world. *Global Change Biology*, *23*(6), 2179–2196. https://doi.org/10.1111/gcb.13642

Hamilton, D. P., Salmaso, N., & Paerl, H. W. (2016). Mitigating harmful cyanobacterial blooms: strategies for control of nitrogen and phosphorus loads. *Aquat. Ecol.*, *50*, 351–366. https://doi.org/10.1007/s10452-016-9594-z

Hampel, J. J., McCarthy, M. J., Gardner, W. S., Zhang, L., Xu, H., Zhu, G., & Newell, S. E. (2018). Nitrification and ammonium dynamics in Taihu Lake, China: Seasonal competition for ammonium between nitrifiers and cyanobacteria. *Biogeosciences*, *15*(3), 733–748. https://doi.org/10.5194/bg-15-733-2018

Hampel, J. J., McCarthy, M. J., Neudeck, M., Bullerjahn, G. S., McKay, R. M. L., & Newell, S. E. (2019). Ammonium recycling supports toxic *Planktothrix* blooms in Sandusky Bay, Lake Erie: Evidence from stable isotope and metatranscriptome data. *Harmful Algae*, *81*, 42–52. https://doi.org/10.1016/j.hal.2018.11.011

Hampton, S. E., Galloway, A. W. E., Powers, S. M., Ozersky, T., Woo, K. H., Batt, R. D., Labou, S. G., O'Reilly, C. M., Sharma, S., Lottig, N. R., Stanley, E. H., North, R. L., Stockwell, J. D., Adrian, R., Weyhenmeyer, G. A., Arvola, L., Baulch, H. M., Bertani, I., Bowman, L. L., … Xenopoulos, M. A. (2017). Ecology under lake ice. *Ecology Letters*,

*20*(1), 98–111. https://doi.org/10.1111/ele.12699

Harke, M. J., Steffen, M. M., Gobler, C. J., Otten, T. G., Wilhelm, S. W., Wood, S. A., & Paerl, H. W. (2016). A review of the global ecology, genomics, and biogeography of the toxic cyanobacterium, *Microcystis* spp. *Harmful Algae*, *54*, 4–20. https://doi.org/10.1016/j.hal.2015.12.007

Heisler, J., Glibert, P. M., Burkholder, J. M., Anderson, D. M., Cochlan, W., Dennison, W. C., Dortch, Q., Gobler, C. J., Heil, C. A., Humphries, E., Lewitus, A., Magnien, R., Marshall, H. G., Sellner, K., Stockwell, D. A., Stoecker, D. K., & Suddleson, M. (2008). Eutrophication and harmful algal blooms: A scientific consensus. *Harmful Algae*, *8*(1), 3–13. https://doi.org/10.1016/j.hal.2008.08.006

Hellweger, F. L., Martin, R. M., Eigemann, F., Smith, D. J., Dick, G. J., & Wilhelm, S. W. (2022). Models predict planned phosphorus load reduction will make Lake Erie more toxic. Science. https://doi.org/abm6791

Herrero, A., Muro-Pastor, A. M., & Flores, E. (2001). Nitrogen control in cyanobacteria. *Journal of bacteriology*, 183(2), 411-425. https://doi.org/10.1128/JB.183.2.411-425.2001

Hoffman, D. K., McCarthy, M. J., Boedecker, A. R., Myers, J. A., & Newell, S. E. (2022). The role of internal nitrogen loading in supporting non-N-fixing harmful cyanobacterial blooms in the water column of a large eutrophic lake. *Limnology and Oceanography*, *67*(9), 2028–2041. https://doi.org/10.1002/lno.12185

Hoorman, J., Hone, T., Sudman, T., Dirksen, T., Iles, J., & Islam, K. R. (2008). Agricultural impacts on lake and stream water quality in Grand Lake St. Marys, western Ohio. *Water, Air, and Soil Pollution*. *193*, 309–322. https://doi.org/10.1007/s11270-008-9692-1

Huser, B. J., Egemose, S., Harper, H., Hupfer, M., Jensen, H., Pilgrim, K. M., Reitzel, K., Rydin, E., & Futter, M. (2016). Longevity and effectiveness of aluminum addition to reduce sediment phosphorus release and restore lake water quality. *Water Research*, *97*, 122–132. https://doi.org/10.1016/j.watres.2015.06.051

Jacquemin, S. J., Doll, J. C., Johnson, L. T., & Newell, S. E. (2023). Exploring long-term trends in microcystin toxin values associated with persistent harmful algal blooms in Grand Lake St Marys. *Harmful Algae*, *122*(April 2022), 102374. https://doi.org/10.1016/j.hal.2023.102374

Jacquemin, S. J., Johnson, L. T., Dirksen, T. A., & McGlinch, G. (2018). Changes in water quality of Grand Lake St. Marys watershed following implementation of a distressed watershed rules package. *Journal of Environmental Quality*, *47*(1), 113–120. https://doi.org/10.2134/jeq2017.08.0338

James, R. T., Gardner, W. S., McCarthy, M. J., & Carini, S. A. (2011). Nitrogen dynamics in Lake Okeechobee: Forms, functions, and changes. *Hydrobiologia*, *669*(1), 199–212. https://doi.org/10.1007/s10750-011-0683-7

Jančula, D., & MarŠálek, B. (2011). Critical review of actually available chemical compounds for prevention and management of cyanobacterial blooms. *Chemosphere*, *85*(9), 1415–1422. https://doi.org/10.1016/j.chemosphere.2011.08.036

Kana, T. M., Darkangelo, C., Hunt, M. D., Oldham, J. B., Bennett, G. E., & Cornwell, J. C. (1994). Membrane inlet mass spectrometer for rapid high-precision determination of N2, O2, and Ar in environmental water samples. *Analytical Chemistry*, *66*(23), 4166–4170. https://doi.org/10.1021/ac00095a009

Kane, D. D., Conroy, J. D., Peter Richards, R., Baker, D. B., & Culver, D. A. (2014). Re-eutrophication of Lake Erie: Correlations between tributary nutrient loads and phytoplankton biomass. *Journal of Great Lakes Research*, *40*(3), 496–501. https://doi.org/10.1016/j.jglr.2014.04.004

Lomas, M. W., & Glibert, P. M. (2000). Comparisons of nitrate uptake, storage, and reduction in marine diatoms and flagellates. *Journal of Phycology*, 36(5), 903-913. https://doi.org/10.1046/j.1529-8817.2000.99029.x

McCarthy, M. J., Carini, S. A., Liu, Z., Ostrom, N. E., & Gardner, W. S. (2013). Oxygen consumption in the water column and sediments of the northern Gulf of Mexico hypoxic zone. *Estuarine, Coastal and Shelf Science*, *123*, 46–53. https://doi.org/10.1016/j.ecss.2013.02.019

McCarthy, M. J., Gardner, W. S., Lavrentyev, P. J., Moats, K. M., Jochem, F. J., & Klarer, D. M. (2007). Effects of hydrological flow regime on sediment-water interface and water column nitrogen dynamics in a Great Lakes coastal wetland (Old Woman Creek, Lake Erie). *Journal of Great Lakes Research*, *33*(1), 219–231. https://doi.org/10.3394/0380-1330(2007)33[219:EOHFRO]2.0.CO;2

McCarthy, M. J., Gardner, W. S., Lehmann, M. F., & Bird, D. F. (2013). Implications of water column ammonium uptake and regeneration for the nitrogen budget in temperate, eutrophic Missisquoi Bay, Lake Champlain (Canada/USA). *Hydrobiologia*, *718*(1), 173–188. https://doi.org/10.1007/s10750-013-1614-6

McCarthy, M. J., Gardner, W. S., Lehmann, M. F., Guindon, A., & Bird, D. F. (2016). Benthic nitrogen regeneration, fixation, and denitrification in a temperate, eutrophic lake: Effects on

the nitrogen budget and cyanobacteria blooms. *Limnology and Oceanography*. *61*(4), 1406–1423. https://doi.org/10.1002/lno.10306

McCarthy, M. J., Lavrentyev, P. J., Yang, L., Zhang, L., Chen, Y., Qin, B., & Gardner, W. S. (2007). Nitrogen dynamics and microbial food web structure during a summer cyanobacterial bloom in a subtropical, shallow, well-mixed, eutrophic lake (Lake Taihu, China). *Hydrobiologia*, *581*(1), 195–207. https://doi.org/10.1007/s10750-006-0496-2

Monchamp, M. E., Pick, F. R., Beisner, B. E., & Maranger, R. (2014). Nitrogen forms influence microcystin concentration and composition via changes in cyanobacterial community structure. *PLoS ONE*, *9*(1). https://doi.org/10.1371/journal.pone.0085573

Newell, S. E., Davis, T. W., Johengen, T. H., Gossiaux, D., Burtner, A., Palladino, D., & McCarthy, M. J. (2019). Reduced forms of nitrogen are a driver of non-nitrogen-fixing harmful cyanobacterial blooms and toxicity in Lake Erie. *Harmful Algae*, *81*, 86–93. https://doi.org/10.1016/j.hal.2018.11.003

Newell, S. E., McCarthy, M. J., Gardner, W. S., & Fulweiler, R. W. (2016). Sediment nitrogen fixation: A call for re-evaluating coastal N budgets. *Estuaries and Coasts*, *39*(6), 1626–1638. https://doi.org/10.1007/s12237-016-0116-y

Nogaro, G., Burgin, A. J., Schoepfer, V. A., Konkler, M. J., Bowman, K. L., & Hammerschmidt, C. R. (2013). Aluminum sulfate (alum) application interactions with coupled metal and nutrient cycling in a hypereutrophic lake ecosystem. *Environmental Pollution*, *176*, 267–274. https://doi.org/10.1016/j.envpol.2013.01.048

OEPA. (2007). *Total Maximum Daily Loads for the Beaver Creek and Grand Lake St. Marys Watershed*.

O'Reilly, C. M., Sharma, S., Gray, D. K., Hampton, S. E., Read, J. S., Rowley, R. J., Schneider, P., Lenters, J, D., McIntyre, P. B., Kraemer, B. M., Weyhenmeyer, G. A., Straile, D., Dong, B., Adrian, R., Allan M. G., Anneville, O., Arvola, L., Austin, J., Bailey, J. L., … Guoqing, Z., (2015). Rapid and highly variable warming of lake surface waters around the globe. *Geophysical Research Letters*, *42*(24), 10773–10781. https://doi.org/10.1002/2015GL066235

Paerl, H. W., Havens, K. E., Xu, H., Zhu, G., McCarthy, M. J., Newell, S. E., Scott, J. T., Hall, N. S., Otten, T. G., & Qin, B. (2020). Mitigating eutrophication and toxic cyanobacterial blooms in large lakes: The evolution of a dual nutrient (N and P) reduction paradigm. *Hydrobiologia*, *847*(21), 4359–4375. https://doi.org/10.1007/s10750-019-04087-y

Paerl, H. W., & Otten, T. G. (2013). Harmful cyanobacterial blooms: causes, consequences, and controls. *Microb. Ecol*. *65*, 995–1010. https://doi.org/10.1007/s00248-012-0159-y

Paerl, H. W., & Paul, V. J. (2012). Climate change: Links to global expansion of harmful cyanobacteria. *Water Research*, *46*(5), 1349–1363. https://doi.org/10.1016/j.watres.2011.08.002

Paerl, H. W., Xu, H., McCarthy, M. J., Zhu, G., Qin, B., Li, Y., & Gardner, W. S. (2011). Controlling harmful cyanobacterial blooms in a hyper-eutrophic lake (Lake Taihu, China): The need for a dual nutrient (N & P) management strategy. *Water Research*, *45*(5), 1973–1983. https://doi.org/10.1016/j.watres.2010.09.018

Schindler, D. W. (2012). The dilemma of controlling cultural eutrophication of lakes. *Proceedings of the Royal Society B: Biological Sciences*, *279*(1746), 4322–4333. https://doi.org/10.1098/rspb.2012.1032

Schindler, D. W., Hecky, R. E., Findlay, D. L., Stainton, M. P., Parker, B. R., Paterson, M. J., Beaty, K. G., Lyng, M., & Kasian, S. E. M. (2008). Eutrophication of lakes cannot be controlled by reducing nitrogen input: Results of a 37-year whole-ecosystem experiment. *Proceedings of the National Academy of Sciences of the United States of America*, *105*(32), 11254–11258. https://doi.org/10.1073/pnas.0805108105

Scott, J. T., McCarthy, M. J., Gardner, W. S., & Doyle, R. D. (2008). Denitrification, dissimilatory nitrate reduction to ammonium, and nitrogen fixation along a nitrate concentration gradient in a created freshwater wetland. *Biogeochemistry*, *87*(1), 99–111. https://doi.org/10.1007/s10533-007-9171-6

Scott, T. J., & McCarthy, M. J. (2010). Nitrogen fixation may not balance the nitrogen pool in lakes over timescales relevant to eutrophication management. *Limnology and Oceanography*, *55*(3), 1265–1270. https://doi.org/10.4319/lo.2010.55.3.1265

Scott, T. J., & McCarthy, M. J. (2011). Response to Comment: Nitrogen fixation has not offset declines in the Lake 227 nitrogen pool and shows that nitrogen control deserves consideration in aquatic ecosystems. *Limnology and Oceanography*, *56*(4), 1548–1550. https://doi.org/ 10.4319/lo.2011.56.4.1548

Scott, T. J., McCarthy, M. J., & Paerl, H. W. (2019). Nitrogen transformations differentially affect nutrient-limited primary production in lakes of varying trophic state. *Limnology and Oceanography Letters*, *4*(4), 96–104. https://doi.org/10.1002/lol2.10109

Smith, V. H., Tilman, G. D., & Nekola, J. C. (1999). Eutrophication: impacts of excess nutrient inputs on freshwater, marine, and terrestrial ecosystems. *Environmental Pollution*, *100*, 179–196. https://doi.org/10.1016/S0269-7491(99)00091-3

Solomon, C. M., Collier, J. L., Berg, G. M., & Glibert, P. M. (2010). Role of urea in microbial metabolism in aquatic systems: A biochemical and molecular review. *Aquatic Microbial Ecology*, *59*(1), 67–88. https://doi.org/10.3354/ame01390

Steffen, M. M., Li, Z., Effler, T. C., Hauser, L. J., Boyer, G. L., & Wilhelm, S. W. (2012). Comparative metagenomics of toxic freshwater cyanobacteria bloom communities on two continents. *PLoS ONE*, *7*(8), 1–9. https://doi.org/10.1371/journal.pone.0044002

Steffen, M. M., Zhu, Z., McKay, R. M. L., Wilhelm, S. W., & Bullerjahn, G. S. (2014). Taxonomic assessment of a toxic cyanobacteria shift in hypereutrophic Grand Lake St. Marys (Ohio, USA). *Harmful Algae*, *33*, 12–18. https://doi.org/10.1016/j.hal.2013.12.008

Treuer, G., Kirchhoff, C., Lemos, M. C., & McGrath, F. (2021). Challenges of managing harmful algal blooms in US drinking water systems. *Nature Sustainability*, *4*(11), 958–964. https://doi.org/10.1038/s41893-021-00770-y

U.S. Environmental Protection Agency. (2009). National lakes assessment: a collaborative survey of the nation's lakes. In *US Environmental Protection Agency* (Issue EPA 841-R-09-001).

U.S. Environmental Protection Agency. (2011). Reactive nitrogen in the United States: An analysis of inputs, flows, consequences, and management options. United States Environmental Protection Agency (EPA). In *US Environmental Protection Agency* (Issue EPA-SAB-11-013).

WHO. (2021). WHO guidelines on recreational water quality. Volume 1, Coastal and freshwaters. In *World Health Organization*.

Wolf, D., & Klaiber, H. A. (2017). Bloom and bust: Toxic algae's impact on nearby property values. *Ecological Economics*, *135*, 209–221. https://doi.org/10.1016/j.ecolecon.2016.12.007

Wu, T., Boquiang, Q., Brookes, J. D., Yan, W., Ju, X., & Feng, J. (2019) Spatial distribution of sediment nitrogen and phosphorus in Lake Taihu from a hydrodynamics-induced transport perspective. *Science of the Total Environment*, *650*, 1554–1565. https://doi.org/10.1016/j.scitotenv.2018.09.145

Xu, H., Mccarthy, M. J., Paerl, H. W., Brookes, J. D., Zhu, G., Hall, N. S., Qin, B., Zhang, Y., Zhu, M., Hampel, J. J., Newell, S. E., & Gardner, W. S. (2021). Contributions of external nutrient loading and internal cycling to cyanobacterial bloom dynamics in Lake Taihu, China: Implications for nutrient management. *66*(4), 1492–1509. https://doi.org/10.1002/lno.11700

Zhu, L., Shi, W., Van Dam, B., Kong, L., Yu, J., & Qin, B. (2020). Algal accumulation decreases sediment nitrogen removal by uncoupling nitrification-denitrification in shallow eutrophic lakes. *Environmental Science and Technology*, *54*(10), 6194–6201. https://doi.org/10.1021/acs.est.9b05549

# VII. APPENDIX

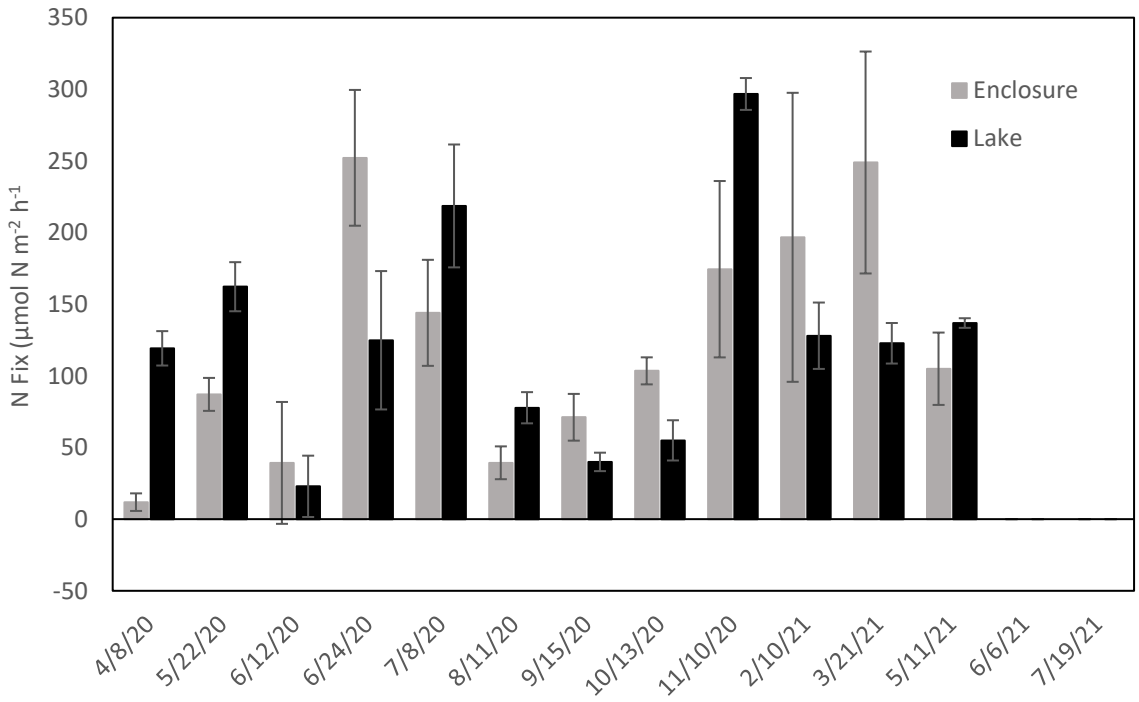


*Figure 21: Calculated N Fixation.*

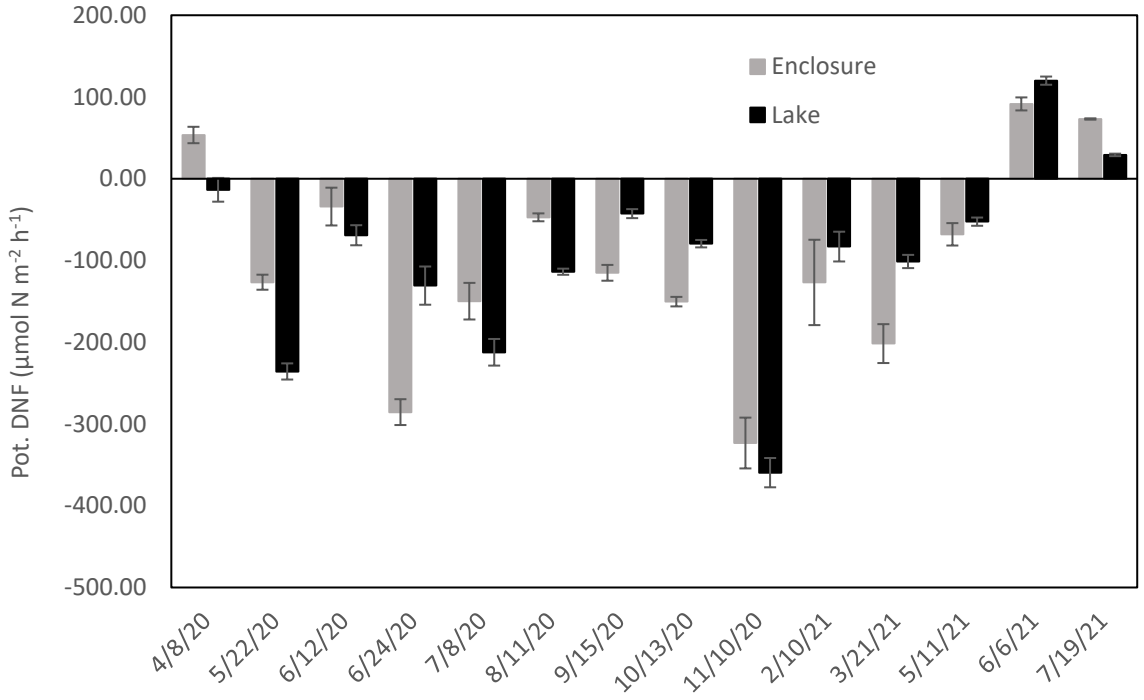


*Figure 22: Potential denitrification ($^{28}N_2$ + $^{29}N_2$ + $^{30}N_2$ + any N fixation).*

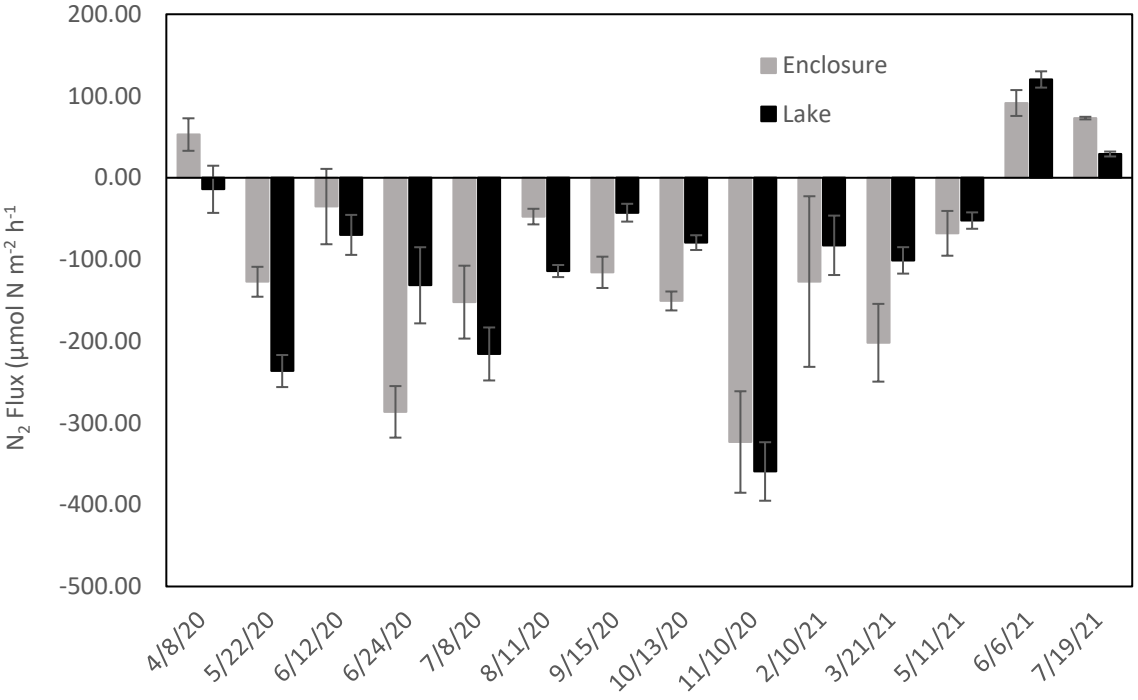


*Figure 23: In-Situ $N_2$ flux ($^{28}N_2$ fluxes + any N fixation).*

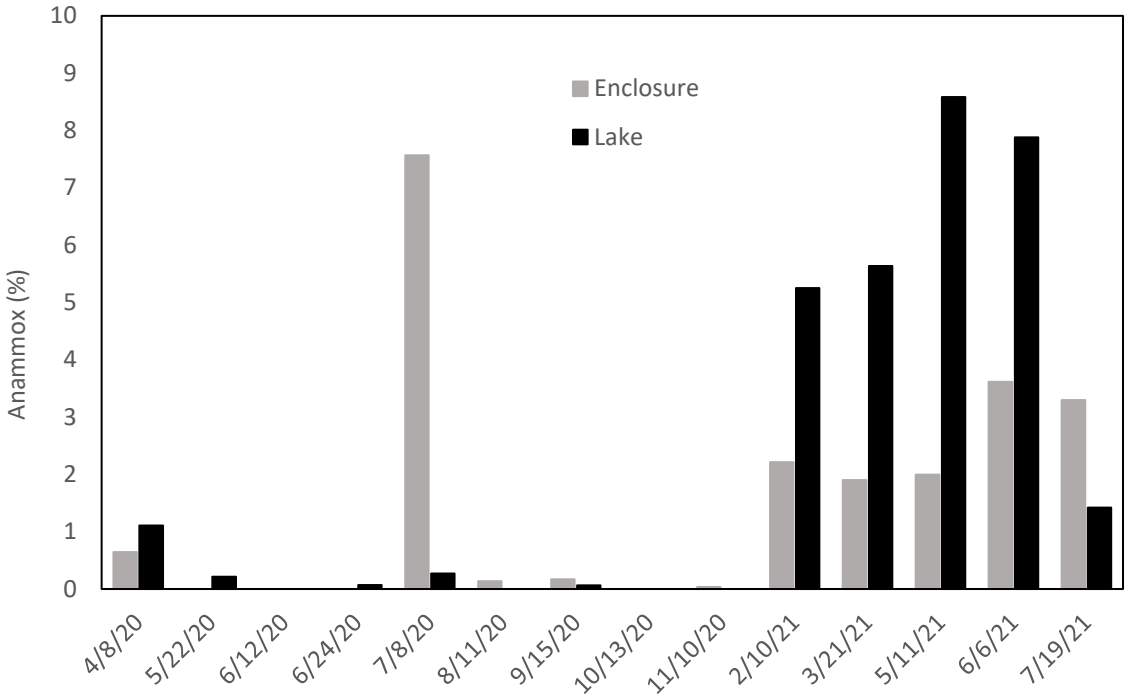


*Figure 24: Percentage of potential denitrification accounted for by annamox.*